The Dissertation Committee for Li-Jung Chen Certifies that this is the approved version of the following dissertation:

Biological Treatment of Hazardous Air Pollutants from Corn-to-Biofuel Dry Mill Production Facilities

Committee:

Kerry A. Kinney, Co-Supervisor

Lynn E. Katz, Co-Supervisor

Mary Jo Kirisits

A. Frank Seibert

Gerald E. Speitel Jr.

Biological Treatment of Hazardous Air Pollutants from Corn-to-Biofuel Dry Mill Production Facilities

by

Li-Jung Chen, B.S.; M.S.

Dissertation

Presented to the Faculty of the Graduate School of

The University of Texas at Austin

in Partial Fulfillment

of the Requirements

for the Degree of

Doctor of Philosophy

The University of Texas at Austin

May 2009

Dedication

To my husband Jeremy

and my parents.

Thank you for all your love and support.

Acknowledgements

I would like to express my gratitude to my advisors Dr. Kerry A. Kinney and Dr. Lynn E. Katz for their advice, encouragement and support throughout my doctoral work. I would also like to thank my committee Dr. Gerald E. Speitel Jr., Dr. Mary Jo Kirisits, and Dr. A. Frank Seibert for providing guidance along the way.

I want to particularly thank Paula Kulis, Shipeng Fu, Nate and Rebekah Johnson, Shannon Stokes, Becky Teasley, Susan De Long and Mara London for their wonderful friendship. The past and present members in Drs. Kinney, Katz and Speitel research groups have made my research work possible. I would like to recognize Dr. Soondong Kwon for sharing his expertise; Dr. Chia-Chen Chen and Charles Perego for helping with the instruments. Special thanks go to Brandt Miller for his excellent assistance with lab work during the final stage of my research.

I am so grateful to my parents and my siblings Gillian, Peggie, Vincent, and Ethan, and also my in-laws grandmother Dorothy, parents Fred and Carla, and brother Christopher for their love. Thank you baby Luke for granting me strength to finish my Ph.D. dissertation. Last but not least, my deepest appreciation goes to my best friend and husband, Jeremy Seibert, for always believing in me and being such a cheer in life. I could not have accomplished this much without him.

Biological Treatment of Hazardous Air Pollutants from Corn-to-Biofuel Dry Mill Production Facilities

Publication No._____

Li-Jung Chen, Ph.D.

The University of Texas at Austin, 2009

Supervisors: Kerry A. Kinney and Lynn E. Katz

Development of renewable energy sources such as ethanol has become a priority to meet growing energy demands. In the United States, the majority of ethanol is produced at dry mill facilities that convert corn to ethanol; these facilities can be a major emission source for volatile organic compounds (VOCs). Biofiltration is a promising VOC control technology but its effectiveness for the VOC mixtures emitted from ethanol production facilities has yet to be determined.

The main goal of this research was to evaluate the feasibility of using biofiltration to treat ethanol plant air pollutants. To accomplish this, microbial degradation of four representative pollutants (formaldehyde, acetaldehyde, ethanol and acetic acid) was examined first in simplified batch reactors and then in a laboratory-scale biofilter system. The batch data indicate that, at a neutral pH, an enriched microbial consortium was capable of completely degrading formaldehyde, acetaldehyde and ethanol, and the Monod model was successfully utilized to describe single substrate degradation kinetics for these pollutants. However, the consortium only partially

degraded acetic acid. In binary substrate experiments, acetaldehyde degradation was not significantly affected by either ethanol or formaldehyde. However, acetaldehyde inhibition of ethanol degradation was observed and inhibition kinetics were necessary to describe the observed ethanol removals. Formaldehyde degradation was inhibited in the presence of acetaldehyde and/or ethanol; however, further research will be required to identify the inhibtion.

The biofilter study was performed to investigate the effects of pollutant loading, substrate mixtures and low pH on system performance. The results indicate that it is feasible to achieve greater than 97% overall removal efficiency at a short contact time of 5 seconds under neutral pH conditions. The level of substrate inhibition observed in the batch experiments was not evident in the biofilter experiments. However, low pH conditions gradually decreased the biofilter performance with a more significant impact on acetaldehyde, a result that was supported by batch data. Finally, a numerical model that integrated degradation kinetics was able to describe the biofilter performance under the test conditions. This research demonstrates that biofiltration has the potential to be a viable VOC treatment technology at corn-derived ethanol production facilities.

Table of Contents

List of Tables

List of Figures

Chapter 1: Introduction

With an increasing world population and declining availability of fossil fuels, the development of renewable energy sources has become a global priority to meet our growing energy demands. Recently, the United States Congress passed the *Energy Independence and Security Act of 2007* that set production targets for renewable fuels in the United States over the next 15 years. The Act mandates that the production of renewable fuels reach 36 billion gallons by 2022, with up to 15 billion gallons of this fuel generated from conventional biofuels such as corn-derived ethanol (U.S. Congress, 2007).

Greater than 97% of U.S. domestic ethanol is made from corn stock, and dry milling facilities provide 79% of corn-based ethanol production (Shapouri and Salassi, 2006). Approximately 7.7 billion gallons of corn-based ethanol were produced in the U.S. in 2008 (RFA, 2009). Even though ethanol is widely viewed as an attractive renewable energy source, the potential environmental implications of corn to ethanol production have sparked debate on the merits of this approach. In particular, the net energy gain and carbon debt associated with corn to ethanol production have been discussed extensively in many recent studies (McAloon *et al*., 2000; Shapouri *et al.*, 2002; Pimentel and Patzek, 2005; Farrell *et al*., 2006; Searchinger *et al*., 2008; Fargione *et al*., 2008; Kim *et al*., 2009). However, much less attention has focused on the hazardous air pollutants (HAPs) that can be emitted from corn to ethanol production facilities.

1.1. PROBLEM IDENTIFICATION

The U.S. Environmental Protection Agency (USEPA) has investigated the emissions of air pollutants from ethanol production facilities and discovered that some of these facilities are sources of volatile organic compounds (VOCs), particulate matter (PM) and odors (USEPA, 2002; MDH, 2003). At dry milling facilities, in particular, the distillers dried grains with solubles (DDGS) dryer stack can be a significant emission source of VOCs consisting of alcohols, aldehydes and organic acids (MDH, 2003). It has also been confirmed that other process units such as distillation and fermentation tanks can generate similar VOC emissions (MDH, 2003; Brady and Pratt, 2006). Since sources such as the DDGS dryer emit HAPs at levels that can violate the National Emissions Standards for Hazardous Air Pollutants (NESHAP), ethanol production facilities have been required to install air pollution control devices to treat these emissions. Exhaust gases from a DDGS dryer are typically at high temperatures (100-140°C) and often passed through a scrubber or a cyclone to control PM emissions and reduce exit gas temperatures. Incinerators are then used to destroy the VOCs remaining in the waste gas streams. As for distillation and fermentation processes, a wet scrubber is widely used to control soluble VOC emissions such as ethanol and acetic acid. Sometimes, it is necessary to install a downstream incinerator or carbon adsorber for destruction of volatile VOCs (e.g. acetaldehyde) that are not removed in the scrubber.

Representative air pollutants emitted from corn-based ethanol production facilities consist of formaldehyde, acetaldehyde, ethanol and acetic acid. Formaldehyde and acetaldehyde are the major pollutants of concern since they are probable human carcinogens and have been classified as HAPs by the USEPA. To effectively treat waste gases containing these pollutant mixtures, treatment technologies such as incineration, adsorption, absorption and biofiltration can be utilized alone or coupled with

one another. Although incineration can achieve high VOC destruction efficiencies, it is energy intensive, produces greenhouse gases from the combustion process and is subject to the volatility of natural gas prices. Adsorption is an option for waste gas treatment but the removal efficiency of an adsorption system will be limited by the relatively low adsorption capacities for the major HAPs. Absorption is feasible for the organic acids and formaldehyde in the gas streams but would likely be ineffective for acetaldehyde due to its high Henry's Law constant ($atm \cdot m^3/mol$). Biofiltration may be an attractive treatment option due to its moderate operating costs, minimal energy consumption and the potential for high pollutant removal efficiencies. However, the feasibility of utilizing biofilters for ethanol plant emissions has not been evaluated.

Formaldehyde and acetaldehyde are known to be biodegradable individually, but the biodegradability of aldehyde mixtures in real waste gas streams is not well established. To date, most studies have focused on biofiltration of single aldehydes and little research has been conducted to investigate the effectiveness of biofilters for treating binary aldehyde mixtures. Thus, it is important to investigate the response of biofilters to pollutant mixtures containing aldehydes and the other constituents that are typically found in the waste gases emitted from ethanol production facilities. In addition to the effect of substrate mixtures, low pH conditions due to the presence of acidic fermentation byproducts in ethanol plant emissions may pose another challenge to biofiltration applications. Thus, the resiliency of the microbial consortium to acidic conditions must be evaluated.

1.2. RESEARCH OBJECTIVES

The overall objective of the research was to evaluate the feasibility of biofiltration as an alternative air pollution control technology to treat air emissions from corn-derived

biofuel production facilities. This study focused on the biological treatment of formaldehyde, acetaldehyde, ethanol and acetic acid, which are representative of the hazardous and non-hazardous air pollutants typically found in ethanol plant emissions.

Specific objectives of this research included:

- Evaluate aldehyde degradation kinetics and investigate the effect of pH and substrate mixtures on aldehyde degradation in batch studies.
- Determine Monod kinetic parameters for the selected substrates and evaluate inhibition models to describe substrate interactions.
- Examine how key operating factors, including pollutant loading rates, contact time, substrate mixtures and pH affect pollutant removal in a biofilter.
- Develop a steady-state biofilter model that describes biofilter system performance.

1.3. RESEARCH SCOPE

This research evaluated the potential for applying biofiltration technology to the control of VOC emissions from ethanol production facilities. Specifically, the fundamental kinetics of aldehyde degradation were first investigated in batch reactors for both single substrate and binary substrate mixtures. The effect of dissolved oxygen, pH and enrichment condition was also evaluated in these batch experiments. Next, the performance of a laboratory-scale biofilter was evaluated as a function of pollutant loading rate, waste gas composition and pH. In these experiments, the biofilter treated a series of simulated waste gas streams that progressed in complexity from a single aldehyde component to a four component mixture of formaldehyde, acetaldehyde, ethanol and acetic acid. Finally, a state-steady numerical model incorporating biofilter

system characteristics and substrate degradation kinetics was developed to describe and interpret the pollutant removals observed in this research.

This research provides not only a fundamental understanding of the biodegradation of HAP mixtures but also demonstrates the potential of biofiltration technology as a treatment alternative for corn-derived ethanol production facilities. In addition, the research provides insights regarding the pretreatment requirements for waste gas streams prior to biofiltration and feasible operating strategies for ethanol plant biofilter applications.

Chapter 2: Literature Review

The production of corn-based ethanol is soaring in the United States. It is known that volatile organic compounds (VOCs) and particulate matter (PM) are generated during ethanol production processes, and some of the VOCs are classified as hazardous air pollutants (HAPs). The Clean Air Act's New Source Review (NSR) program requires ethanol production facilities to install control devices and undertake other pre-construction obligations to control the emissions of pollutants (USEPA, 2002). Incineration has been utilized frequently at these facilities to treat VOC emissions, but its high energy costs have provoked the industry to begin considering alternative air pollution control technologies. Biofiltration is a promising technology that has been applied successfully in many industries. Evaluating the feasibility of biofiltration to treat the HAPs present in ethanol plant emissions can help to determine its potential for application at corn-based ethanol production facilities.

This chapter provides an overview of corn-based ethanol production and evaluates the potential for using biofiltration technology to treat air emissions from ethanol facilities. Section 2.1 describes corn-based ethanol production processes and identifies the common air pollutants that require treatment. Next, primary biodegradation pathways for the aldehyde pollutants of concern are discussed in Section 2.2. Section 2.3 reviews substrate degradation kinetics, which is a crucial factor for assessing biodegradation potential. Then, biofiltration technology and the parameters affecting biofilter performance are described in Section 2.4. Finally, Section 2.5 describes the use of computer models to predict biofilter performance.

2.1. CORN-BASED ETHANOL PRODUCTION

2.1.1. Ethanol Production Processes

Ethanol production in the U.S. has risen in the past few years because ethanol is viewed as a renewable energy source and has the potential to ease our dependence on foreign oil. Approximately 7.7 billion gallons of ethanol was produced in the U.S. in 2008, which is approximately 96% of the annual ethanol demand (RFA, 2009). Growing ethanol demands have motivated farmers to produce more corn and inspired scientists to look into various feed stocks that can be used to produce ethanol.

Due to an ever increasing demand for ethanol, expansion of corn-based ethanol production has become a priority for the U.S. ethanol industry. There are 171 plants in current production and 21 plants under expansion and construction. A total ethanol production capacity of 12 billion gallons per year (MGY) is expected once the new and expanded production capacity is in place (RFA, 2009). The ethanol market is dominated by its use as an oxygenate in reformulated gasoline and as a replacement for petroleum-based fuels. Some areas of the country mandate the use of E10 (10% ethanol and 90% gasoline) to improve air quality. Some newer vehicles can run on reformulated gasoline containing a higher level of ethanol, such as E85 or any mixture of ethanol and gasoline (USDOE, 2007).

The majority (97%) of ethanol produced in the U.S. is made from corn kernels; 79% of corn-based ethanol comes from the dry milling process (Figure 2.1) and the remainder comes from the wet milling process (Figure 2.2) (USEPA, 1994a; Shapouri and Salassi, 2006; RFA, 2009).

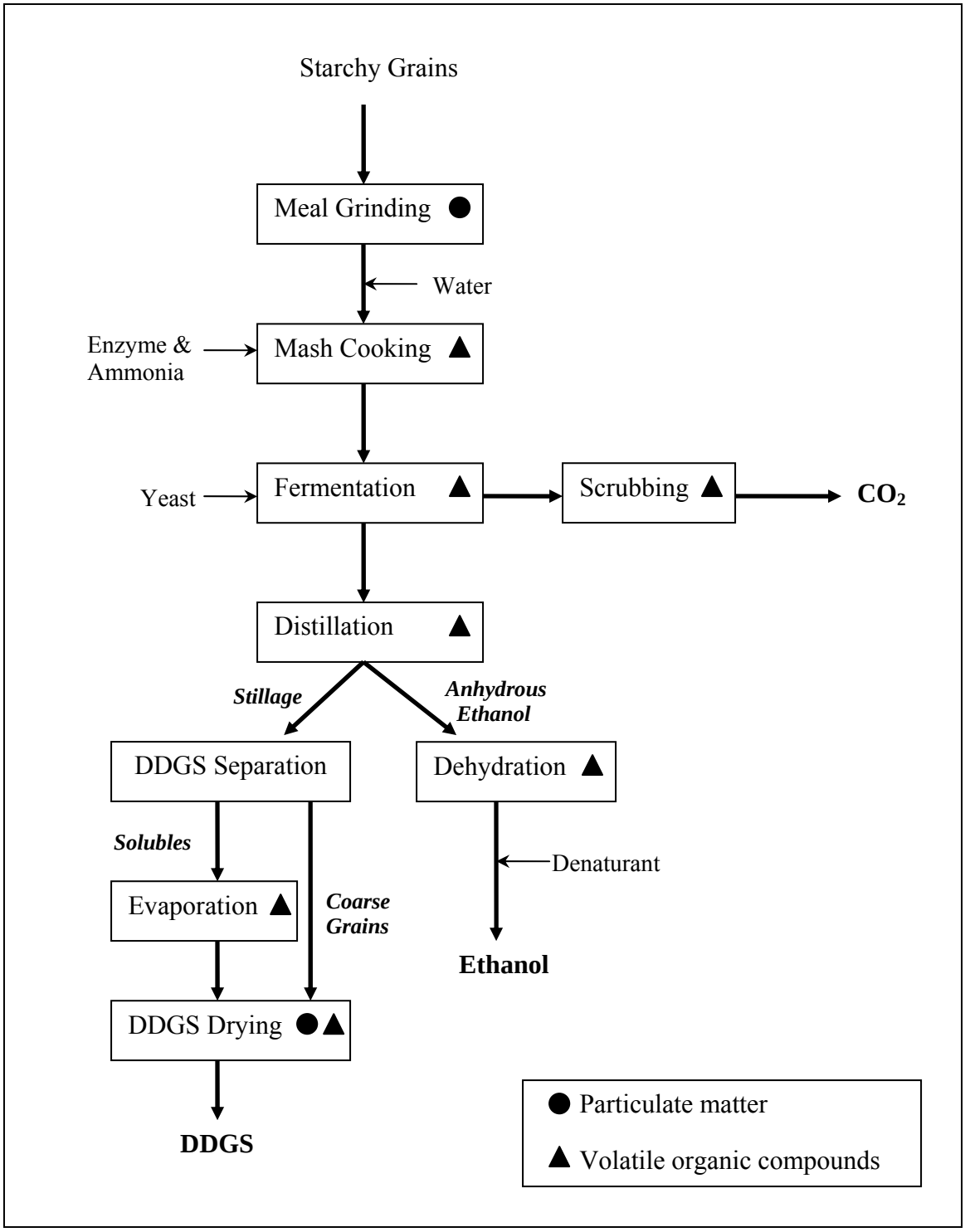

Figure 2.1. Typical corn dry milling process and emission sources.

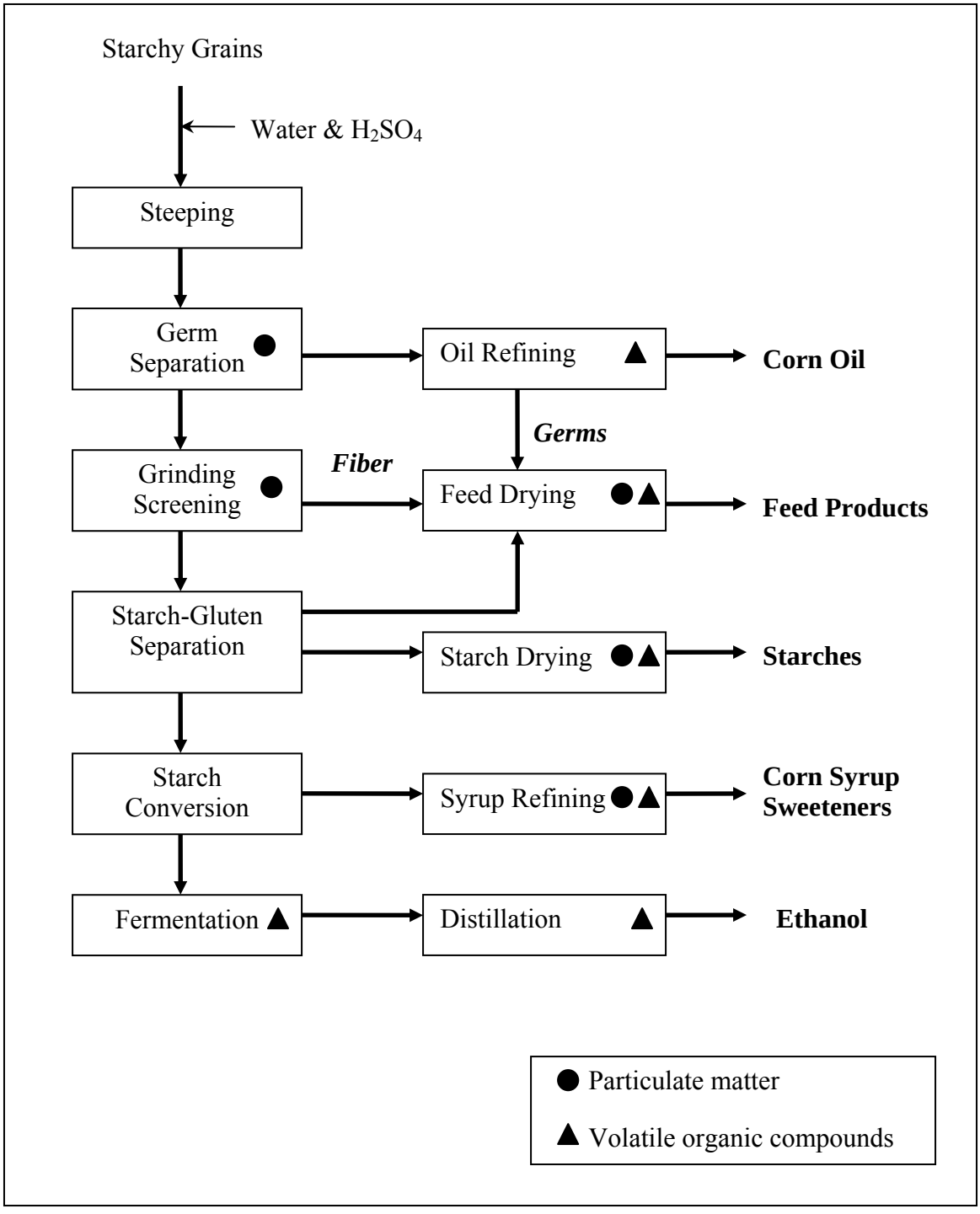

Figure 2.2. Typical corn wet milling process and emission sources.

As seen in Figures 2.1 and 2.2, the dry milling process produces ethanol and distillers dried grains with solubles (DDGS), while the wet milling process provides a greater variety of products. However, the dry milling process has become the preferred production system for new and/or small-scale plants due to its lower capital investment requirements.

2.1.2. Sources, Characteristics and Control of Air Emissions

The USEPA began investigating emissions from ethanol production facilities in 2002 and discovered that a number of the active ethanol plants failed to meet emission standards outlined in their permits. Specifically, the USEPA announced civil settlements with 12 ethanol production facilities in Minnesota for alleged the Clean Air Act (CAA) violations. Each of these plants was required to install a thermal oxidizer and other air pollution control devices valued at $2 million per facility and pay a fine ranging from $29,000 to $39,000 (USEPA, 2002). One of these facilities owned by Gopher State Ethanol, Inc. was closed in May 2004 due to emissions of corrosive pollutants and PM that negatively impacted the local neighborhood. In 2003, Archer Daniels Midland (ADM) was charged a civil penalty of $4.6 million by the U.S. Department of Justice (USDOJ) and USEPA because ADM failed to accurately estimate its emissions from hundreds of process units and expanded other units without the installation of required air pollution control technology (USEPA, 2003). In 2005, the USDOJ and USEPA announced a CAA settlement with Cargill, Inc. after the company had significantly underestimated emissions from its operation at 26 facilities in 13 states. Cargill was charged a civil penalty of $1.6 million and required to spend $3.5 million on environmental projects (USEPA, 2005a).

Corn-based ethanol production processes generate a variety of air pollutants including VOCs, PM, odorous compounds and combustion byproducts such as nitrogen oxides (NO_x), sulfur oxides (SO_x), carbon monoxide (CO) and carbon dioxide (CO_2). VOCs and PM are generated during the production processes while the combustion byproducts are produced by dryers, boilers and incinerators. In the dry milling process, the DDGS dryer has been reported to be the most significant source of VOC emissions, while other units such as fermentation tanks and distillation tanks are also significant VOC sources (see Figure 2.1). Similarly, air emissions containing PM and VOCs are also detected in various operation units in the wet milling process, shown in Figure 2.2.

The composition and exit temperatures of waste gas streams at dry milling facilities depend on the particular production process and their downstream treatment systems. Waste gases emitted from a DDGS dryer stack contain a variety of VOCs such as alcohols, aldehydes and organic acids. The waste gas temperature of the exhaust from the DDGS dryer stack is usually in the range of 100 to 140°C; however, after passing through a cyclone or scrubber for particulate matter removal, the temperature usually decreases to approximately 35 to 55°C. Exhaust gases from fermentation and distillation systems contain fewer VOCs and the emitting temperature is often lower than 35°C. Table 2.1 summarizes the VOC emissions from several dry milling facilities to provide a better understanding of the VOC composition of the exhaust gases from different processes at corn-based ethanol production plants (Interpoll, 2001 & 2003 & 2005; ADM, 2002; MDH, 2003; AET, 2005).

.

Table 2.1. Characteristics of exhaust gases emitted from major dry milling process units at ethanol facilities

Process	Typical Treatment Unit	Gas Temp. Exiting Treatment Unit (°C)	Pollutant	Concentration Range (ppm_v)
Fermentation	Scrubber	15~35	Methanol Ethanol Formaldehyde Acetaldehyde Acetic acid	< 1 5~170 < 1 1~140 < 1
Distillation				
DDGS Drying	Scrubber	35~55	Methanol Ethanol Formaldehyde Acetaldehyde Acetic acid	1~85 1~80 1~5 1~70 1~10
	Cyclone			
	Bypass Stack (Untreated)	100~140	Methanol Ethanol Formaldehyde Acetaldehyde Acetic acid Lactic acid	up to 5 10~50 10~90 15~60 100~250 up to 60

Hazardous air pollutants (HAPs) are air pollutants that can cause serious human health problems and harm to the environment. The 188 HAPs listed in the 1990 CAA Amendment are regulated by the USEPA (USEPA, 1990). Installing air pollution control devices to reduce HAP emissions is a priority to ensure that air quality will not degrade. According to a recent public health assessment of an ethanol facility completed by the Minnesota Department of Health, approximately half of the VOCs emitted from the DDGS dryer stack at the dry mill facility were HAPs (MDH, 2003). Table 2.2 provides an overview of the VOCs emitted and the corresponding emission rates from the DDGS dryer stack. It is important to note that acetaldehyde and formaldehyde were present in the highest concentrations among the HAPs that were identified in the off-gases from the dryer stack

Table 2.2. Emission rates of the VOCs emitted from a DDGS dryer (MDH, 2003)

Compound	HAP	Emission rate (lb/hr)	Concentration* (ppm_v)
Acetic Acid		18.43	97.4
Lactic Acid		17.45	61.5
Aectaldehyde	√	2.87	20.7
Ethanol		1.85	12.7
Formaldehyde	√	1.55	16.4
Furfuraldehyde		0.25	0.8
Acrolein	√	0.09	0.3
Benzene	√	0.03	0.1

*: Volumetric flow rate from the DDGS dryer for this test was not reported. For a 20 million-gallons-per-year (MGY) ethanol plant, $Q_{DDGS\ dryer}$ is estimated to be 26,000 acfm, T= 103°C and P= 1 atm (Kolb, 2005).

Given that a variety of air pollutants are emitted from corn-based ethanol production plants, adequately reducing these emissions is important to mitigate the

potential impacts that they may have on human health and the environment. Air pollution control treatment units have been installed downstream of production units at ethanol production facilities. For instance, cyclones, baghouses, or scrubbers are typically used to remove PM and cool down DDGS dryer exhaust gases. Subsequent treatment in an incinerator is often used to destroy the remaining VOCs in waste gas streams to CO_2 and water. To treat VOC emissions, ethanol facilities often either utilize a thermal oxidizer to treat waste gas streams followed by a heat recovery steam generator (HRSG) to provide additional steam for operations, or a regenerative thermal oxidizer (RTO) containing heat transfer units to recover heat from post-incineration gases to preheat the waste gas to be incinerated (USEPA, 2005b). In addition to PM control, scrubbers are commonly used in fermentation and distillation processes to remove and/or recover soluble VOCs from exhaust gases. For instance, CO_2 scrubbers (also known as fermentation scrubbers) are used to remove ethanol from CO_2 gas streams produced in fermentation process, and a water scrubber downstream of distillation tanks is used for ethanol recovery from process exhaust gases.

Among the treatment units that have been implemented at these facilities to reduce undesired air emissions, incinerators are in fact a significant source of the greenhouse gas CO_2. Biofiltration and incineration both produce CO_2 while treating VOCs by converting the carbon molecules in VOCs to CO_2; however, incineration produces additional CO_2 from combustion of the fuel gas that is necessary to maintain its operating temperature. For example, it was estimated in this research that an incinerator treating 26,000 acfm of DDGS dryer exhaust at a 20 MGY facility would generate an additional 110 lbs of CO_2 per lb of VOC incinerated. Based on this case study, using a treatment technology alternative to incineration can help reduce the amount of CO_2 released to the environment by approximately 14,000 tons per year.

2.2. ALDEHYDE DEGRADATION

Several compounds in the aldehyde group, including formaldehyde, acetaldehyde, furfuraldehyde and acrolein, are major constituents of ethanol plant emissions, and some are classified as HAPs by the USEPA. Specifically, formaldehyde and acetaldehyde have consistently been detected in the waste gas streams emitted from a variety of processes at ethanol production facilities. In order to develop a biological treatment system for these aldehyde compounds, the characteristics of the aldehydes and their biodegradation pathways must be well understood.

2.2.1. Characteristics of Formaldehyde and Acetaldehyde

Compounds classified in the aldehyde group (RCHO) are polar and reactive. In the presence of reductants, they can be reduced to alcohols ($R\text{-}CH_2OH$), or in the presence of oxidants, they can be oxidized to carboxylic acids (R-COOH). Formaldehyde (H-CHO) is extremely unstable and its polymerization readily occurs in the presence of air and water at room temperature. The concentration of a commercial formaldehyde solutions is 37% (w/w) dissolved in water, with the addition of 10~15% methanol as a stabilizer to prevent oxidation and polymerization of formaldehyde. Even with methanol present in the solution, formaldehyde monomers slowly polymerize into paraformaldehyde (Andrawes, 1984). Acetaldehyde ($CH_3\text{-}CHO$) is highly flammable and has a high vapor pressure of 740 mmHg at 20°C (USEPA, 2007).

The apparent Henry's law constant for formaldehyde and acetaldehyde at 25°C are 3.4×10^{-4} atm·m^3/mol and 8.8×10^{-2} atm·m^3/mol, respectively (Betterton and Hoffman, 1988). These values highlight the difference in volatility of the two compounds in aqueous systems. Formaldehyde and acetaldehyde both have a pungent suffocating odor; the odor threshold is 0.83 ppm_v for formaldehyde and 0.05 ppm_v for acetaldehyde

(Amoore and Hautala, 1983). In addition, both aldehydes have been listed as probable human carcinogens. Formaldehyde and acetaldehyde concentrations in the air of 0.07 and 0.27 ppb_v respectively pose an additional cancer risk of 1 in 10^6 (USEPA, 2009).

2.2.2. Formaldehyde Degradation Pathways

Formaldehyde damages proteins and nucleic acids in cells nonspecifically due to its high reactivity. Aqueous solutions containing formaldehyde are commonly used as a disinfectant or preservative. Nevertheless, formaldehyde has been reported to be biodegradable under aerobic conditions (Bonastre *et al.*, 1986, Adroer *et al.*, 1990; Azachi *et al.*, 1995; Yamazaki *et al.*, 2001; Hidalgo *et al.*, 2002; Eiroa *et al*., 2004; Eiroa *et al.*, 2005), as well as under anaerobic conditions (Qu and Bhattacharya, 1997; Lu and Hegemann, 1998; Omil *et al*., 1999; Gonzalez-Gil *et al.*, 2002; Oliveira *et al*., 2004).

Methylotrophic bacteria and yeasts can grow on a number of C_1 substrates including methane, methanol, methylene chloride and several methylated compounds. Formaldehyde, an intermediate in the degradation of these compounds, can be utilized in subsequent catabolism and anabolism (Kaszycki *et al.*, 2001; Madigan *et al*., 2003). The metabolic pathways of one-carbon compounds through formaldehyde by aerobic methylotrophic bacteria (Vorholt, 2002) are shown in Figure 2.3. Oxidation of formaldehyde to formic acid by a methylotroph is carried out via a cyclic ribulose monophosphate pathway or one of several linear pathways. These linear pathways are involved with either a dye-linked, NAD(P)-independent formaldehyde dehydrogenase which is associated with cytoplasmic membrane, or a formaldehyde dehydrogenase that is dependent on NAD(P) and also requires a cofactor such as tetrahydrofolate, tetrahydromethanopterin, glutathione, or mycothiol (Hanson and Hanson, 1996; Vorholt, 2002). The glutathione-dependent formaldehyde pathway is also the most common

pathway in both prokaryotes and eukaryotes (Barber and Donohue, 1998; Vorholt, 2002). Once formaldehyde is oxidized to formic acid, a NAD-dependent formate dehydrogenase converts formic acid to CO_2. As shown in Figure 2.3, formaldehyde can also be assimilated into cell material by methanotrophic bacteria via two cycles: the ribulose monophosphate (RuMP) cycle by Type I methylotrophs, and the serine cycle by Type II methylotrophs. The main differences between Type I and II methylotrophs are the structures of their internal membrane systems in cytoplasm, and if they possess a complete set of enzymes for the citric acid cycle (Madigan *et al.*, 2003).

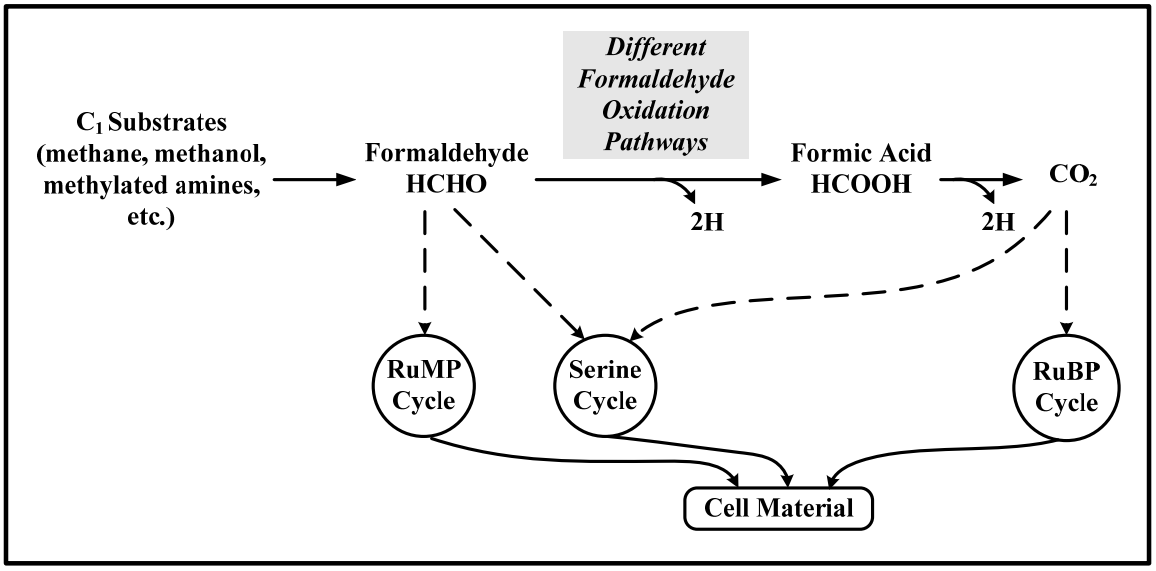

Figure 2.3. Formaldehyde metabolism by aerobic methylotrophic bacteria (Vorholt, 2002).

In addition to methylotrophs, aerobic biodegradation of formaldehyde has been extensively studied using bacteria isolated from soil (Mehta, 1975; Azachi *et al.*, 1995), seawater (Yamazaki *et al.*, 2001), contaminated sites (Hidalgo *et al.*, 2002), and industrial wastewater/sludge (Bonastre *et al*. 1986; Adroer *et al*., 1990; Glancer-Šoljan *et al.*, 2001;

Eiroa *et al.*, 2004; Eiroa *et al.*, 2005). Some studies have shown that aerobic formaldehyde biodegradation leads to the appearance of formic acid (Barber and Donohue, 1998; Glancer-Šoljan *et al.*, 2001) or the co-occurrence of methanol and formic acid (Kato et al., 1984; Adroer *et al*., 1990; Eiroa *et al.*, 2005). The former pathway is similar to the reaction of oxidizing formaldehyde to CO_2 by methylotrophic organisms. As shown in Pathway A, formaldehyde and formate dehydrogenases are involved, and they are mostly NAD-linked enzymes, as discussed in the previous section. [Note that the degradation pathways in this section have been labeled A, B, C, etc. to facilitate the discussions within the text].

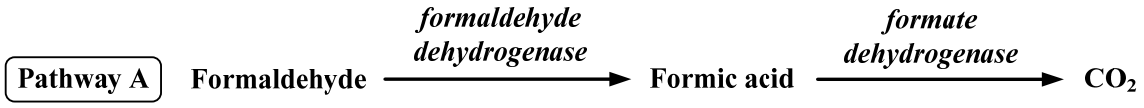

A few studies have showed *Pseudomonas putida* possesses a formaldehyde dismutase that can catalyze two moles of formaldehyde to one mole of methanol and one mole of formic acid, shown in Pathway B (Kato *et al.*, 1984; Adroer *et al.*, 1990). This type of reaction does not require the addition of electron acceptors such as NAD^+ or $NADP^+$, and can occur as a cross-dismutation reaction between two different aldehydes, or between one alcohol and one aldehyde (Kato *et al.*, 1984).

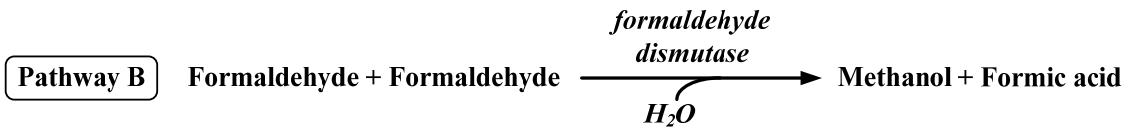

Acetic acid bacteria are known to oxidize ethanol to acetic acid through acetaldehyde as the intermediate. In addition, it has been confirmed that some acetic acid bacteria are capable of formaldehyde oxidation (Schinagawa *et al*., 2006 & 2008). Schinagawa *et al.* (2006) studied an alcohol dehydrogenase (ADH) isolated from the cytoplasmic membrane of an acetic acid bacterium strain, *Acetobacter* sp. SKU 14. The enzyme activity was tested using several types of substrates including sugars, sugar alcohols, alcohols, aldehydes and organic acids. The membrane-bound ADH showed broad substrate specificity toward alcohols (e.g. ethanol, n-propanol and n-butanol) and aldehydes (e.g. formaldehyde and acetaldehyde), and it had higher activities in oxidation of alcohols than aldehydes. In addition, the authors confirmed the membrane-bound ADHs isolated from two other acetic acid bacteria, A. *aceti* IFO 3284 and *Gluconobacter suboxydans* IFO 12528, were also capable of oxidizing formaldehyde. Schinagawa *et al.* (2008) further compared formaldehyde oxidizing activity between *Acetobacter* sp. SKU 14 and *G. suboxydans* IFO 12528. They discovered the ADH in *Acetobacter* sp. SKU 14 showed a higher activity in formaldehyde oxidation than *G. suboxydans* IFO 1252. Based on the previous discussion, substrate specificity and activity of the membrane-bound ADHs in acetic acid bacteria will be crucial to pollutant removals when these bacteria are utilized to degrade pollutant mixtures consisting of ethanol, formaldehyde and acetaldehyde. Competition occurring among these ethanol plant pollutants in a biological treatment system can attribute to substrate specificity and activity of enzymes.

2.2.3. Acetaldehyde Degradation Pathways

Acetaldehyde is widely used to synthesize chemicals such as acetic acid and esters, and it is also known as an important intermediate in numerous biodegradation

pathways. Some microorganisms are capable of converting acetaldehyde to ethanol during fermentation processes in reduced environments, while ethanol oxidation under aerobic conditions leads to the formation of acetaldehyde. The common aerobic ethanol biodegradation pathway is shown in Pathway C with acetaldehyde and acetic acid as the main intermediates. Alcohol dehydrogenase (ADH) catalyzes ethanol to acetaldehyde followed by aldehyde dehydrogenase (ALDH) converting acetaldehyde to acetic acid. ADH and ALDH can be found in many bacteria and yeast due to the widespread existence of ethanol in the environment. A few studies of ethanol biofiltration have reported that ethyl acetate was observed in addition to acetaldehyde and acetic acid during ethanol degradation by yeast *Candida utilis* (Domenech *et al*., 1999; Christen *et al*., 2002). They attributed the occurrence of ethyl acetate to the esterification of ethanol and acetic acid in the biofilter systems.

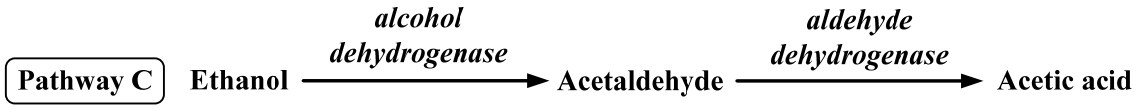

Acetic acid bacteria are among the microorganisms that have been identified as aerobic ethanol degraders and are known to perform ethanol oxidation to acetic acid (Pathway C). As a result, they have been extensively utilized in vinegar production. Although acetic acid bacteria are strict aerobes, adequate control of oxygen supplies is crucial for acetic acid production in a system. Insufficient or excess oxygen concentrations can damage enzymatic activities that are involved in ethanol oxidation and respiration, leading to low acid production (Muraoka *et al*., 1982 &1983; Park *et al*., 1989; Matsushita *et al*., 1995). Park *et al*. (1989) studied the effect of dissolved oxygen

(DO) concentration on acetic acid production using *A. aceti*. They found the optimal DO concentration range for rates of respiration and ethanol oxidation was 3-7 mg/L; a DO concentration lower than 3 mg/L or higher than 7 mg/L inhibited both rates. In addition, although acetic acid bacteria can grow well at low pH conditions, prompt pH regulation is crucial for acetic acid production in terms of maintaining ethanol oxidation activity. For instance, Park *et al*. (1989) reported that an increasing acetic acid concentration in the growth media led to a decrease in the ethanol oxidation rate. In addition, Matsushita *et al*. (1995) discovered that an inactive ADH form was more abundantly present at pH 5.0-6.5 than at pH 7.0-8.5. They also reported that the inactivation can be reversed by shifting pH from acidic to neutral/alkaline region.

Acetic acid bacteria consist of two key genera: *Acetobacter* can oxidize acetic acid to CO_2 and H_2O, while *Gluconobacter* cannot oxidize acetic acid because they lack a complete set of catalytic enzymes for the TCA cycle (Madigan *et al*., 2003). It has been reported that *Gluconobacter oxydans* does not possess succinate dehydrogenase (Sugiyama *et al*., 2003). It is believed that quinoprotein ADH and ALDH, located on the outer cytoplasm membrane of acetic acid bacteria, are responsible for ethanol oxidation as well as acetic acid accumulation in the media. Typically, acetic acid is transported into the cytoplasm by passive diffusion for acetate assimilation in the TCA cycle. Membrane-bound ADHs are found NAD(P)-independent and less substrate-specific; some purified ADHs are capable of oxidation of both alcohols and aldehydes (Shinagawa *et al*., 2006).

Interestingly, additional NAD(P)-dependent ADH and ALDH have been found in the cytoplasm of acetic acid bacteria. Chinnawirotpisan *et al*. (2003) used *Acetobacter pasteurianus* SKU 1108 and its membrane-bound ADH deficient mutant strain to clarify the roles of the membrane-bound quinoprotein ADH and the cytoplasmic NAD(P)-

dependent ADH in the metabolism of acetic acid bacteria. They suggest that the membrane-bound ADH and ALDH are mainly responsible for producing acetic acid extracellularly, resulting in accumulation of acetic acid, while the cytoplasmic ADH and ALDH are involved in acetic acid assimilation in the cytoplasm. Matsushita *et al*. (2005) further proposed a proton motive force-dependent efflux pump exists in *Acetonacter aceti*, which can specifically transfer intracellular acetic acid from the cytoplasm to outside of membrane. In other words, this unique mechanism and passive diffusion can simultaneously regulate intercellular and extracellular concentrations of acetic acid during ethanol oxidation.

The yeast strain *Saccharomyces cerevisiae* is predominantly used in alcoholic fermentation of sugar to ethanol in the absence of oxygen through glycolysis, and the facultative bacterium *Zymomonas mobilis* also plays an important role in alcoholic fermentation (Madigan *et al.*, 2003). Ethanol fermentation from glucose by yeast and the genus *Zymomonas* is shown in Pathway D. It is important to note that the pathways for converting glucose to pyruvate utilized by yeast and *Zymomonas* are different; yeast converts glucose through glycolysis while *Zymomonas* uses the Entner-Doudoroff Pathway.

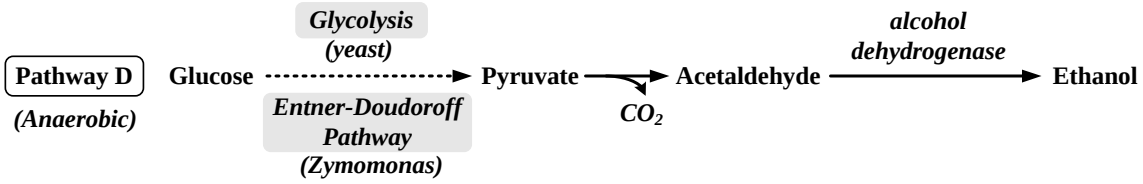

Research on the strain *Zymomonas mobilis* has shown that the bacterium possesses two ADH isoenzymes located in the cytoplasm: ADH I containing zinc and

ADH II containing iron respectively at their active sites (Kalnenieks *et al.*, 2002; Kalnenieks *et al.*, 2006). The isoenzymes can catalyze a reversible reaction between ethanol and acetaldehyde, and both are NADH-dependent eznymes. It has been reported that ADH I catalyzes acetaldehyde reduction faster than ethanol oxidation while ADH II behaves the opposite way (Kalnenieks *et al.*, 2002). Under anaerobic conditions, both enzymes carry out ethanol synthesis using acetaldehyde as expected in a typical fermentation to form alcohol. It has been confirmed that the ADH isoenzymes have higher affinities for NADH than NADH dehydrogenase, given the fact that the half-saturation constants of ADH I, ADH II and NADH dehydrogenase for NADH are 27, 12, and 58 μM (Kinoshita *et al.*, 1985; Kalnenieks *et al.*, 1996). As a result, the ADH isoenzymes of *Z. mobilis* compete for NADH with the respiratory NADH dehydrogenase under aerobic conditions.

Although acetaldehyde reduction to ethanol makes perfect sense in an anaerobic environment, this reaction is also possible aerobically. Kalnenieks *et al.* (2002) observed net ethanol synthesis from glucose occurred in a steady-state aerobic chemostat cultivating *Z. mobilis*. Even though the intracellular NADH level in the aerobic cultures was much lower than in the anaerobic cultures, the ratio of [Acetaldehyde]×[NADH]×[H^+] to [Ethanol]×[NAD^+] was still higher than reported equilibrium constants (as low as 6.9×10^{-12} M) for the ethanol oxidation reaction. Kalnenieks *et al.* (2006) studied the parent strain of *Z. mobilis* and its ADH II-deficient mutant; they concluded that ADH II was the primary ethanol-oxidizing enzyme and ADH I was the acetaldehyde-reducing enzyme under aerobic conditions. However, the opposite reactions are not thermodynamically feasible without introducing external energy. They further proposed that ADH II has a dual role in aerobic catabolism of *Z. mobilis*; that is, a fraction of ADH II carries out ethanol oxidation while ADH I along with the rest of ADH II fraction

catalyze ethanol synthesis. The proposed aerobic ethanol cycle by *Z. mobilis* is shown as Pathway E.

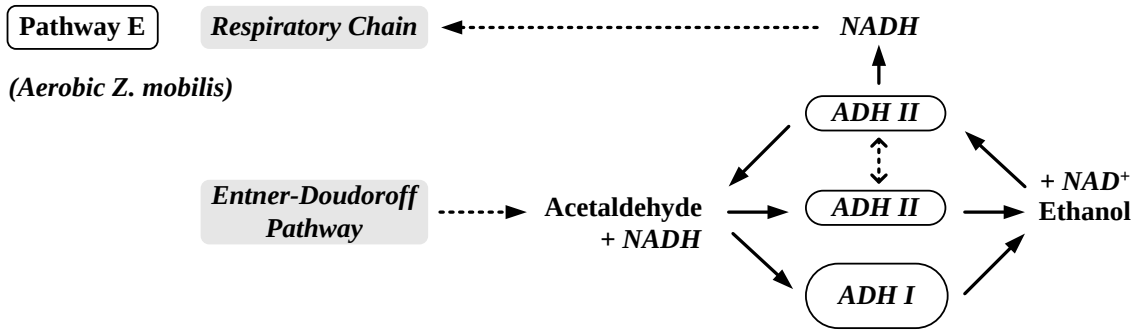

Given the unique characteristics of acetic acid bacteria and facultative bacteria *Zymomonas*, it is possible for acetic acid bacteria to rely on yeast and *Zymomonas* for ethanol production in a natural environment (Madigan *et al.*, 2003). In fact, Kondo and Kondo (1996) examined the feasibility of utilizing a mixed culture of ethanol-producing organisms (*S. cerevisiae* or *Z. mobilis*) and acetic acid bacteria (*Acetoacter sp.*, *Acetobacter aceti* or *Gluconobacter suboxydans*) for acetic acid production. Their results demonstrated the feasibility of glucose conversion aerobically to ethanol by *Z. mobilis* at the first stage and subsequent acetic acid production by *Acetoacter sp.* at the second stage. Therefore, the possibility exists for acetaldehyde conversion to ethanol by the facultative bacteria *Zymomonas* and ethanol degradation to acetic acid by the acetic acid bacteria in a biological system that is operated under aerobic conditions.

2.3. SUBSTRATE DEGRADATION KINETICS

Substrate utilization rates are generally related to microbial growth rates and can be characterized through kinetic studies. Fundamental questions such as

biodegradability, toxicity and the biodegradation rates of single and multiple substrates can be modeled through substrate degradation kinetics. Modeling can be used to assess treatment technology feasibility, to evaluate the impact of operational parameters, and to guide further research. Therefore, it is important to understand degradation kinetics of pollutants before employing the microorganisms of interest in a biological treatment system.

2.3.1. Kinetic Models for Substrate Degradation

One of the kinetic models frequently used to describe microbial growth kinetics employs the Monod equation. The original equation relates specific microbial growth rate (μ, 1/hr) to substrate concentration (S, mg/L) in a system. From the perspective of substrate utilization, the Monod equation with respect to substrate i can be expressed as Equation 2.1.

$$r_{s,i} = \frac{dS_i}{dt} = -\frac{k_i S_i X}{K_{s,i} + S_i} \qquad \text{(Equation 2.1; } \textit{Monod Kinetics}\text{)}$$

where $r_{s.i}$ = utilization rate of substrate i (mg/L/hr);

k_i = maximum specific utilization rate of substrate i (mg substrate/mg biomass/hr);

S_i = concentration of substrate i (mg/L);

X = biomass concentration (mg/L);

$K_{s,i}$ = half-saturation constant of substrate i (mg/L).

The Monod equation can be used to describe single substrate degradation in a single-substrate system or in a multiple-substrate system where the degradation of one substrate is not affected by the presence of the other substrates. However, the classical Monod equation does not consider substrate/product inhibition of a single substrate, or substrate competition/inhibition among multiple substrates. Numerous forms of kinetic models have been developed to account for inhibition by incorporating additional constants into the original Monod model (for a review see Kovárová-Kovar and Egli, 1998). When the substrate concentration exceeds a critical value, known as the inhibition concentration, it can be toxic to the microorganisms. This type of inhibition is referred to as *Self-Inhibition* (Rittmann and McCarty, 2001). Several substrate inhibition kinetic models have been utilized to describe substrate toxicity to microbial growth. One example is the Andrews model (Equation 2.2), which is similar to the Monod kinetic model but incorporates a term for self-inhibition constant of the substrate (K_{IS}, mg/L).

$$r_{s,i} = -\frac{k_i S_i X}{K_{s,i} + S_i + \frac{S_i^{\,2}}{K_{IS}}} \qquad \text{(Equation 2.2; } \textit{self-inhibition}\text{)}$$

Inhibition can also arise from the presence of multiple substrates in a system. To successfully model inhibition kinetics in a system, the assumptions inherent in the model must be matched to the system and the model must be experimentally verified. Three major types of inhibition have been proposed to address potential growth effects when a second substrate inhibits the degradation of the primary substrate (Rittmann and McCarty, 2001). The first type of inhibition is called *Competitive Inhibition*, in which two substrates i and j compete for an active site of the same enzyme. In this situation,

the utilization rate of substrate i, which is subject to competitive inhibition by substrate j, can be expressed as Equation 2.3.

$$r_{s,i} = -\frac{k_i S_i X}{K_{s,i}(1 + \frac{S_j}{K_{I,j}}) + S_i} \qquad \text{(Equation 2.3; } \textit{competitive inhibition}\text{)}$$

where $K_{I,j}$ = inhibition constant of substrate j (mg/L);

S_i and S_j = concentrations of substrates i and j (mg/L).

For a binary substrate system with occurrence of competitive inhibition between substrates i and j, the assumption of $K_{I,i}=K_{s,i}$ and $K_{I,j}=K_{s,j}$ has been successfully applied in modeling competitive degradation kinetics of BTEX (Chang *et al*., 1993; Bielefeldt and Stensel, 1999) and chlorinated organic compounds (for a review see Alvarez-Cohen and Speitel, 2001).

The second type of inhibition is *Noncompetitive Inhibition*. In this type of inhibition, an inhibitor can bind to an enzyme at a site different than the active site and change the configuration of the enzyme, thus lowering the maximum utilization rate of the primary substrate. As a result, the presence of a noncompetitive inhibitor will impede binding of the primary substrates with the enzyme, and increasing the primary substrate concentrations will not overcome the effect. The utilization rate of substrate i, which is noncompetitively inhibited by the presence of substrate j, can be described as follows:

$$r_{s,i} = -\frac{k_i S_i X}{\left(K_{s,i} + S_i\right)\left(1 + \frac{S_j}{K_{I,j}}\right)}$$ (Equation 2.4; *noncompetitive inhibition*)

Sometimes inhibition can result from a combination of competitive and noncompetitive substrate inhibition within a multiple substrate system. This type of inhibition is referred to as *Uncompetitive (Mixed) Inhibition* and the expression is shown in the following equation, where inhibition constants $K_{I,j1}$ and $K_{I,j2}$ of substrate j can have the same or different values.

$$r_{s,i} = -\frac{k_i S_i X}{\left(K_{s,i}\left(1 + \frac{S_j}{K_{I,j1}}\right) + S_i\right)\left(1 + \frac{S_j}{K_{I,j2}}\right)}$$ (Equation 2.5; *mixed inhibition*)

2.3.2. Aldehyde Degradation Kinetics

The focus of most previous research studies related to formaldehyde and acetaldehyde degradation was to qualitatively assess the biodegradability of the substrates and to quantify their removals in a given treatment system. Quantitative modeling of the data has been limited in the published literature. The following section summarizes the few studies that have reported kinetic model parameters for formaldehyde or acetaldehyde biodegradation under aerobic conditions.

Formaldehyde Degradation

Bonastre *et al*. (1986) studied aerobic biodegradation of formaldehyde over a concentration range of 100 to 2300 mg/L by activated sludge at different temperatures

(15, 25 and 35°C). Based on the experimental data, the authors discovered that formaldehyde degradation in their systems cannot be described by the Monod model. Instead, the Vavilin model (Equation 2.6) was utilized to derive the kinetic parameters for formaldehyde degradation.

$$-\frac{1}{X}\frac{dS}{dt} = \mu_{\max}\frac{S^n}{K_s^{n-p}\,S_0^p + S^n} \qquad \text{(Equation 2.6)}$$

where X = microorganism concentration (mg/L);

S = formaldehyde concentration (mg/L);

S_0 = formaldehyde initial concentration (mg/L);

μ_{max} = specific rate of formaldehyde consumption (mg/mg/hr);

K_s = kinetic constant (mg/L);

n, p = kinetic constant (dimensionless).

The constant p was determined as 2, and the fitting results of the kinetic data are summarized in Table 2.3. The fitting results indicate that the specific consumption rate of formaldehyde increased with increasing temperature in the activated sludge systems. Moreover, the parameter K_s^{n-2} was reported as a range of fitting values, depending on the fitting values of the parameter n.

Table 2.3. Formaldehyde kinetic parameters determined using the Vavilin model

Kinetic Parameter		Value
μ_{max} (mg /mg/hr)	15°C	0.4 - 0.8
	25°C	1.0 - 2.2
	35°C	4.0 - 6.0
K_s^{n-2} (K_s in mg/L)		1.0 - 2.0
n		1.7 - 2.1

Eiroa *et al*. (2004) investigated aerobic formaldehyde biodegradation in the absence and presence of 12.5% methanol in the batch flasks. Each of the flasks was inoculated with sludge from the aerobic chamber of the wastewater treatment plant at a synthetic resin factory. The authors observed that there was no inhibition of formaldehyde degradation in the presence of high formaldehyde concentrations (up to 3890 mg/L) and the presence of methanol did not inhibit formaldehyde degradation. The initial formaldehyde degradation rates in the absence and presence of methanol suggest that formaldehyde degradation followed first order kinetics. The estimated first order rate constant for formaldehyde degradation with and without the presence of methanol was 0.31 and 0.51 hr^{-1}, respectively. However, no other kinetic parameters were reported in this study, and there was not sufficient information included to estimate k and K_s for use in this research.

Acetaldehyde Degradation

Rajagopalan *et al*. (1998) studied acetaldehyde degradation using activated sludge samples with two test methods: oxygen addition (BOX) and serum bottle (SB). The experimental results were applied to the Monod equation, and the maximum specific degradation rate (k) and half-saturation constant (K_s) were determined. The kinetic parameters for acetaldehyde degradation from the BOX and SB tests at 37°C are summarized in Table 2.4; the k and K_s values determined by the two tests were similar.

Table 2.4. Kinetic parameters for aerobic acetaldehyde biodegradation determined using the results from the BOX and SB tests

Test	k (mg/mg VSS/hr)	K_s (mg/L)
BOX	0.089±0.025	2 ± 1
SB	0.077	1.8

Ibrahim *et al*. (2001a) also determined the kinetic parameters for the biodegradation of acetaldehyde or propionaldehyde using immobilized activated sludge gel beads in the batch reactors. They used the following equation to calculate the specific degradation rate (r_i) of each aldehyde compound:

$$-r_i = -\frac{dC_{il}}{dt} = \frac{k_1 C_{il} X}{1 + k_2 C_{il}} \qquad \text{(Equation 2.7)}$$

where C_{il} = concentration of pollutant i in the gel bead (kmol/m^3);

X = concentration of activated sludge immobilized in the bead (kg MLSS/m^3);

k_1 = specific biodegradation rate constant (m^3/kg MLSS/hr);

k_2 = equilibrium constant (m^3/mmol).

Table 2.5 shows the kinetic data obtained from their batch assays at two temperatures (25 and 30°C). The authors reported that the specific degradation rates of both aldehydes were faster at higher temperatures, and the k_1 value of propionaldehyde was slightly higher than that of acetaldehyde at a given temperature. It is worth noting that k_1/k_2 (mmol/kg MLSS/hr) and $1/k_2$ (mmol/m^3) from this study are equivalent to k and K_s in the Monod equation (Equation 2.1). Thus, it is possible to estimate k and K_s values for both aldehydes based on the data reported by Ibrahim *et al*. (2001a). At 25°C, 0.051 mg/mg MLSS/hr of k and 19.2 mg/L of K_s for degradation of acetaldehyde in the gel beads were then determined.

Table 2.5. Kinetic parameters for acetaldehyde and propionaldehyde biodegradation in immobilized activated sludge gel beads

Compound	Temperature (°C)	k_1 (m^3/kg MLSS/hr)	k_2 (m^3/mmol)
Acetaldehyde	25	2.64	0.0023
	30	3.61	0.0015
Propionaldehyde	25	3.15	0.0030
	30	4.28	0.0022

Pirnie-Fisker and Woertz (2007) utilized the fungi *Exophiala lecanii-corni* and *S. cerevisiae* to determine single substrate degradation rates of several byproducts from corn to ethanol production facilities: acetic acid, lactic acid, acetaldehyde, ethanol, glycerol, formaldehyde and methanol. The batch studies showed that, with the exception of

methanol and formaldehyde, both strains can utilize each of the compounds as the sole carbon and energy source to grow. Monod kinetic parameters for ethanol, acetaldehyde and acetic acid were determined from batch studies. Table 2.6 summarizes the maximum specific substrate utilization rate (k), the half-saturation constant (K_s) and the maximum specific growth rate (μ_{max}) for the two fungi growing on ethanol, acetaldehyde and acetic acid.

Table 2.6. Summary of kinetic parameters for ethanol, acetaldehyde and acetic acid biodegradation by two fungi

Substrate	Microbial Strain	k (mg/mg/hr)	K_s (mg/L)	μ_{max} (hr^{-1})
Ethanol	*E. lecanii-corni*	1.09	0.04	0.072
	S. cerevisiae	1.34	0.02	0.044
Acetaldehyde	*E. lecanii-corni*	0.15	NA	0.023
	S. cerevisiae	0.43	1×10^{-8}	0.071
Acetic acid	*E. lecanii-corni*	2.97	0.11	0.079
	S. cerevisiae	1.33	0.34	0.023

2.4. VAPOR PHASE BIOREACTORS

Biofiltration is commonly used to control odors at wastewater treatment plants and to treat VOC laden waste gas streams emitted from various industries (Ottengraf *et al*., 1986; van Groebestujin and Hessslink, 1994; Swanson and Loehr, 1997). In the biofiltration process, a contaminated gas stream is passed through a packed bed where microorganisms attach. Pollutants in the gas phase can serve as carbon and energy sources for microorganisms and will be converted into water, new biomass and carbon

dioxide under aerobic biodegradation. Three basic types of bioreactors used to control air pollution are biofilters, biotrickling filters and bioscrubbers. Biofilters and biotrickling filters are similar in that microorganisms growing on the packing media degrade pollutants from the gas streams. The major difference between the two bioreactors is that a liquid stream containing nutrients is supplied and recirculated continuously in biotrickling filters while nutrient solutions are added periodically to biofilters. In bioscrubbers, pollutants are transferred into the liquid phase from the gas phase in a scrubber unit, and subsequently degraded within a separate activated sludge unit of the bioscrubber. Both biofilters and biotricking filters can be utilized to treat waste gases containing aldehydes, such as those generated during the production of corn-based ethanol.

2.4.1. Aldehyde Biofiltration

Although biofiltration effectively treats air pollutants, studies associated with aldehyde biofiltration are limited. Experiments using a vapor phase bioreactor to treat aldehyde concentrations ranging from 10 to 100 ppm_v have been reported in the literature. The following section summarizes the studies regarding aldehyde biofiltration.

Prado *et al*. (2004) investigated elimination capacity of formaldehyde and methanol in four different biofilters and biotrickling filters. The inlet formaldehyde loading to the bioreactors was maintained at approximately 15 $g/m^3/hr$ at an empty bed contact time (EBCT) of 80 seconds. After one week of operation, formaldehyde removal was inhibited when the methanol loadings were increased from 0.5-26 $g/m^3/hr$ to 374-644 $g/m^3/hr$. Although the presence of high methanol loadings affected formaldehyde elimination in the bioreactors in this study, Prado *et al*. (2006) later

reported that methanol loadings up to 600 $g/m^3/hr$ had no effects on removal of 50 $g/m^3/hr$ formaldehyde in another biotrickling filter. The authors attributed this observation to the different system operating periods between two studies. The biotrickling filter used in Prado *et al*. (2006) had been continuously treating mixtures of formaldehyde and methanol for 8 months, while the bioreactors examined in Prado *et al*. (2004) were in their startup periods when inhibition of formaldehyde degradation by methanol was observed.

Garner (2002) also demonstrated that high removal efficiencies of formaldehyde (>95%) and methanol (>90%) were achieved simultaneously in a pilot-scale biofilter treating 42,000 cfm of waste gas streams emitted from a particleboard manufacturing facility. However, the influent concentrations of both pollutants were not reported in this study so it is difficult to make comparisons with the studies completed by Prado *et al*. (2004 & 2006).

Ibrahim *et al*. (2001a) studied single aldehyde biofiltration using acetaldehyde and propionaldehyde in two separate columns. The columns were packed with immobilized activated sludge gel beads and operated at an EBCT of less than 5 seconds. During the nearly 30 day biofiltration test, the influent concentration of each aldehyde was increased stepwise from 10 to 100 ppm_v, and each concentration was maintained for several days before stepping up to the next concentration. The results show that removal of both aldehydes decreased with their increasing influent concentration. The acetaldehyde removal dropped from 100% to 60% when its loading was increased from 14 to 135 $g/m^3/hr$. Similarly, the propionaldehyde removal decreased from 100% to 70% when the loading was increased from 18 to 143 $g/m^3/hr$. The authors concluded that the aldehyde removals decreased because biodegradation rates of the gel beads were approaching their maximum. Ibrahim *et al*. (2001b) also examined biofiltration of the

aldehyde mixtures using the same column setup. The results suggest that removal of the aldehyde mixtures decreased with increasing total influent aldehyde concentrations, and the presence of propionaldehyde exerted an adverse effect on acetaldehyde removal in the column.

2.4.2. Parameters Affecting Biofilter Performance

The characteristics of a waste gas stream will affect biofilter performance and may need to be adjusted in order to achieve desired pollutant removal efficiencies in a biofilter. Several parameters including substrate mixtures, pollutant loading rates, nutrient supply, operating temperature, pH and moisture content are critical to biofilter performance. Among these operating parameters, substrate mixtures, temperature and pH are likely to play important roles in the biofiltration of ethanol plant emissions since the waste gases contain multiple pollutants including organic acids and could potentially be emitted at elevated temperatures. However, pollutant loading rates, nutrients and moisture content can also potentially affect the performance of a biofilter in an ethanol plant application. The following sections summarize how these parameters affect pollutant biodegradation. While many of the pollutants discussed in the following sections are not being studied in this research, the effects that these parameters have on pollutant degradation were assumed to be generally applicable to biofilter performance and were used to guide the biofilter study performed in this research.

Substrate Mixtures

The composition of actual waste gas streams is usually complex and varies with industry. It is difficult to predict whether a microbial community will be able to degrade

all the components of a mixture of substrates even if each substrate is biodegradable individually. The presence of a more biodegradable compound can enhance or inhibit the degradation rate of a less biodegradable compound depending on the microbial culture and metabolic pathways.

Stanley *et al*. (1993) investigated the impact of acetaldehyde on yeast growth in an ethanol-containing medium; the results indicated addition of small amounts of acetaldehyde to the medium reduced the lag phase for yeast growth on ethanol. However, when more than 0.3 g/L of acetaldehyde was present in the medium, it inhibited yeast growth. Bhattacharya and Baltzis (2001) showed that the presence of ethanol increased the degradation rate of o-dichlorobenzene by enhancing biomass growth. Similarly, Lovanh *et al*. (2002) also reported ethanol in low concentrations (1 mg/L) increased benzene removal, but high concentrations of ethanol (>5 mg/L) inhibited the degradation rate of benzene due to oxygen limitations in the aqueous chemostat system. Mohseni and Allen (2000) reported that methanol suppressed the growth of the α-pinene degrading community in the biofilters; however, the methanol removal was not affected for α-pinene loadings ranging from 15 to 45 $g/m^3/hr$.

The studies discussed above offer a wide range of conclusions on the impact of substrate mixtures on pollutant removals in a system. The extent to which substrate interactions affect pollutant removals appears to depend on operating parameters such as pollutant types and loadings.

Pollutant Mass Loading

Pollutant mass loading rate (QC/V, $g/m^3/hr$) of a vapor phase bioreactor is usually expressed in terms of gas flow rate (Q), pollutant inlet concentration (C), and packed bed volume (V). Biofilters can effectively treat waste gas streams containing pollutants in a

typical concentration range of 10-160 g/m^3/hr. Higher pollutant mass loadings can lead to lower removal efficiencies, biomass clogging of packing materials and emissions of toxic or acidic intermediates (Swanson and Loehr, 1997). One case of an overloaded biofilter treating a total ethanol loading of 156 g/m^3/hr was reported by Devinny and Hodge (1995). The overloaded biofilter experienced breakthroughs of ethanol and accumulations of its byproducts (acetaldehyde, acetic acid and ethyl acetate) after one month of high ethanol removals. They postulated that the oxidation rate of ethanol in the biofilter was faster than the degradation rates for the intermediates produced in the biodegradation. The accumulation of intermediates caused a reduction in pH in the upper two-thirds of the biofilter which further inhibited pollutant degradation. A similar observation was reported in a yeast-based biofilter (Christen *et al*., 2002). A higher gas flow rate and shorter EBCT yielded a higher ethanol mass loading rate which detrimentally affected biofilter performance. Low final pH values and the accumulation of two ethanol degradation byproducts, acetaldehyde and ethyl acetate, in the gas effluent were reported.

Nutrient Supply

Nutrient limitation may be responsible for reduced biodegradation rates in a biological treatment system. To study effects of operating parameters other than nutrient supply, it is important to assure that no nutrient limitation occurs in the system. Microorganisms require carbon, nitrogen, phosphorus, oxygen, and hydrogen along with some other nutrients and trace elements for biomass growth and cell function maintenance. Grady and Lim (1980) suggest that the ratio of total carbon to nitrogen and phosphorous (C:N:P)of at least 100:5:1 is generally necessary to maintain microbial activity without serious nutrient limitation. Nitrogen availability is especially important

for microbial growth and successful biodegradation. Inorganic forms of nitrogen, such as nitrate and ammonia, are more available than organic nitrogen for microbial growth (Gribbins and Loehr, 1998). Corsi and Seed (1995) found that a minimum of 200 mg/kg total available nitrogen levels was required to obtain high toluene removal efficiencies in compost biofilters. Gribbins and Loehr (1998) reported that microbially available nitrogen affected biofilter performance and the soluble nitrogen concentration in the media had to be above about 1000 mg N/kg dry weight for optimal operation of a biofilter. Ammonia was found to be distributed more uniformly throughout the packing media than nitrate. One possible reason for this difference is that the positive ammonium ion binds to the compost media, so it resists leaching better than nitrate when water is added to prevent media drying. In another study, high concentrations of ammonia had an inhibitory effect on biofiltration while nitrate at high concentrations did not affect the methanol removal rate (Yang *et al*., 2002).

The effect of nitrogen availability on VOC degradation has also been observed when a complex mixture of pollutants is present in a waste gas stream. Song *et al*. (2003) found that virtually no toluene or xylene was removed from a paint VOC mixture under nitrogen limited conditions even though methyl propyl ketone (MPK), n-butyl acetate (NBA) and ethyl ethoxy proprionate (EEP) were removed completely. However, when nitrogen was supplied in excess, nearly all of the VOCs could be removed.

Temperature

The temperatures of waste gas streams emitted from ethanol production facilities are dependent on the processes and their downstream units. For example, the temperature of waste gases from the fermentation and distillation scrubbers is in the

range of 15 to 35°C. The temperature of waste gases from the DDGS dryers ranges from 100 to 140°C prior to treatment in a scrubber or cyclone; even after treatment, the waste gas stream temperature can still range from 35 to 55°C. The temperature of mesophilic biofiltration is typically maintained between 20 and 40°C (Leson and Winer, 1991), while thermophilic biofiltration is operated at a gas temperature above 40-45°C. Maintaining a constant moisture content in a biofilter at mesophilic temperatures is easier than at thermophilic temperatures. Also, the usage life of natural packing materials, such as compost, is longer for mesophilic biofiltration.

Although mesophilic biofiltration has been successfully applied to treat a variety of industrial emissions, it has also been reported that thermophilic biofiltration systems were utilized to treat VOCs including BTEX (Matteau and Ramsay, 1999; Strauss *et al*., 2004), alcohols (Cox *et al*., 2001; Kong *et al*., 2001) and hydrogen sulfide (Datta *et al*., 2007). Although thermophilic biofiltration can reduce the costs associated with cooling a waste gas stream, some issues still must be overcome to achieve desired pollutant removals in thermophilic bioreactors. For instance, it is challenging to maintain a constant humidity across packing materials in biofilters at higher temperatures. Moreover, increasing volatility and decreasing solubility of pollutants and nutrients occur with increasing temperature (Kennes and Viega, 2002).

Among ethanol plant emissions, dryer off-gases will likely pose the greatest potential temperature issue for biofiltration (see Table 2.1). Based on the current pollution control devices installed in ethanol plants, dryer off-gases are primarily sent to particulate matter removal systems such as scrubbers or cyclones. The temperature of the gas streams exiting these systems are reported to be in the range of 35°C to 55°C; therefore, this type of waste gas might need to be cooled to some extent for mesophilic biofiltration. Cooling inlet gas streams can be achieved using heat exchange devices or

pretreatment systems upstream of biofiltration systems. For instance, wet scrubbers used to remove PM from waste gases in ethanol plants can also help to reduce gas phase temperatures to within an appropriate temperature range for mesophilic biofiltration operation (Ferranti and Conca, 2000). It is also important to note that the temperature of gas streams exiting fermentation/distillation scrubbers at ethanol production facilities typically range from 15 to 35°C, so temperature should not be an issue for treating these types of waste gases.

pH

The ideal pH range for microbial growth depends on the microbial species present. To effectively remove organic pollutants via biofiltration, the optimal pH values typically range from 6 to 9 for most bacterial biofilters. Although fungal biofilters are known to tolerate lower pH values, extremely acidic conditions will still have a significant impact on biofilter performance (Christen *et al*., 2001; Terán Pérez *et al*., 2002).

Microbial metabolism in biofilters is usually accompanied by the production of acidic metabolites such as inorganic acids (sulfuric acid, nitric acid or hydrochloric acid) and/or organic acids (Swanson and Loehr, 1997). Decreased biofilter performance due to the accumulation of acetic and formic acids has been reported by several researchers for ethanol and methanol-degrading biofilters, respectively (Devinny and Hodge, 1995; Swanson and Loehr, 1997; Christen *et al*., 2002; Terán Pérez *et al*., 2002; Prado *et al*., 2004 & 2006). Biofilter acidification can likely be prevented by lowering the pollutant mass loading or decreasing the gas flow rate (Devinny and Hodge, 1995). Using nutrient solutions or packing materials to provide a higher buffer capacity, selecting an

appropriate nitrogen source (e.g., use ammonia instead of ammonium sulfate) (Terán Pérez *et al*., 2002), or adjusting pH on a regular basis (Prado *et al*., 2004) may also help.

Moisture Content

Biofiltration performance is also affected by the moisture content of the packing materials, which is a function of inlet gas temperature and water content in the waste gases. The water content in waste gases emitted from ethanol plants varies with the emission sources. For instance, the DDGS dryer off-gases contain 40-60% water by volume, while the post-scrubber gas streams usually consist of 5-12% water by volume. It is important to ensure that the waste gas stream treated in a vapor phase bioreactor contains adequate water content so it does not cause the bioreactors to dry out, or conversely, over-wet the packing materials inside the bioreactor. Overly wet biofilters will result in high backpressures, low gas retention time, oxygen transfer problems, creation of anaerobic zones and nutrient wash out (Swanson and Loehr, 1997). On the other hand, poor humidity control leads to drying and poor pollutant elimination capacity in biofilters.

Krailas *et al*. (2000) investigated the effect of water on methanol elimination in biofilters. It was found that when the moisture content in the compost-based biofilter was below 35% by weight, microbial activity was impaired. Moisture contents of 40 to 60% by weight should be maintained for optimal biofilter operation (Ottengraf *et al*., 1986). However, different packing media require slightly different moisture contents. For example, Moe and Irvine (2000) suggested a 65% moisture content for hydrophilic polyurethane foam packing media.

2.4.3. Hybrid Systems Integrating Vapor Phase Bioreactors

Although various treatment technologies can be used individually to treat ethanol plant emissions, it may be more cost-effective to use a hybrid system. Integrating biofiltration with another treatment technology to treat air emissions has gained more attention in industry. For example, a coupled pilot system consisting of a prescrubber followed by a vapor phase bioreactor was used to successfully treat formaldehyde in the exhaust air from a composite panel board facility (Ferranti and Conca, 2000). Prior to entering the prescrubber unit of the hybrid system, the exhaust air was passed through a filter to remove PM and then a thermal exchange device to reduce the inlet gas temperature from 90 to 65°C. The gas temperature exiting the prescrubber and entering the bioreactor was 35°C. The prescrubber not only served as a humidifier/cooler but also removed PM from the gas streams. A constant, neutral pH was maintained in the prescrubber and in the bioreactor. The results from the 20-week pilot tests indicated that the hybrid system removed greater than 95% of the formaldehyde from the industrial exhaust air.

Kastner and Das (2005) compared the removal efficiencies of the VOCs emitted from three poultry-rendering facilities using absorption and biofiltration. Conventional wet scrubbers using a ClO_2 solution exhibited low overall removals efficiencies (23-64%) due to their lack of reactivity with aldehydes. In contrast, a biofilter was able to achieve overall VOC removals of 71-99%. It is interesting to note that the wet scrubber inlet temperature of 45-60°C was reduced to 30-40°C after the waste gas streams passed through the scrubber. Therefore, they suggest that a hybrid process combining a wet scrubber and biofilter in series could improve overall VOC removals and process stability.

Bangs (2005) conducted a series of scrubber experiments to evaluate removal of acetic acid and acetaldehyde in a wet scrubber. Three different scrubbing solutions were evaluated for their ability to remove acetic acid from the gas phase via absorption: water, 0.1N NaOH solution and 0.25N NaOH solution. The wet scrubber was found to be efficient at removing acetic acid at pH levels above approximately 6.5. Acetaldehyde passed through the water scrubber rapidly due to its high Henry's Law constant ($atm \cdot m^3/mol$). However, acetaldehyde was found to be degraded in a biofilter at inlet concentrations ranging from 18 to 197 ppm_v. The result implies that it is feasible to use a coupled system composed of a scrubber and a biofilter to treat a mixture of hydrophilic and hydrophobic compounds such as those found in the emissions from ethanol plants.

2.4.4. Potential Pretreatment for Biofiltration of Ethanol Facility Emissions

Biofiltration is an attractive treatment option for ethanol plant emissions for several reasons. Compared to incineration, it is relatively inexpensive to operate and can achieve high removal efficiencies while generating less greenhouse gases. Although it is a promising air pollution control technology, biofiltration of ethanol plant emissions can be problematic due to the complex characteristics of the waste gas streams. First of all, substrate inhibition or competition effects may limit the degradation of certain substrates and lead to low overall VOC removals. As discussed in Section 2.1.2, some waste gas emissions downstream of drying processes can potentially be found at elevated temperatures (35-55°C). Also, due to the presence of acidic pollutants in the ethanol off-gases, low pH conditions might pose a challenge to the biodegradation of ethanol plant emissions. Finally, PM from a variety of emission sources can clog the packing media of biofilters.

It may be more effective to condition waste gas streams prior to introducing them to biofilters, since the gas phase only resides in biofilters for a relatively short period of time – on the order of seconds to minutes. To apply biofiltration to treat the HAPs produced at ethanol production facilities, pretreatment requirements for ethanol plant emissions prior to biofiltration may include:

- PM control to prevent clogging in a bioreactor system by passing the waste streams through a wet scrubber, cyclone or baghouse.
- Neutralizing the waste gas streams in a wet scrubber to prevent microorganisms in the downstream biofilter from being inactivated at low pH.
- Removing excess heat from the waste gas streams using heat exchangers or wet scrubbers to obtain desired inlet gas temperatures for the biofilter.

2.5. BIOFILTER MODELING

To more accurately predict treatment system performance, efforts have been made to establish biofilter models for several scenarios (Ottengraf and van den Oever, 1983; Zarook *et al*., 1993; Deshusses *et al*., 1995a & 1995b; Hodge and Devinny, 1995; Mohseni and Allen, 2000). The biofilter models published in the literature are based on several simplifying assumptions that vary from one modeling scenario to another. Therefore, some limitations exist in applying a model developed for a specific scenario to different biofilter systems (Kennes and Veiga, 2002). Oxygen limitation, for example, is considered in some models (Zarook *et al*., 1993 & 1997) while others assume oxygen is present in excess (Deshusses *et al*., 1995a & 1995b; Hodge and Devinny, 1995; Mohseni and Allen, 2000).

For pollutant degradation to occur in a bioreactor, the pollutant must be transferred from the gas phase to the biofilm. Figure 2.4 represents the biodegradation of pollutants in a vapor phase bioreactor (VPB). Several biofilter models that have been developed to describe single and multiple substrate systems are summarized in the following sections.

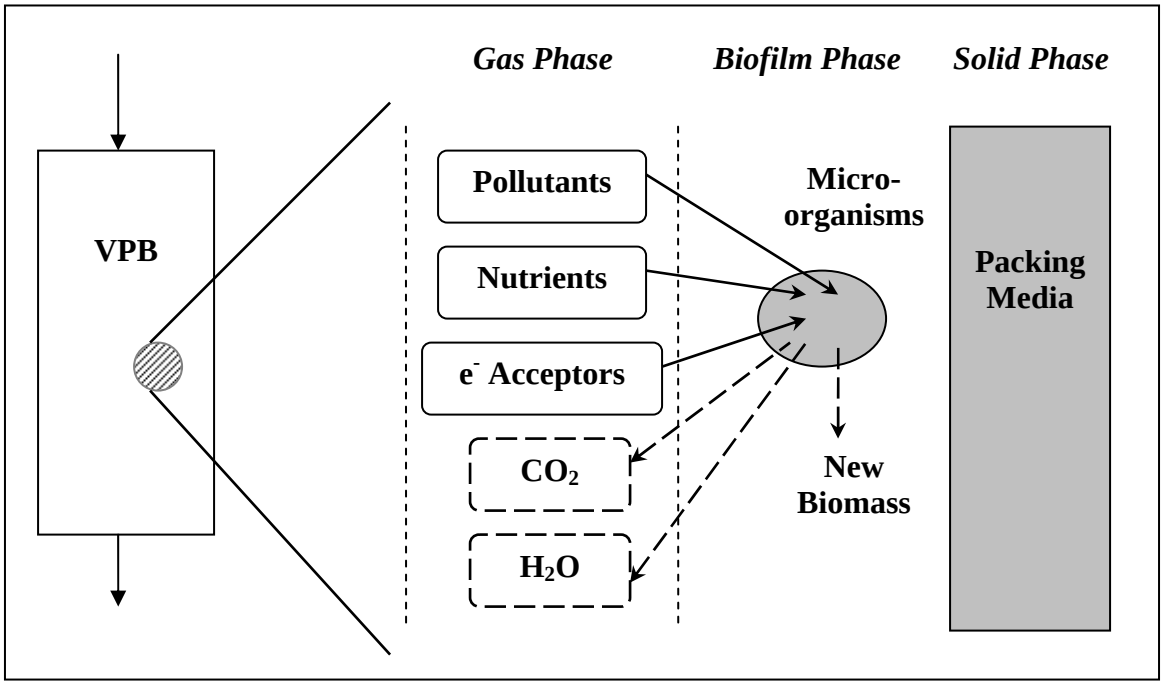

Figure 2.4. Biodegradation of pollutants in a VPB (Gunsch, 2004).

2.5.1. Single Substrate Biofiltration Models

Hodge and Devinny (1995) developed a model for ethanol biofiltration using a two-phase system: the gas phase and the water/solids phase. The model treats the water and solids as a single phase; therefore, it ignores phenomena such as diffusion in the water/biofilm and adsorption at the interface between the water and the solids. Since

the solid phase is accounted for in the model, the characteristics of the packing media including adsorptive capacity, porosity and buffer capacity are required input parameters of the model. The mass balance equation describing ethanol mass transfer in the gas phase, shown in Equation 2.8, includes pollutant dispersion and advection in the gas phase and pollutant transfer from the gas phase into the water/solids phase.

$$\frac{\partial C}{\partial t} = D\frac{\partial^2 C}{\partial x^2} - V\frac{\partial C}{\partial x} - \left(\frac{1-\theta}{\theta}\right)\left[k(k_h C - C_{ads})\right] \qquad \text{(Equation 2.8)}$$

where C = ethanol concentration in the gas phase (mg/cm^3);

C_{ads} = ethanol concentration in the water/solids phase (mg/cm^3);

D = ethanol dispersion coefficient in the gas phase (cm^2/hr);

x = distance of travel in filter (cm);

V = axial interstitial velocity of the gas stream (cm/hr);

θ = filter material porosity at field capacity;

k = ethanol transfer rate constant (hr^{-1});

k_h = equilibrium value for the ratio of ethanol concentration in the water/solids phase to its gas-phase concentration.

In the water/solids phase, two mass balance equations are written to account for ethanol biodegradation (Equation 2.9) and CO_2 production (Equation 2.10). The rate at which the processes occur is assumed to follow first-order kinetics.

$$\frac{\partial C_{ads}}{\partial t} = k(k_h C - C_{ads}) - bC_{ads} \qquad \text{(Equation 2.9)}$$

$$\frac{\partial [CO_2]_{ads}}{\partial t} = k_c (k_{hc} [CO_2] - [CO_2]_{ads}) + R_c (bC_{ads}) \quad \text{(Equation 2.10)}$$

where b = biodegradation constant (hr^{-1});

$[CO_2]_{ads}$ = CO_2 concentration in the water/solids phase(mg/cm^3);

$[CO_2]$ = CO_2 concentration in the gas phase (mg/cm^3);

k_c = CO_2 transfer rate constant (hr^{-1});

k_{hc} = equilibrium value for the ratio of carbon dioxide concentration in the water/solids phase to its gas-phase concentration;

R_c = ratio of mass of CO_2 released to mass of ethanol degraded.

Tang *et al*. (1996) proposed a biofilm model for the treatment of triethylamine (TEA) in waste gases. In this model mass balances over two phases, bulk gas phase and biofilm, were carried out in the modeling processes under the general assumptions described in Section 2.5.3. An effective biofilm thickness (δ_e) (assumed to be 15% of actual biofilm thickness) was used to correct for the thickness of the anaerobic biolayer, which does not contribute to aerobic biodegradation of TEA. At steady state, the mass balance for the biofilm (Equation 2.11) can be written as the flux of the pollutant into the biofilm equal to the pollutant biodegradation rate, where the biodegradation rate can be described by the degradation kinetic expression proposed by Luong (1987). In the gas-phase mass balance (Equation 2.12), the advection of the pollutant in the gas phase is equal to the pollutant flux into the biofilm.

$$D_e \frac{d^2 S_l}{dx^2} = \frac{X_V}{Y} \frac{\mu_{max} S_l}{K_s + S_l} \left[1 - \frac{S_l}{S_{lm}} \right]^n \quad \text{(Equation 2.11)}$$

$$U_g \frac{dS_g}{dz} = A_s D_e \left[\frac{dS_l}{dx} \right] \qquad \text{(Equation 2.12)}$$

where D_e = effective diffusion coefficient (m^2/hr);

S_l = pollutant concentration in the biofilm (g/m^3);

S_{lm} = maximum pollutant liquid-phase concentration above which microbial growth is completely inhibited (g/m^3);

S_g = pollutant concentration in the gas phase (g/m^3);

X_v = biofilm dry density (g/m^3);

Y = yield coefficient (g biomass/g substrate);

μ_{max} = maximum specific growth rate (hr^{-1});

K_s = half-saturation constant (g/m^3);

U_g = superficial gas velocity (m/hr);

A_s = specific surface area (m^2/m^3);

x = distance in the biofilm (m);

z = height of the biofilter (m);

n = kinetic constant.

Ibrahim *et al*. (2001a) developed a model to describe single-aldehyde (acetaldehyde or propionaldehyde) biofiltration in a column packed with immobilized activated sludge gel beads and inert hollow plastic balls. The assumption made in the model was that the rate of pollutant biodegradation in the gel beads is much lower than that of pollutant diffusion through the gel beads. As a result, the pollutant flux from the gas phase to the gel beads is assumed to be equal to the pollutant biodegradation rate in

the gel beads, shown in Equation 2.13. It is important to note that no mass transfer effects were considered in the model.

$$-U_G \frac{dC_{ig}}{dz} = \frac{k_1 C_{il}}{1 + k_2 C_{il}} \eta X \left(1 - \varepsilon - \varepsilon_p\right) \qquad \text{(Equation 2.13)}$$

where U_G = superficial gas velocity (cm/s);

C_{ig} = concentration of component *i* in the gas phase (kmol/m^3);

C_{il} = concentration of component *i* in a gel bead (kmol/m^3);

z = height of a packed bed (cm);

k_1 = specific biodegradation rate constant of component *i* (m^3/(kg MLSS-hr));

k_2 = equilibrium constant (m^3/mmol);

ε = fractional void of packed bed;

ε_p = fractional volume of hollow plastic balls;

X = activated sludge concentration in gel beads (kg MLSS/m^3).

2.5.2. Binary Substrate Biofiltration Models

Ottengraf and van den Oever (1983) proposed a theoretical model describing the elimination of pollutants in a biofilter bed. It is assumed that pollutants transfer from the gas phase to the biofilm by advection so the mass balance equation for the gas phase is similar to Equation 2.12. Moreover, pollutant elimination in the biofilm is assumed to follow zero-order kinetics. Two scenarios are distinguished in this model: (1) reaction limitation applies when the biofilm is fully active and hence the biodegradation rate controls the overall removal efficiency, and (2) diffusion limitation applies when

pollutants can only diffuse to a certain depth of the biofilm due to lower gas concentrations and hence the overall removal efficiency is controlled by the diffusion rate.

Deshusses *et al*. (1995a & 1995b) developed a multi-layer diffusion reaction model to describe both the steady- and transient-state behavior of biofilters. Three main phases are modeled within each layer: the gas phase, the biofilm and the liquid volume within the packing media are considered for mass balances. The mass balance equations for the biofilm and the gas phase are similar to Equations 2.11 and 2.12, respectively. The biofilm is further divided into four subdivisions and it is assumed that there is no net biomass growth. In the liquid volume where sorption occurs, it is assumed no biological activity and pollutant mass transfer coefficient in the sorption volume equal to that in the biofilm. Experimental biofiltration results for methyl ethyl ketone (MEK) and methyl isobutyl ketone (MIBK) were compared with model simulations, which assumed Monod type kinetics and competition between MEK and MIBK. The model provided adequate predictions for the removals of a range of MEK and MIBK as a single pollutant at most steady-state and dynamic situations. However, when the model was applied to the removals of the MEK/MIBK mixtures, agreement between experimental data and model predictions was less satisfactory than single pollutant removal. The authors suggested that it is necessary to apply more appropriate quantification of the inhibition kinetics of mixed MEK/MIBK biodegradation to the model.

Mohseni and Allen (2000) developed a model describing the simultaneous biodegradation of a hydrophilic (methanol) and a hydrophobic (α-pinene) VOC. Instead of using conventional air/water partition coefficients (normally the reciprocal of Henry's Law constants), experimentally determined air/biofilm partition coefficients were used in the model to more accurately describe the enhanced partitioning of hydrophobic

compounds to the biofilm. The governing mass balance equations describing the removal of methanol (subscript m) and α-pinene (subscript p) in the biofilm at steady state are shown in Equations 2.14 and 2.15, respectively. The parameters X, Y, μ_{max} and K_s used in the equations have been previously defined for Equations 2.11 and 2.12.

$$D_{e(m)} \frac{d^2 S_m}{dx^2} = r_{s(m)} = \frac{X}{Y_m} \frac{\mu_{max(m)} S_m}{K_{s(m)} + S_m} \qquad \text{(Equation 2.14)}$$

$$D_{e(p)} \frac{d^2 S_p}{dx^2} = r_{s(p)} = \alpha \frac{X}{Y_p} \frac{\mu_{max(p)} S_p}{K_{s(p)} + S_p} \qquad \text{(Equation 2.15)}$$

and $\alpha = \left(\frac{1}{1 + (C_m / K_i)^2} \right)$

where D_e = substrate effective diffusivity in the biofilm at 40°C (m^2/hr);

r_s = substrate utilization rate (kg/(m^3-hr));

S = substrate concentration in the biofilm (g/m^3);

C = substrate concentration in the gas phase (g/m^3);

K_i = inhibition constant of methanol (g/m^3).

The authors proposed that different microbial communities degraded the two compounds and the presence of methanol inhibited the α-pinene degrading microorganisms, but the presence of α-pinene did not affect methanol removal. The results showed that methanol removal followed first-order kinetics and noncompetitive inhibitory kinetics better described α-pinene degradation. As for the mass balance of the two pollutants over the gas phase, it was described by an equation similar to Equation

2.12. Sologar *et al*. (2003) also reported that the biodegradation of methanol in the presence of hydrogen sulfide can be described by a first-order kinetic expression. It was found that hydrogen sulfide degradation was not affected by the presence of methanol and could be described by Monod kinetics. Both a reaction-limited model (similar to the one proposed by Ottengraf and van den Oever, 1983) and a biofilm-based model (Mohseni and Allen, 2000) described the binary-substrate system well.

Zarook *et al*. (1993) used similar assumptions to those described above, but took oxygen limitation into consideration in developing a mathematical model to describe methanol biofiltration. The mass balances were performed on the biofilm (an equation similar to Equation 2.11) and the gas phases (an equation similar to Equation 2.12). The specific growth rate was dependent on both methanol and oxygen concentrations and was described by Andrews kinetics (Equation 2.2) in the presence of excess of oxygen. For a binary-substrate system under oxygen limited and transient state conditions, the model described in Zarook *et al*. (1993) was modified to include adsorption to the solid phase (Zarook *et al.*, 1997). Mass balances were developed for benzene, toluene and oxygen in each of the three phases (gas, biofilm and solid). The mass balance equations over the biofilm and the gas phase are similar to Equations 2.11 and 2.12, respectively. The mass balance equation for the solids phase is described using an equation similar to Equation 2.8 with the adsorption isotherm of benzene and toluene considered. Degradation of benzene was described by Monod kinetics in the absence of toluene and the presence of excess oxygen, and the Andrews kinetic model described toluene removal in the absence of benzene and the presence of excess oxygen.

Ibrahim *et al*. (2001b) also studied the biofiltration of a mixture of acetaldehyde and propionaldehyde using immobilized activated sludge gel beads. The model, which was originally developed for single aldehyde biofiltration (Ibrahim *et al*., 2001a), was

modified to account for the mixture effect by adding an inhibitory term to the original Monod type kinetic expression in the mass balance with respect to each aldehyde compound. The model predictions for the mixed aldehyde biofiltration in the packed column agreed well with the experimental results, even though mass transfer effects are not considered in this model. However, mass transfer phenomena like diffusion can be significant in biofilter systems with different packing media when treating a similar waste gas stream.

2.5.3. Summary of Biofiltration Models

While some assumptions differ among the biofiltration models, many of the same general assumptions are made in most of the models discussed above. These general assumptions are summarized as follows:

- Biofiltration operation is at steady state and the gas flow pattern is plug flow.
- Gas phase mass transfer resistance is negligible.
- The concentration of substrate at the gas/biofilm interface is in equilibrium with its gas phase concentration.
- Substrates and nutrients are transported by diffusion within the biofilm.
- The biofilm thickness and density, as well as moisture content and porosity of packing media are homogenous across the biofilter.
- The target pollutant is the only growth-limiting substrate.

While the general assumptions of the models remained the same, there were differing assumptions used in the development of each model. Based upon this evaluation, the governing equations used by Mohseni and Allen (2000) to describe simultaneous degradation best represent the experimental conditions of this research.

The substrate specific degradation parameters used in these governing equations will be determined during the batch reactor studies.

Chapter 3: Batch Kinetic Experiments

The main goal of this research was to develop a biofiltration system for removing aldehyde mixtures from corn-derived ethanol plant emissions. To this end, the experimental plan included collection of batch kinetic data and laboratory scale biofilter data for single and multiple substrate systems containing acetaldehyde, formaldehyde, ethanol and acetate. The aldehydes were selected based on a review of emissions data. Ethanol and acetic acid are also present in ethanol plant emissions and are reported as byproducts of aldehyde degradation. Batch biodegradation experiments were conducted to characterize the key parameters affecting degradation of the substrates, verify the biodegradation pathways of the two aldehydes and characterize the kinetics of biodegradation. In this chapter, the effects of dissolved oxygen (DO) concentration and pH are examined. In addition, the effect of enrichment condition on non-aldehyde substrate (ethanol or acetate) degradation was also evaluated. Finally, the potential for substrate inhibition by either co-substrates or biodegradation byproducts is also evaluated in a series of batch kinetic experiments.

3.1. MATERIALS AND METHODS

3.1.1. Chemicals and Microorganisms

Chemicals

The properties of the four compounds studied in this research are summarized in Table 3.1. Comparison of the two aldehydes shows that acetaldehyde is significantly more soluble and more volatile than formaldehyde. In addition, formaldehyde has a strong tendency to polymerize at room temperature. As a result, commercial

formaldehyde solutions are usually supplied at concentrations below 40% (w/w) dissolved in water, with or without 10 to 15% methanol added as a stabilizer to prevent formaldehyde polymerization. A 16% methanol-free formaldehyde solution of Electron Microscopy (EM) grade manufactured by Ted Pella Inc. was used in the batch experiments. The other three compounds (acetaldehyde, ethanol and acetic acid) were of ACS reagent grade (> 99.5%) and obtained from Sigma-Aldrich (St. Louis, MO).

Table 3.1. Properties of the selected ethanol plant pollutants

Compound	Formula	Molecular Weight (g/mol)	Density (g/ml)	Solubility (mg/L)	Henry's Law Constant [c] ($atm \cdot m^3/mol$)
Formaldehyde	CH_2O	30.03	1.090	5.5×10^{5} [a]	3.37×10^{-7}
Acetaldehyde	C_2H_4O	44.05	0.789	10^{6} [b]	6.67×10^{-5}
Ethanol	C_2H_6O	46.07	0.788	10^{6} [b]	5.00×10^{-6}
Acetic Acid	$C_2H_4O_2$	60.05	1.049	10^{6} [b]	1.00×10^{-7}

[a] Chemfinder (2007)
[b] Yaws (1999)
[c] Gaffiney *et al*. (1987)

Microbial Consortium

To reduce the potential for substrate inhibition during microorganism enrichment each substrate was enriched separately. Previous research indicates that this approach preserves microbial diversity (Park, 2004). Thus, the aldehyde-degrading consortium used in this research was developed by combining formaldehyde- and acetaldehyde-degrading microbial cultures. Each aldehyde-degrading microbial culture was enriched from an activated sludge sample obtained from the Walnut Creek Wastewater Treatment Plant in

Austin, TX. One (1) mL of activated sludge and 100 mL of phosphate buffer solution (PBS) (Table 3.2) were added to a 250-mL amber glass bottle and then sealed with Teflon tape and a Mininert® valve. After injection of 100 mg/L of one of the aldehyde compounds through the valve, each bottle was placed on a shaker table at a speed of 100 rpm and incubated at ambient temperature (21-23°C). Once complete substrate degradation was observed in a bottle, the biomass solution was aerated for 20 minutes using 0.2μm-filtered air before the same substrate was re-injected into the bottle. This process was repeated several times and the formaldehyde- and acetaldehyde-degrading microbial cultures were then combined in 1:1 ratio (v/v) to form an aldehyde-degrading consortium.

Table 3.2. Composition of phosphate buffer solution (PBS)

Phosphate buffer solution (g/L)		Trace element solution* (g/L)	
KH_2PO_4	2.72	$MgSO_4 \cdot 7H_20$	50
Na_2HPO_4	1.42	$CaCl_2 \cdot 2H_2O$	14.7
$(NH_4)_2SO_4$	3.96	H_3BO_3	2.86
Trace element solution*	1mL/L	$MnSO_4 \cdot H_2O$	1.54
		$FeSO_4 \cdot 7H_2O$	2.5
		$CuCl_2 \cdot 2H_2O$	0.027
		$ZnSO_4 \cdot 7H_2O$	0.044
		$CoCl_2 \cdot 6H_2O$	0.041
		$NaMoO_4 \cdot 2H_2O$	0.025
		$NiCl_2 \cdot 6H_2O$	0.020

3.1.2. Protocols for the Batch Experiments

Enrichment of the aldehyde-degrading consortium used in each batch experiment was performed by transferring 5 mL of an inoculum solution to a 2L gas-tight glass bottle

containing 800 mL of sterile PBS. Filtered air was used to aerate the PBS daily before adding substrate(s) to the bottle during the enrichment period of 3 to 5 days. For each experiment, biomass was harvested through centrifugation, washed and mixed with sterile and pre-aerated PBS to obtain the desired solid concentration. The biomass solution was then transferred to a 500 mL gas-tight, headspace-free syringe (VICI, Magnum syringe) containing a stir bar for complete mixing. The experimental method was developed and described by Aziz (1997). A run time of 3 hours or less was applied to each set of batch experiments to ensure that the kinetics were representative of the physiological state of the original biomass. Initial and final biomass concentrations were measured to confirm that the amount of microbial growth over the course of an experiment was less than 10 percent. Dissolved oxygen (DO), pH, and volatile suspended solids (VSS) were measured prior to the addition of any substrates, and at the end of each experiment. Periodically, liquid samples were withdrawn from the tip of the 500 mL syringe using a 10 mL gas-tight syringe, and then filtered through 0.2 μm syringe filters for analysis of substrate concentrations.

(A) Control Experiments

Due to the high volatility of acetaldehyde as well as the high reactivity of formaldehyde and acetaldehyde, it is important to ensure no volatilization and/or biomass adsorption occurred in the headspace-free syringes that were used as the batch reactors. Therefore, abiotic and killed control experiments were conducted in the batch reactors using a single aldehyde (formaldehyde or acetaldehyde).

An abiotic experiment was conducted in the head-space free batch reactor for both aldehyde compounds but including no biomass. The killed control experiments were conducted by injecting the substrates into a head-space free batch reactor containing

biomass that had been autoclaved at 121°C and 18 psi for 30 minutes. Table 3.3 summarizes the experimental conditions used in the control experiments.

Table 3.3. Experimental conditions in the abiotic and killed control experiments

Type of Experiment	Substrate	Substrate Conc. (mg/L)	Initial pH	Initial DO (mg/L)
Abiotic	Formaldehyde	12.3	7.1	8.5
	Acetaldehyde	22.7	7.0	8.2
Killed Control	Formaldehyde	13.0	7.1	7.8
	Acetaldehyde	26.6	7.1	7.9

(B) Effect of Dissolved Oxygen Concentration on Aldehyde Degradation

Since the batch reactor systems used in this research were maintained in headspace-free conditions, available oxygen for aerobic substrate degradation by the aldehyde-degrading consortium was provided solely from DO in the PBS. Different initial DO concentrations were tested in single substrate batch systems to ensure that neither duel substrate limitations at low oxygen concentrations nor oxygen toxicity at high concentrations were confounding the degradation kinetics.

Sterile PBS was either aerated with 0.2 μm-filtered air or pure oxygen for 30 minutes to provide low or high initial DO concentrations in the batch experiments. Table 3.4 summarizes the experimental conditions used in the different DO experiments with either formaldehyde or acetaldehyde in the single substrate systems.

Table 3.4. Experimental conditions for the single substrate systems at different initial DO values

Experiment	Substrate	Substrate Conc. (mg/L)	Initial pH	Initial DO (mg/L)
F-DO-1	Formaldehyde	11.5	7.0	4.9
F-DO-2		12.2	7.1	11.8
A-DO-1	Acetaldehyde	22.4	7.1	5.8
A-DO-2		22.2	7.0	12.8

(C) Effect of pH on Aldehyde Degradation

Waste gas streams from ethanol production facilities could potentially be acidic due to the presence of organic acids (e.g. acetic acid or lactic acid) that are generated during fermentation. To determine the effect of low pH on aldehyde degradation, formaldehyde and acetaldehyde elimination by the aldehyde-degrading consortium was studied for several pH conditions in single-substrate batch systems.

The pH experiments were conducted to determine the pH range over which single-aldehyde degradation was inhibited. The initial pH values of the PBS in the experiments were adjusted using phosphoric acid, potassium dihydrogen phosphate and disodium hydrogen phosphate. The experimental conditions for the pH experiments are summarized in Table 3.5.

Table 3.5. Experimental conditions for the single substrate systems for different initial pH values

Experiment	Substrate	Substrate Conc. (mg/L)	Initial pH	Initial DO (mg/L)
F-pH4	Formaldehyde	12.1	3.9	6.4
F-pH5		12.1	4.9	6.1
F-pH7		12.2	7.0	5.1
A-pH6	Acetaldehyde	22.3	5.8	5.1
A-pH7		22.2	7.0	12.8

(D) Effect of Enrichment Condition on Non-Aldehyde Substrate Degradation

As shown in Table 2.1, the composition of waste gas streams emitted from ethanol facilities varies with the production process. It is, therefore, important to understand how a change in waste gas composition impacts substrate degradation. Since the microbial culture was developed using formaldehyde and acetaldehyde as enrichment carbon sources, it was necessary to assess the ability of the culture to degrade non-aldehyde substrates, and to determine whether an acclimation period would be required to degrade substrates other than formaldehyde or acetaldehyde.

The consortia used in these experiments were cultivated under two enrichment conditions: one condition where formaldehyde and acetaldehyde were provided as the carbon sources, and the other where a non-aldehyde substrate (ethanol or acetate) was supplied in addition to formaldehyde and acetaldehyde during the enrichment process. Following enrichment, the subsequent degradation of either ethanol or acetate was

assessed in the batch reactor described above. Table 3.6 summarizes the experimental conditions for these experiments.

Table 3.6. Experimental conditions used to assess the effect of enrichment conditions

Experiment	Carbon Sources for Enrichment	Substrate in Batch Experiment	Substrate Conc. (mg/L)	Initial pH	Initial DO
E-X	Formaldehyde Acetaldehyde	Ethanol	1.1	7.1	4.5
E-O	Formaldehyde Acetaldehyde Ethanol		1.3	7.0	9.8
AA-X	Formaldehyde Acetaldehyde	Acetate	6.1	6.9	5.5
AA-O	Formaldehyde Acetaldehyde Acetate		5.8	7.0	6.7

(E) Single Substrate Degradation and Byproduct Formation

The literature review presented in Chapter 2 identified potential pathways for acetaldehyde and formaldehyde degradation. A number of key intermediates in these pathways included methanol, acetate, ethanol, and formate. Batch experiments were conducted to identify the presence of these byproducts during aldehyde degradation as well as to examine the biodegradability of the two byproducts commonly found in ethanol emissions, acetate and ethanol. The experimental conditions utilized in each of these single substrate experiments are summarized in Table 3.7; S_0 and X_0 represent the initial concentrations of substrate and biomass, respectively.

Table 3.7. Experimental conditions used in the single substrate experiments

Experiment	Substrate	S_0		X_0	Initial pH	Initial DO
		mg/L	mM	mg VSS/L		
SS-F-7	Formaldehyde	5.7	0.2	40	7.1	8.0
SS-A-8	Acetaldehyde	12.0	0.3	56	7.2	8.0
SS-E-6	Ethanol	8.9	0.2	36	7.1	11.2
SS-Ac-4	Acetate	5.9	0.1	45	7.2	11.4
SS-Ac-5*	Acetate	7.2	0.1	44	7.1	12.2

* Spiked 3.6 mg/L (0.06 mM) of acetate at 90 minutes

(F) Binary Substrate Degradation

Binary substrate experiments were conducted to investigate potential substrate mixture effects that could arise from treating a waste gas stream from an ethanol production facility. As a result, the substrates were paired to examine any interactions between two aldehydes (formaldehyde and acetaldehyde), and between an aldehyde (formaldehyde or acetaldehyde) and a non-aldehyde substrate (ethanol or acetate). The operating conditions for the binary substrate experiments are presented in Table 3.8; S_0 and X_0 represent the initial concentrations of substrate and biomass, respectively. The concentrations of S_0 and X_0 in these experiments were chosen to match those applied in the single substrate experiments.

Table 3.8. Experimental conditions used in the binary substrate experiments

Experiment	Substrate	S_0		X_0	Initial pH	Initial DO
		mg/L	mM	mg VSS/L		
BS-AE	Acetaldehyde Ethanol	27.7 10.2	0.6 0.2	50	7.2	12.6
BS-FA-4	Formaldehyde Acetaldehyde	6.1 11.6	0.2 0.3	56	7.1	10.4
BS-FAc	Formaldehyde Acetate	5.4 10.8	0.2 0.2	38	7.2	11.3
BS-FE-1	Formaldehyde Ethanol	10.5 4.1	0.4 0.1	126	7.1	11.8
BS-FE-2	Formaldehyde Ethanol	5.3 9.5	0.2 0.2	38	7.2	8.6

3.1.3. Analytical Methods

The following section summarizes the analytical methods used during the batch experiments. The analytical methods to determine concentrations of the primary substrates including formaldehyde, acetaldehyde, ethanol and acetate as well as other potential degradation byproducts such as methanol and formate are described first. Other analyses for determination of biomass concentration, dissolved oxygen concentration and pH are also described.

Formaldehyde

Liquid samples containing formaldehyde were measured using the colorimetric reaction described in the USEPA Test Method 316 (USEPA, 2006). Liquid samples containing biomass were filtered through 0.2 μm syringe filters and diluted appropriately

prior to analysis. Then, 2.5 mL of a liquid sample was transferred to a disposable cuvette and 0.25 mL of pararosaniline reagent was added. The cuvette was capped and shaken for 30 seconds to ensure the solution was well-mixed. After 0.25 mL of sodium sulfite reagent solution was added to the solution, the cuvette was again capped and shaken for 30 seconds. The colorimetric reaction was developed at room temperature for one hour before absorbance at 570 nm was measured on an Aglient 8453 UV-visible spectrophotometric system. The minimum detection limit (MDL) for the colorimetric formaldehyde analysis was determined to be 0.146 mg/L according to Standard Method 1030E Method Detection Limit (APHA *et al*., 1998). The linear concentration range for formaldehyde using this method was up to 4.0 mg/L. A calibration curve for formaldehyde standard solutions using this method is shown in Figure 3.1.

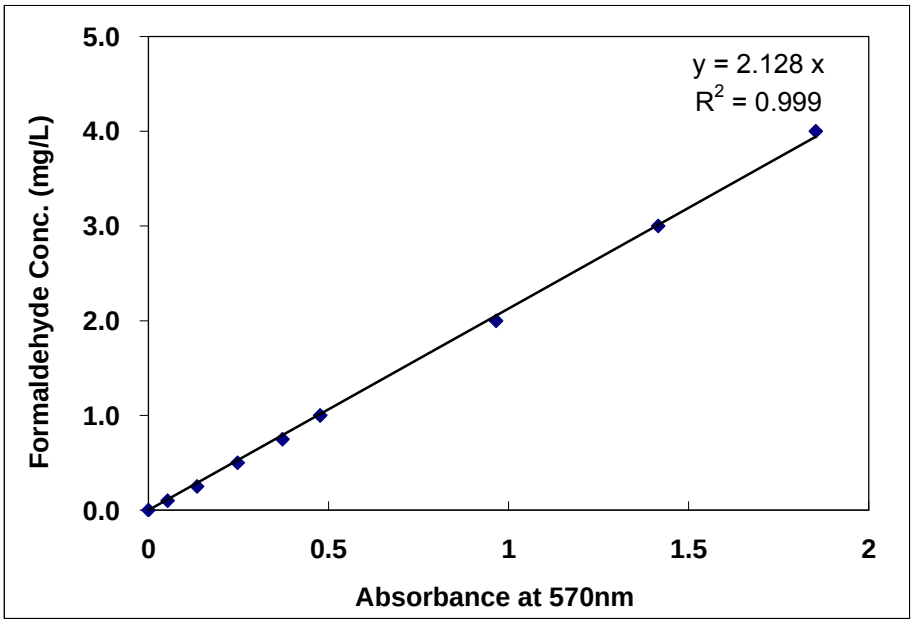

Figure 3.1. Calibration curve for aqueous formaldehyde concentrations.

Acetaldehyde, Ethanol and Methanol

To determine acetaldehyde concentrations in the liquid phase, 1 mL of liquid was transferred to a 2 mL vial which was then capped and equilibrated at 25˚C for 30 minutes. Headspace samples of the vials were withdrawn using a 0.5 mL gastight syringe (VICI, Series A-2) and injected into a Hewlett Packard (HP) 5890 II Plus Gas Chromatograph (GC) equipped with a flame-ionization detector (FID) and a 30 m Restek RTX-624 column. The GC column was operated at 35˚C for 4 minutes, increased at a rate of 50˚C/min to 150˚C and held for 1 minute. Helium was used as the carrier gas at a flow rate of 6.0 mL/min. The injector and the detector were set at 200˚C and 280˚C. Figure 3.2 is an example of a calibration curve for the gas-phase acetaldehyde concentrations. Acetaldehyde headspace concentrations were then used to calculate corresponding aqueous concentrations in the original liquid samples using the Henry's Law constant for acetaldehyde (Table 3.1). The MDL was determined to be 0.4 ppm_v.

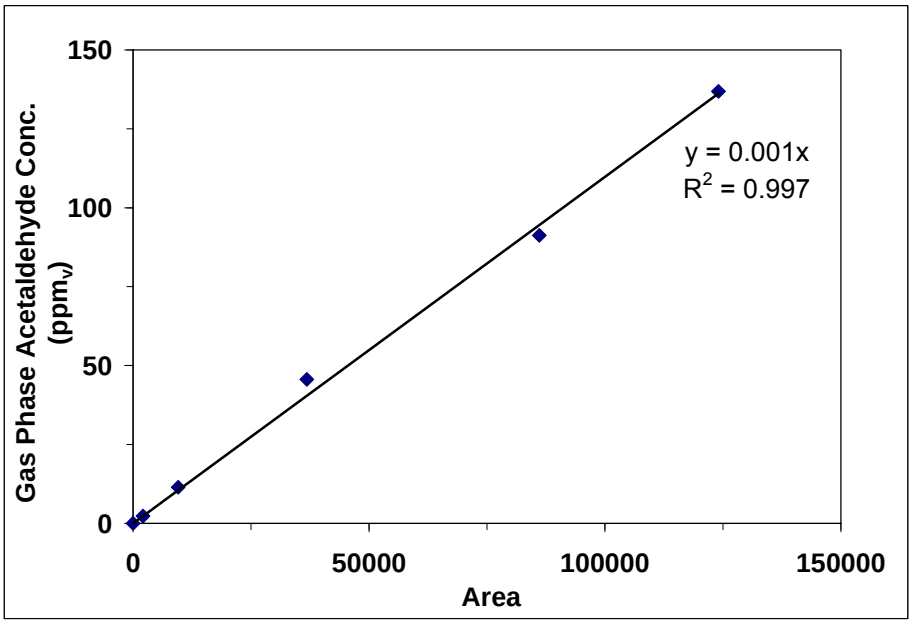

Figure 3.2. Calibration curve for gas phase acetaldehyde concentrations.

A 3 mL aliquot of a liquid sample containing ethanol (or methanol) was placed in a 9 mL headspace vial fitted with a Telflon-faced butyl septum. The vials were then analyzed for ethanol (or methanol) concentrations using a Tekmar 7000 headspace sampler attached to a HP 5890 GC-FID equipped with a 30 m Restek RTX-624 column. The FID was supplied with 30 mL/min nitrogen, 30 mL/min hydrogen, and 300 mL/min air. The GC-FID was operated at an initial oven temperature of 40˚C for 3 minutes, followed by 10˚C/min to 140˚C which was held for 2 minutes, and then increased at 50˚C /min to a final temperature of 220˚C that was held for 3 minutes. The temperatures of the injector and the detector were 250˚C and 275˚C, respectively. A sample calibration curve for liquid phase ethanol concentrations is shown in Figure 3.3.

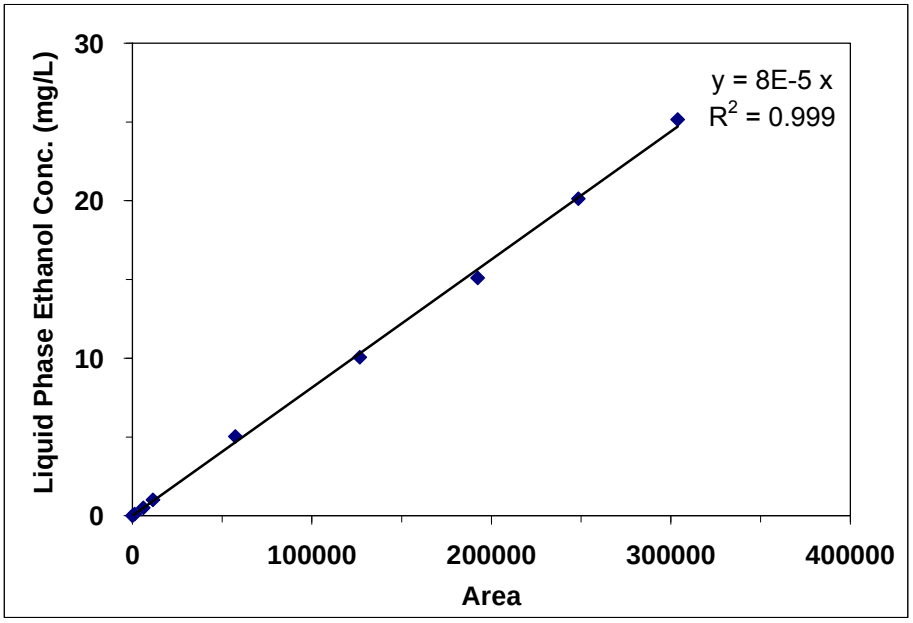

Figure 3.3. Calibration curve for liquid phase ethanol concentrations.

Acetate and Formate

Liquid samples containing acetate and formate were analyzed using a Metrohm Ion Chromatograph (IC) system. The IC system was equipped with the Metrohm 709 IC Pump, 732 IC Detector, 733 IC Separation Center, 752 Pump Unit, 762 IC interface, 838 Advanced Sample Processor and the Metrohm A Supp 5 -250 Column.

The eluent for the IC system consisted of 1.0 mM of sodium hydrogen carbonate and 3.2 mM of sodium carbonate, and the flow rate of the eluent through the column was 0.7 mL/min. Each sample run time on the IC system was 30 minutes, and the retention times for acetate and formate were 6.9 minutes and 7.5 minutes, respectively. Typical calibration curves for acetate and formate standards are plotted in Figure 3.4.

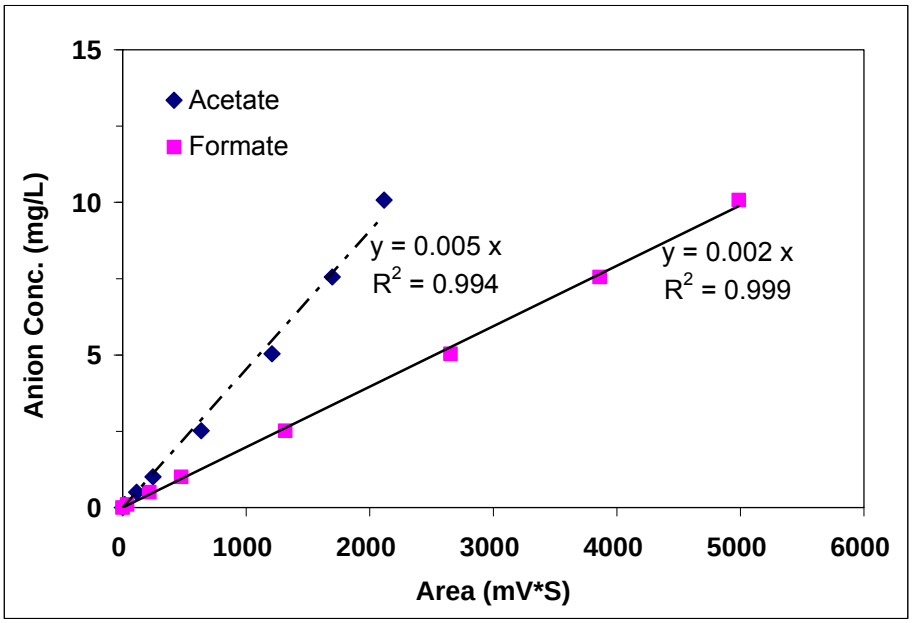

Figure 3.4. Calibration curves for acetate and formate concentrations.

Biomass Concentration

The initial biomass concentration for each batch experiment was estimated by measuring liquid samples on the spectrophotometer at a wavelength of 600 nm. Analysis of volatile suspended solids (VSS) was performed to determine the actual biomass concentrations in the beginning and end of each experiment; VSS was analyzed according to Standard Method 2540E (APHA, 1998). During the preliminary (A), (B), (C) and (D) experiments described in Section 3.1.4, there was inconsistency between the absorbance values at 600 nm and the VSS measurements due to issues with the VSS analysis. Therefore, the absorbance values were used to evaluate the preliminary experimental data. In the subsequent single and binary batch kinetic experiments (E) and (F) in Section 3.1.4, the issues with the VSS analysis were resolved so the VSS measurement results were used.

Dissolved Oxygen Concentration and pH

DO concentrations of liquid samples were determined using a YSI Model 54ARC oxygen meter. The DO meter was calibrated using distilled water at room temperature prior to measurement each day. The pH values of liquid samples were measured using an Orion pH meter (Model 520A) equipped with a VWR Scientific pH probe (No.34105-148). The probe was calibrated with standard pH buffers of 4, 7 and 10 prior to measurement each day.

3.2. RESULTS AND DISCUSSION

3.2.1. Control Experiments

To ensure no occurrence of significant volatilization or biomass adsorption in the headspace-free batch reactors, abiotic and killed control experiments for each aldehyde compound were conducted. The results of the experiments using formaldehyde and acetaldehyde as the single substrate are plotted respectively in Figures 3.5(a) and (b).

As seen in Figure 3.5(a), formaldehyde concentrations during either experiment remained fairly constant; the deviation of any data points from the average formaldehyde concentration was within ±4% for either the abiotic or killed control experiment. Similarly, the acetaldehyde concentration profiles are shown in Figure 3.5(b). Even though the deviation of few data points from the average acetaldehyde concentration was up to ±9% in both experiments, the overall results indicate no substantial losses of acetaldehyde due to volatilization or biomass adsorption in the batch reactors. The deviation of the acetaldehyde concentrations shown in Figure 3.5(b) was due to the periodic variation of the background signals at the GC-FID.

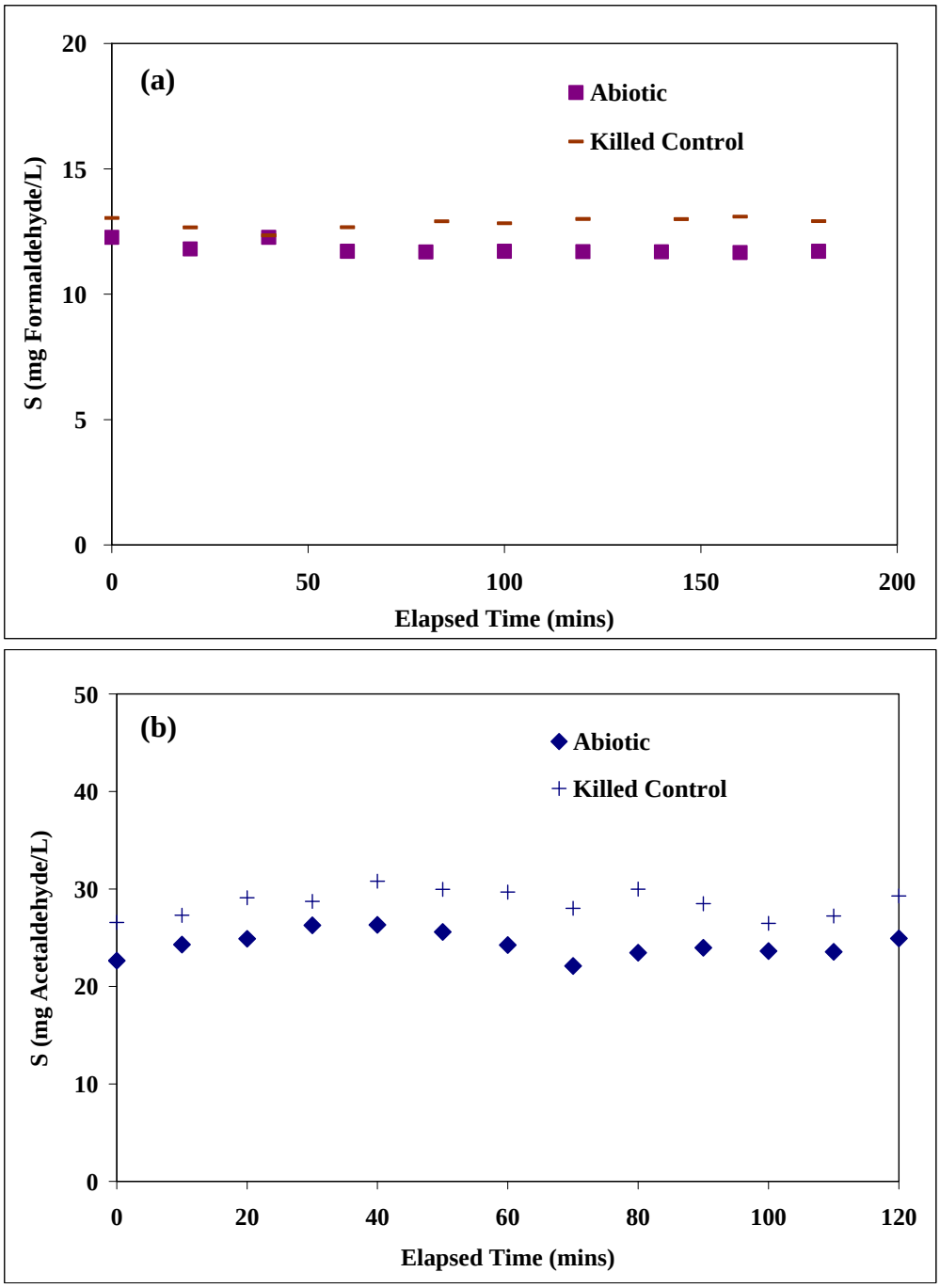

Figure 3.5. Abiotic and killed control experiments conducted in batch reactors with: (a) formaldehyde; or (b) acetaldehyde as the single substrate.

3.2.2. Effects of Key Operating Parameters

(A) Effect of Dissolved Oxygen Concentration on Aldehyde Degradation

Single substrate degradation experiments were conducted at two different initial DO concentrations to verify that oxygen was neither a limiting reagent nor present at toxic concentrations in the substrate degradation experiments. Formaldehyde concentration profiles derived from the experiments conducted with initial DO concentrations of 4.9 and 11.8 mg/L are shown in Figure 3.6(a). As indicated in the figure, the initial substrate concentrations for these two experiments are identical. In addition, the similarity in the absorbance values of the samples measured at 600 nm (A_{600nm}) suggests that the solids concentrations are similar for the two experiments. As a result, comparison of the rates of substrate utilization can be made by directly comparing the data for the two different initial dissolved oxygen concentrations. The results indicate that the curves are nearly identical and formaldehyde removals of approximately 100% were observed for both experiments.

Figure 3.6(b) shows the concentration profiles for acetaldehyde degradation at two different initial DO (5.8 and 12.8 mg/L) conditions. Complete removal of acetaldehyde was observed for low and high initial DO values for this substrate as well. Again, the initial substrate concentrations and absorbance values at 600 nm are similar, suggesting that the initial concentration of oxygen was not limiting during the single aldehyde degradation experiments, and the higher oxygen concentration did not have an adverse impact on either aldehyde degradation. In addition, low values of DO reported at the end of each experiment did not appear to inhibit degradation. Indeed, the concentration of DO at the end of the low DO experiment for formaldehyde (F-DO-1) was 0.6 mg/L compared to a value of 4.6 mg/L for the high DO experiment (F-DO-2).

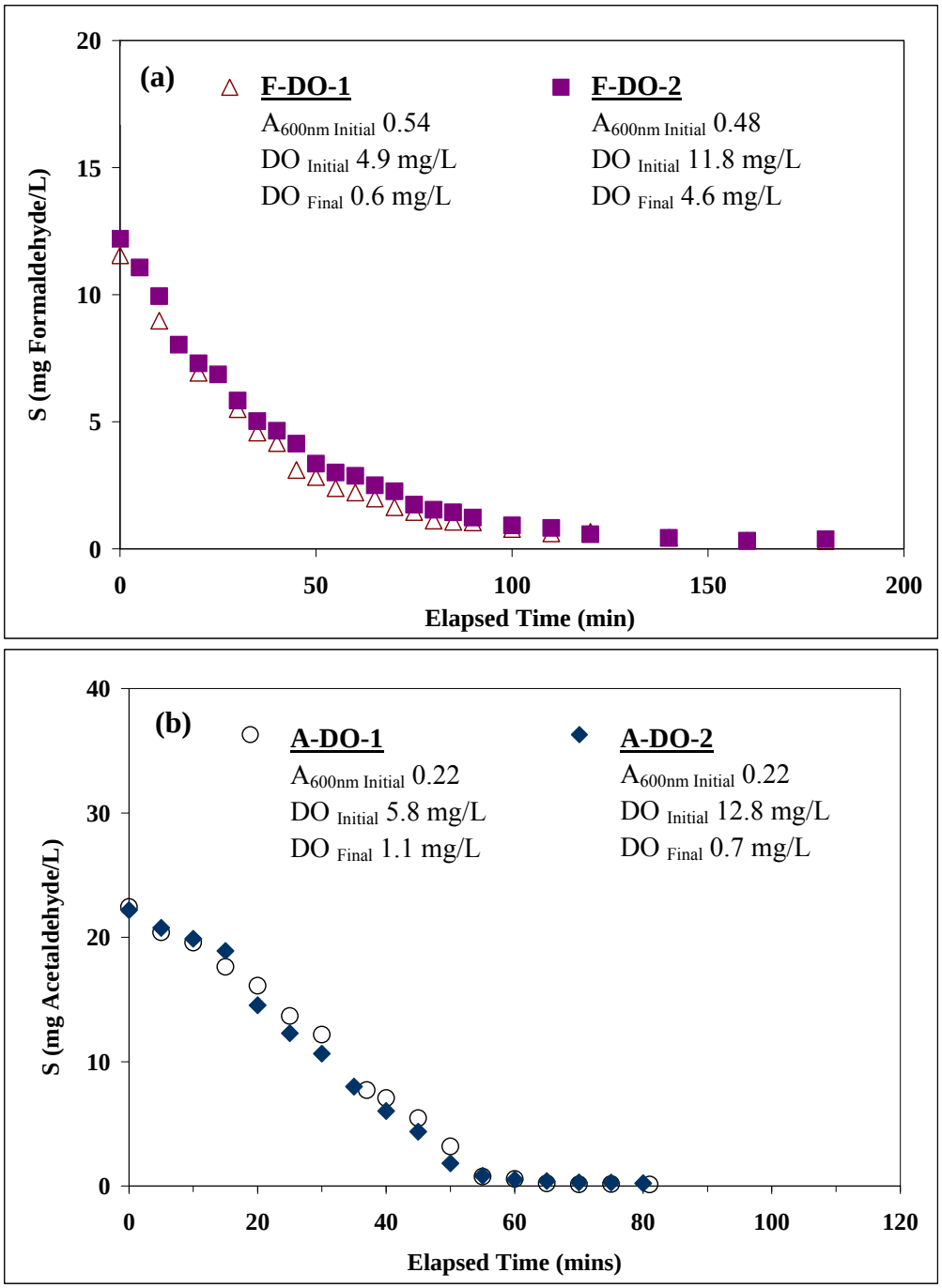

Figure 3.6. Effect of initial DO concentrations on aldehyde degradation in batch reactors with: (a) formaldehyde; (b) acetaldehyde as the single substrate.

(B) Effect of pH on Aldehyde Degradation

The effect of pH on single aldehyde degradation by the enriched aldehyde-degrading consortium in this research was examined for pH values ranging from neutral to acidic conditions. Formaldehyde and acetaldehyde were individually tested in the single substrate batch reactors at different pH conditions.

The formaldehyde degradation batch experiments were conducted at pH 7.0, 4.9 and 3.9. Figure 3.7(a) shows the formaldehyde concentration profiles at three different pH conditions. The initial substrate concentration is similar for all three experiments. The initial absorbance values at 600nm for the three experiments suggest that the solids concentration in the pH 7.0 experiment is approximately 18 percent higher than the pH 4.9 experiment. However, comparison of the two data sets suggests that the rates of substrate removal are similar suggesting that the specific rate of substrate utilization for the pH 4.9 experiment is slightly higher. In contrast, a significant reduction in the rate of substrate utilization is observed when the pH is lowered to a 3.9, even though the absorbance value is approximately seven percent higher than the pH 4.9 experiment. These results suggest that inhibition of formaldehyde degradation did not become obvious until the pH of the batch reactor dropped to 3.9. Indeed, a significant drop in absorbance of the sample (19%) and cell lysis in the reactor were observed at the end of the pH 3.9 experiment. A similar effect of pH on formaldehyde elimination was observed in batch experiments conducted by Prado *et al.* (2006) at significantly higher formaldehyde concentrations. They supplied 200 mg/L of formaldehyde and 3.5 g/L of VSS in three sets of vials containing buffer solutions at pH 7.5, 5.5 or 4.0; the results showed that formaldehyde removals decreased at lower pH. It took much longer to achieve complete removal of formaldehyde at pH 4.0 (55 hours) than at pH 7.5 (5 hours).

The data from this research suggest that removal of formaldehyde was significantly impeded after approximately 150 minutes at pH 3.9.

The effect of pH on acetaldehyde degradation using the consortium was also investigated in the batch reactors for pH values of 7.0 and 5.8. In this case, the absorbance values and initial substrate concentrations were less than one and less than four percent different between the two experiments, respectively. The experimental results of acetaldehyde degradation as the single substrate at two pH conditions are shown in Figure 3.7(b). As is evident in the figure, when pH dropped from 7.0 to 5.8, the microbial activity was significantly impeded as acetaldehyde removal decreased from nearly 100% to 35%.

These pH experimental results indicate that decreasing pH impacted acetaldehyde degradation more significantly than formaldehyde degradation when using the consortium developed in this research, suggesting the potential of two separate communities (or enzymes) being responsible for the conversion of formaldehyde and acetaldehyde in the batch reactors. In addition, given that acetate was found to be an intermediate of acetaldehyde degradation in Pathway C (Section 2.2.3), it is possible that at the lower pH more acetic acid (pK_a 4.76) was present in the system, leading to feedback inhibition of acetaldehyde degradation that was observed during the pH 5.8 experiment.

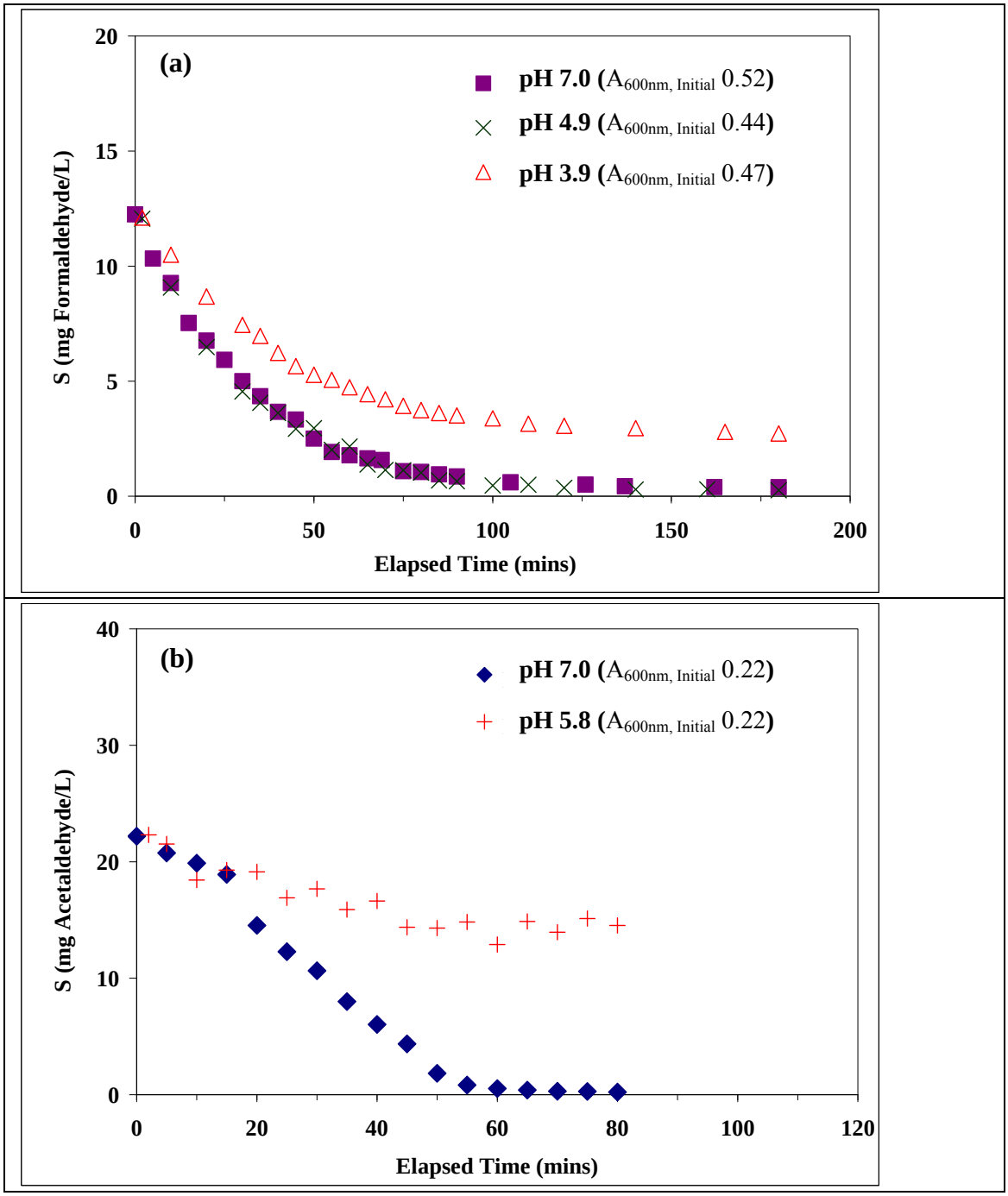

Figure 3.7. Effect of pH on aldehyde degradation in batch reactors with: (a) formaldehyde; (b) acetaldehyde as the single substrate.

(C) Effect of Enrichment Conditions on the Degradation of Ethanol and Acetate

The initial enrichment cultures developed for this research were exposed only to the aldehyde substrates. To assess the impact of enrichment conditions on the other two compounds, substrate degradation data were also collected from the consortium that had been exposed to either ethanol or acetate in addition to the aldehyde compounds. Comparison of the degradation of ethanol for the two different consortia is shown in Figure 3.8(a). The initial substrate concentrations and absorbance values at 600nm are similar so that the results can be compared directly. The results suggest that the consortium was able to degrade ethanol without any acclimation period, and beyond that, the presence of ethanol during biomass enrichment enhanced the ethanol degradation rate. Based on these findings, it is reasonable to speculate that in addition to an aldehyde-degrading community, there was another microbial community responsible for ethanol degradation. When two aldehydes were supplied as the carbon sources during enrichment, the aldehyde-degrading species appears to have dominated the microbial community in the mixed culture. However, when ethanol was provided along with the two aldehydes, the fraction of the ethanol-degrading community in the mixed culture increased and led to a higher ethanol degradation rate.

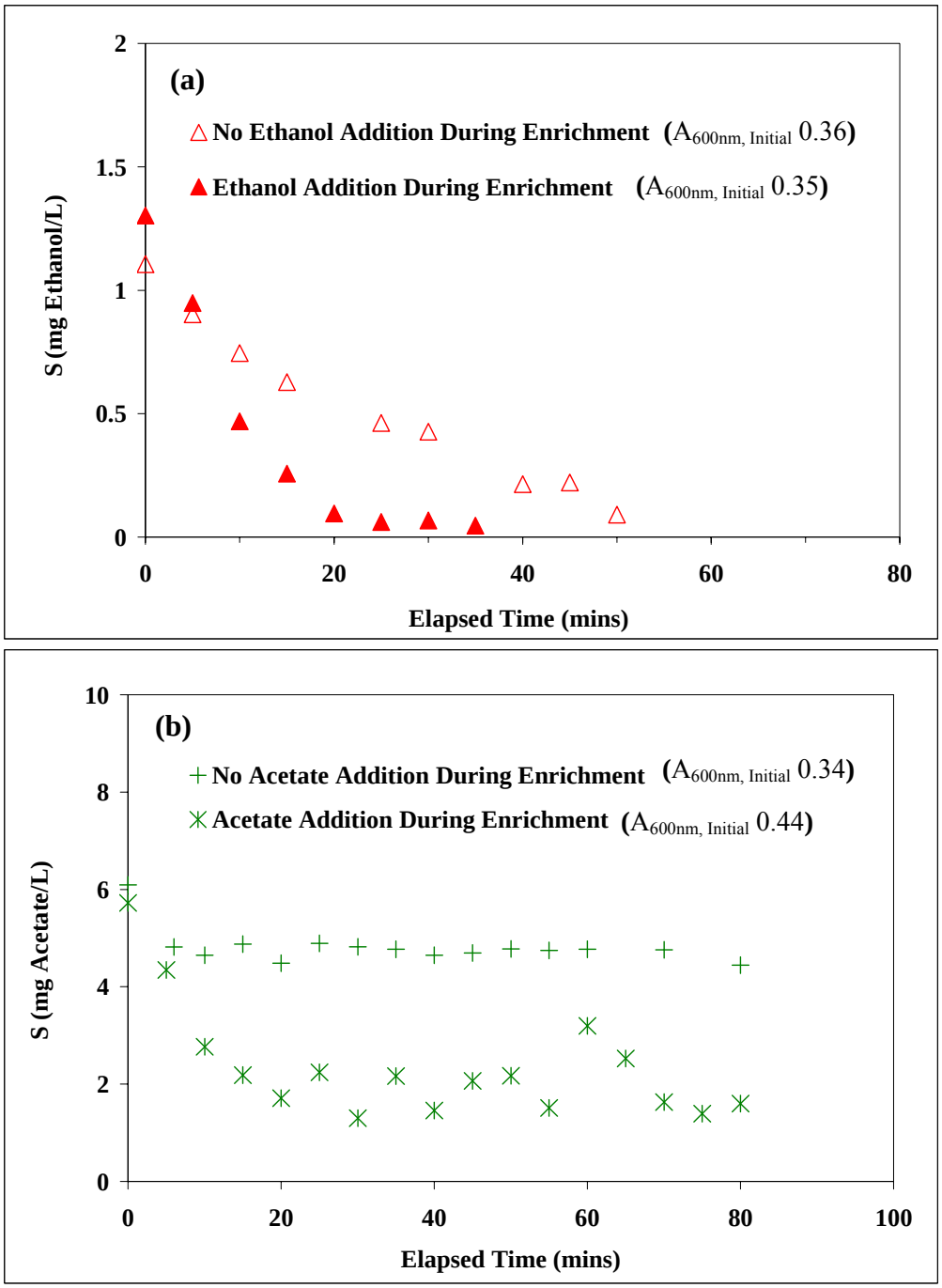

Figure 3.8. Comparison of different enrichment conditions on non-aldehyde substrate degradation with: (a) ethanol; (b) acetate as the single substrate when using the aldehyde-degrading consortium.

Although acetate is widely considered an easily biodegradable carbon source, the results shown in Figure 3.8(b) indicate that acetate degradation depended on whether acetate was used during biomass enrichment of the consortium. When the consortium was cultivated using formaldehyde and acetaldehyde as the carbon sources, only 22% removal of acetate was observed after 6 minutes and no further removal occurred through the course of the experiment. The final acetate concentration of 4.7 mg/L was well above the analytical detection limits of the experiment. Once acetate was supplied as one of the carbon sources for biomass enrichment, acetate removal increased to 65% in the subsequent batch experiment. However, an average acetate concentration of 2.0 mg/L remained in the system after 20 minutes. Based on these experimental results, it is difficult to determine which mechanism(s) led to incomplete removal of acetate in the batch reactors. Thus, further study (Section 3.2.2) was required to verify these observed results.

(D) Single Substrate Degradation and Byproduct Formation

The experimental data from the batch kinetic experiments using formaldehyde, acetaldehyde, ethanol and acetate as a single substrate indicate that all the substrates, except for acetate, were removed by the enriched consortium to below detection limits under the test conditions. For formaldehyde, acetaldehyde and ethanol degradation experiments, the primary degradation byproduct(s) for each of the substrates are also reported. The results for each single substrate experiment are discussed individually as follows.

Formaldehyde Degradation

As shown in Figure 3.9, accumulation of formate was observed with the disappearance of formaldehyde in the single substrate system during Experiment SS-F-7. The formate concentration peaked at 0.06 mM at 50 minutes in this experiment and began to decrease once formaldehyde was nearly eliminated from the system. In addition, methanol was briefly detected at a peak concentration of 0.02 mM but disappeared after 10 minutes of the experiment.

As discussed in Section 2.2.2, two formaldehyde degradation pathways have been reported in the literature. In Pathway A, formaldehyde produces formic acid as an intermediate, which subsequently is degraded to carbon dioxide. The key enzymes associated with these two transformations are formaldehyde dehydrogenase and formate dehydrogenase, repectively. The presence of methanol is not consistent with this path. If formaldehyde degradation follows Pathway B, formaldehyde would be converted to equal moles of methanol and formic acid by formaldehyde dismutase. Both formate and methanol were observed in Experiment SS-F-7 during the course of formaldehyde degradation, with formate detected at much higher molar concentrations than methanol. The presence of methanol in the system suggests that Pathway B is operative. That the relative concentration of the methanol and formate are not equivalent may reflect differences in the relative rates of degradation of the two substrates in this system. However, the possibility that Pathway A was also operative in the batch system cannot be eliminated as the relative rates of formate and methanol degradation were not determined.

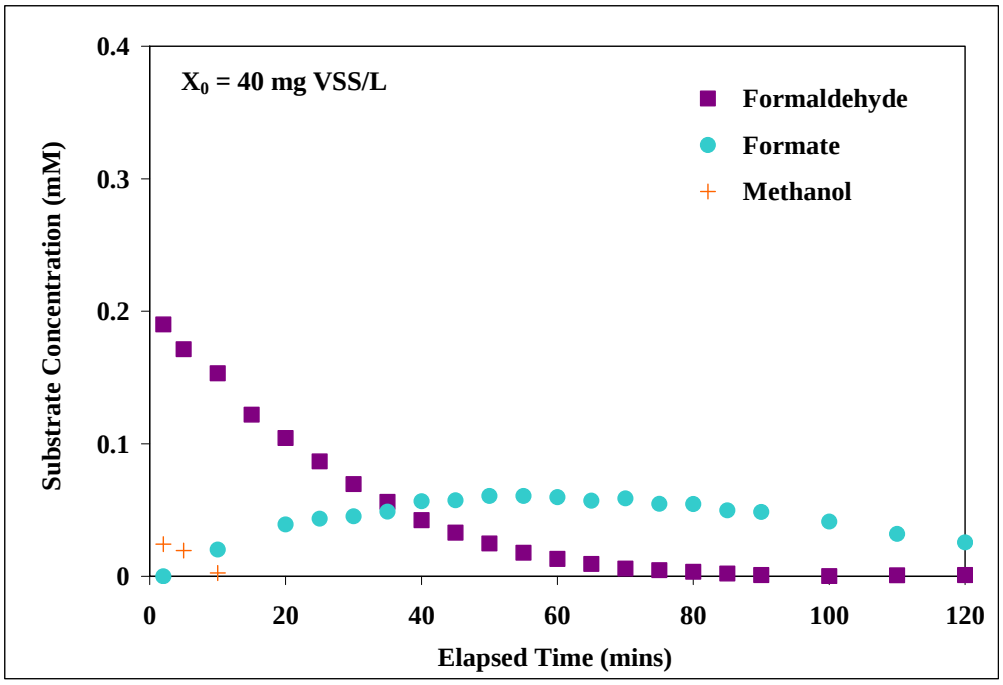

Figure 3.9. Concentration profiles for formaldehyde and it intermediates during single formaldehyde degradation (Experiment SS-F-7).

Acetaldehyde Degradation

The results for single acetaldehyde degradation in Experiment SS-A-8 are plotted in Figure 3.10. In this experiment, ethanol and acetate were produced at equimolar ratios during the first 30 minutes. The presence of ethanol in the experiment suggests that acetaldehyde may have been formed (as well as degraded) as an intermediate by-product of ethanol degradation via Pathway C in which alcohol and aldehyde dehydrogenases degrade ethanol to acetaldehyde and acetate, respectively. Once acetaldehyde was completely removed from the system, ethanol and acetate remained in the system at constant concentrations of 0.07 and 0.06 mM, respectively. Given the final DO concentration of 0.7 mg/L at 100 minutes of this experiment, oxygen limitation

should not have been the cause for inhibition of ethanol degradation. Accumulation of both acetaldehyde degradation byproducts implies some uncharacterized inhibition might be responsible for shutting down ethanol and/or acetate degradation in the batch system during Experiment SS-A-8.

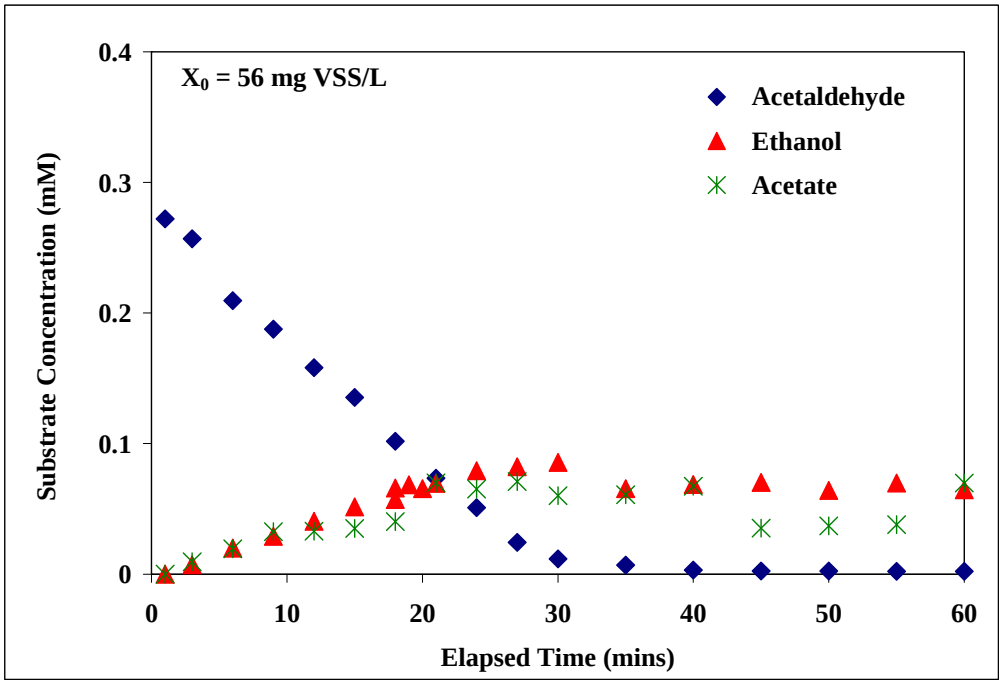

Figure 3.10. Concentration profiles for acetaldehyde and it intermediates during single acetaldehyde degradation (Experiment SS-A-8).

A few studies have reported that some alcohol dehydrogenases (ADHs) in human, horses, insects and yeast possess dismutation activity, and they can oxidize acetaldehyde to equimolar quantities of ethanol and acetic acid (Trivić *et al.*, 1999; Velonia and Smonou, 2000; Höllrigl *et a*l., 2008). Although the co-occurrence of ethanol and acetate in Experiment SS-A-8 could result from dismutation of acetaldehyde, other possibilities might exist in the system since the aldehyde-degrading consortium was a

mixed culture. In other words, it is possible, even under aerobic conditions, that a portion of the acetaldehyde was reduced to ethanol via Pathway E in which net ethanol production from acetaldehyde under aerobic conditions by facultative microbial species, while the rest of the acetaldehyde was oxidized to acetate via Pathway C (see Section 2.2.3 for the pathways).

Ethanol Degradation

Given that the enrichment conditions were shown to affect ethanol degradation in the batch reactors, ethanol was used as the sole carbon source to enrich the biomass for the single ethanol degradation in Experiment SS-E-6. As shown in Figure 3.11, ethanol was completely removed from the batch system within 20 minutes. Acetate accumulation was observed in the batch system during this experiment suggesting ethanol degradation via Pathway C in which ethanol is oxidized to acetaldehyde and then to acetate; however, no acetaldehyde was detected as ethanol was degraded. One possible explanation for not detecting acetaldehyde is that the conversion rates of ethanol to acetic acid were too rapid to allow for acetaldehyde accumulation in the batch system. Based on the presence of acetate, it is still reasonable to assume that the consortium degraded ethanol via Pathway C (Section 2.2.3) in this experiment, implying alcohol and aldehyde dehydrogenases might be involved in ethanol degradation of the consortium.

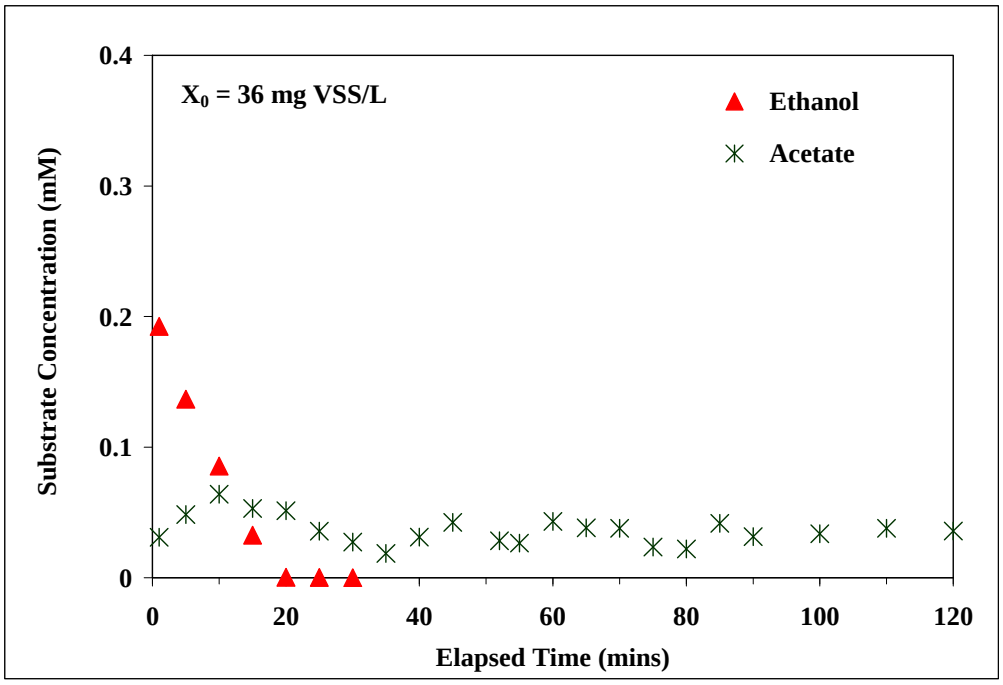

Figure 3.11. Concentration profiles of ethanol and it intermediate derived during single ethanol degradation (Experiment SS-E-6).

Acetate Degradation

The biomass used in the single acetate degradation Experiment SS-Ac-4 was enriched with acetate as the sole carbon source for the same reason discussed in the previous section describing ethanol degradation. Interestingly, this single acetate degradation experiment along with several other preliminary experiments show that the consortium can only partially remove acetate. As shown in Figure 3.12, acetate removal reached 81% approximately 20 minutes after the experiment was initiated, leaving 0.02 mM (1.1 mg/L) of acetate remaining in the reactor until the end of Experiment SS-Ac-4. Given the final DO concentration of 9.7 mg/L in the batch system, oxygen limitations can not explain this observation. To investigate acetate degradation further, Experiment SS-

Ac-5 was conducted identically to Experiment SS-Ac-4, except that an additional 0.06 mM (3.6 mg/L) of acetate was spiked into the system after the acetate degradation had leveled off at 90 minutes. As seen in Figure 3.12, the additional acetate was eliminated immediately, but its concentration in the reactor leveled off again at approximately 0.03 mM (1.8 mg/L), with the final DO concentration of 11.7 mg/L observed. Based on the DO data in Experiments SS-Ac-4 and SS-Ac-5, it is apparent that oxygen was not limiting during acetate degradation in both experiments when using the consortium.

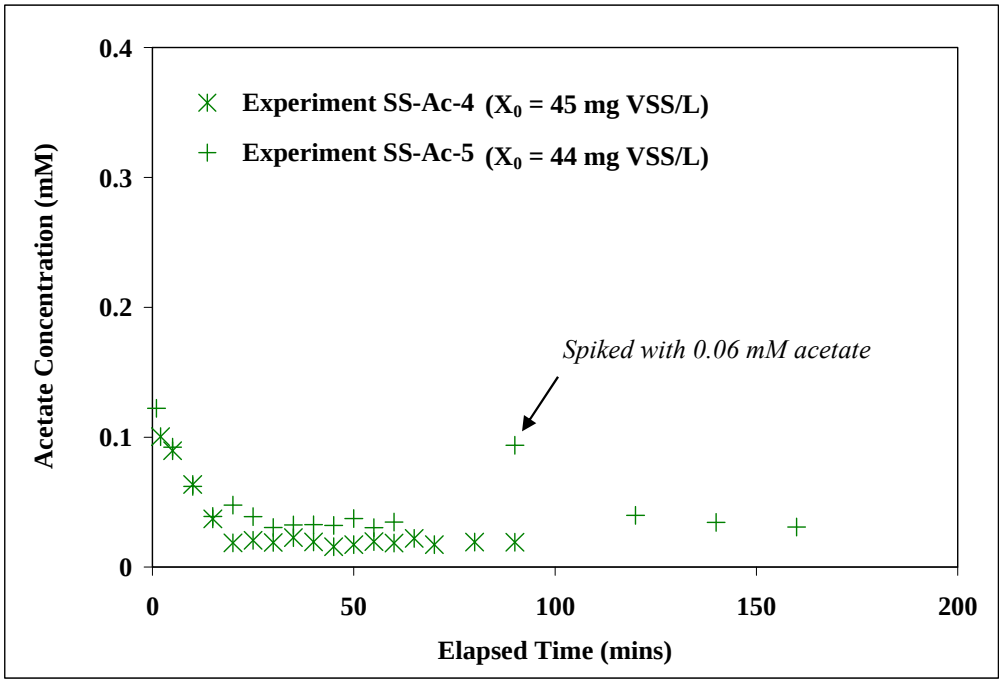

Figure 3.12. Concentration profiles of acetate degradation in single substrate reactor without acetate spiked (Experiment SS-Ac-4) and with 0.06 mM acetate spiked (Experiment AA-Ac-5).

In most microorganisms, acetate must enter the cytoplasm to be incorporated into the TCA cycle for either further oxidation to CO_2 or cell synthesis. Although it is generally accepted that acetate is easily biodegradable, accumulation of acetate in the

cytoplasm can be toxic to cell growth (Russell, 1992; Roe *et al*., 1998). For acetic acid bacteria, it is believed that acetic acid penetrates the cytoplasm through passive diffusion, while a putative ABC transporter and proton motive force-dependent efflux pump possibly export acetic acid in the cytoplasm (Nakano and Fukaya, 2008). Moreover, Boenigk *et al*. (1989) proposed that a carrier-mediated acetate transport mechanism, in addition to passive diffusion, is important for *Acetobacterium woodii* to export intracellular acetate. Since an operating pH of 7 was maintained for the batch experiments in this research, acetate dominated the speciation of the acetic acid system (pK_a= 4.76). One can expect that the amounts of acetate imported intracellularly through passive diffusion were probably limited at neutral pH. However, it is impossible to determine which mechanisms were involved in acetate transport and elimination in the batch systems based on the experimental results. Therefore, additional research will be required to elucidate potential causes for the incomplete acetate degradation observed in this research.

3.2.3. Binary Substrate Degradation

Acetaldehyde & Ethanol Degradation

The concentration profiles for acetaldehyde and ethanol degradation in the binary substrate system during Experiment BS-AE are plotted in Figure 3.13. The results show that acetaldehyde was quickly converted to ethanol, which led to accumulation of ethanol. However, the ethanol concentration only slightly decreased after acetaldehyde was completely eliminated from the batch system. Given the final DO concentration of 0.6 mg/L at 100 minutes of this experiment, oxygen limitation should not have been the cause for ethanol inhibition. Even though acetate was not monitored during this

experiment, it is worth noting that the ethanol concentration profile in this experiment was similar to the one observed during single acetaldehyde degradation (Experiment SS-A-8). Based on the single acetaldehyde degradation data, one can speculate that acetate production occurred concurrently in this binary substrate system, which could be linked to inhibition of ethanol degradation. Further examination is required to clarify the potential inhibition mechanisms.

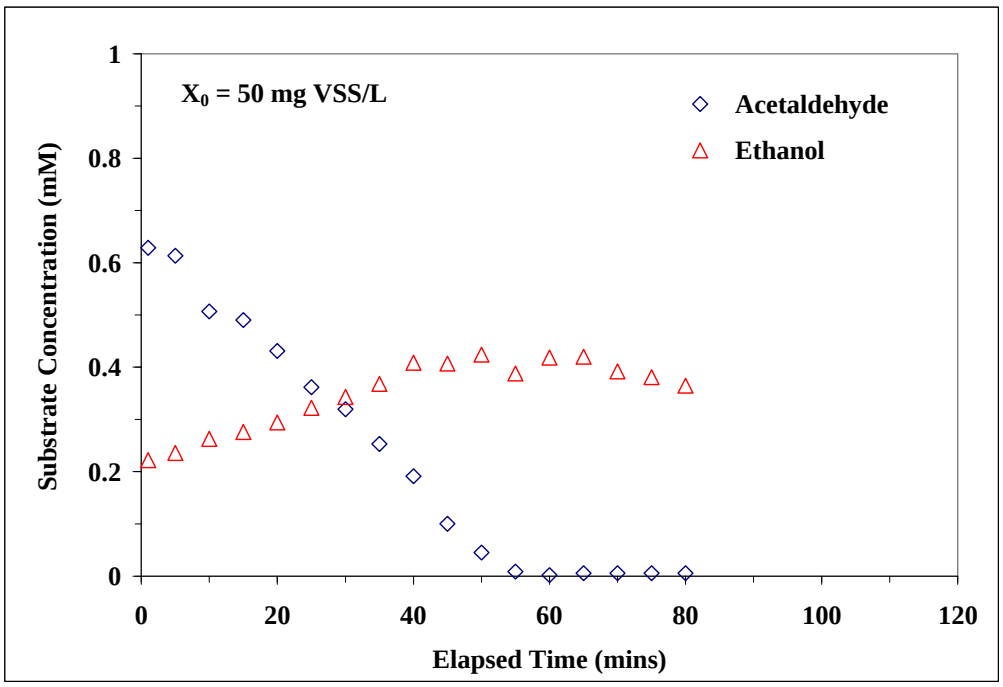

Figure 3.13. Concentration profiles for acetaldehyde and ethanol degradation in the binary substrate system during Experiment BS-AE.

Although the microbial species in the enriched consortium were not identified, the results from Experiments SS-E-6, SS-Ac-4, and BS-AE suggest that there might be at least two microbial communities, such as *Z. mobilis* and acetic acid bacteria, present in the binary substrate system. Per the discussion for Pathway E (in which net ethanol

production from acetaldehyde under aerobic conditions by facultative microbial species) in Section 2.2.3, it is possible that acetaldehyde reduction to ethanol can occur under aerobic conditions when the facultative *Zymomonas* is present. Such a conversion could explain the ethanol formation observed early in Experiment BS-AE as a result of acetaldehyde elimination. The accumulation of ethanol observed in this experiment would require that the acetaldehyde reduction rate by bacteria such as *Zymomonas* was much faster than the ethanol oxidation rate by acetic acid bacteria in the batch system. This hypothesis is indeed supported by the half-saturation constant (K_m) of each corresponding enzyme reported in the literature (Kinoshita *et al*., 1985; Tayama *et al*., 1989; Gómez-Manzo *et al*., 2008). When acetaldehyde was used as a substrate, a K_m of 0.086 mM for *Z. mobilis* ADH I (Kinoshita *et al*., 1985) and a K_m ranging from 2.9 to 4.2 mM for acetic acid bacteria ADH (Tayama *et al*., 1989; Gómez-Manzo *et al*., 2008) have been observed, suggesting that the reduction of acetaldehyde to ethanol in Experiment BS-AE was more likely carried out by *Z. mobilis*.

In addition, the data from the single substrate degradation of ethanol (Experiment SS-E-6) and acetate (Experiment SS-Ac-4) suggest that acetic acid bacteria may play an important role in ethanol degradation in the experimental consortium. A K_m of 0.46-1.2 mM for acetic acid bacteria ADH catalyzing ethanol to acetaldehyde (Tayama *et al*., 1989; Gómez-Manzo *et al*., 2008) is lower than a K_m of 4.8-27 mM for *Z. mobilis* ADH I and ADH II when converting ethanol to acetaldehyde (Kinoshita *et al*., 1985). Thus, it is possible that ethanol degradation was performed by acetic acid bacteria in the binary substrate system containing ethanol (Experiment BS-AE).

Degradation of Formaldehyde and Acetaldehyde

The aldehyde concentration profiles for the binary substrate degradation using formaldehyde and acetaldehyde during Experiment BS-FA-4 are plotted in Figure 3.14. As shown in the single acetaldehyde degradation in Experiment SS-A-8, ethanol and acetic acid were detected during acetaldehyde degradation; therefore, ethanol was monitored during this experiment and its concentration profile is also presented in Figure 3.14.

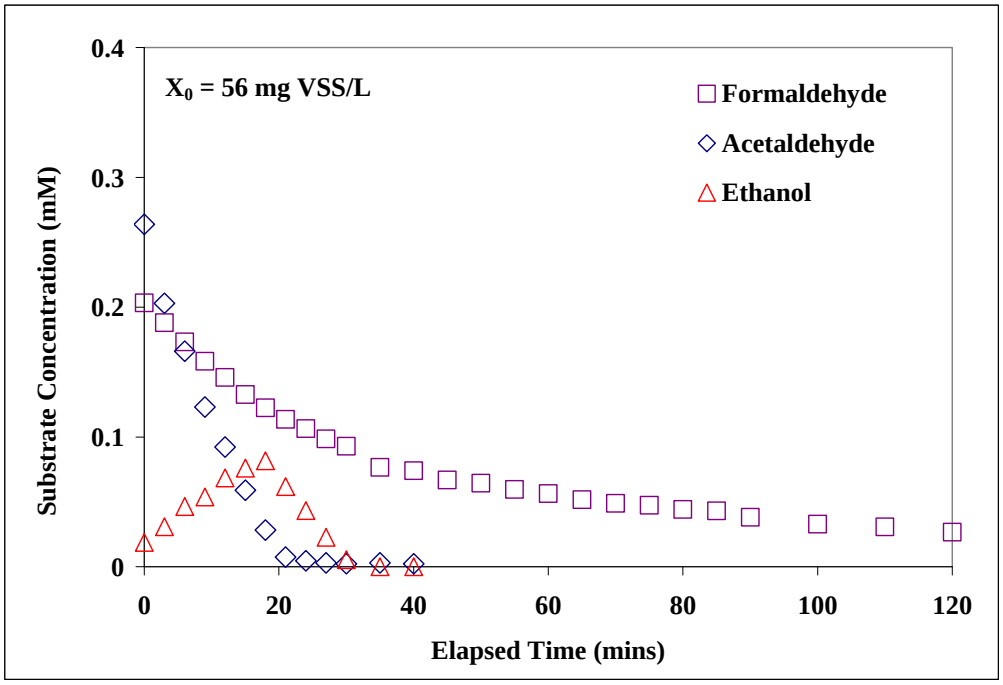

Figure 3.14. Concentration profiles for formaldehyde and acetaldehyde degradation in the binary substrate system (Experiment of BS-FA-4). The concentration profile for ethanol, a byproduct of acetaldehyde degradation, is also included.

Based on the experimental data, acetaldehyde was completely degraded within 30 minutes of the start of the experiment. In contrast to the results reported for

Experiments SS-A-8 and BS-AE, ethanol was completely eliminated following its accumulation as a result of acetaldehyde degradation. On the other hand, only about 87% of the formaldehyde was eliminated by the end of Experiment BS-FA-4 as compared to single formaldehyde degradation in Experiment SS-F-7, even though the biomass concentration in Experiment BS-FA-4 was higher. Thus, formaldehyde degradation was detrimentally affected by the presence of acetaldehyde. It is not clear if formaldehyde degradation was inhibited due to the presence of acetaldehyde itself or due to the production of its degradation byproducts such as ethanol and acetate. No previous studies examining the simultaneous degradation of formaldehyde and acetaldehyde or the degradation of formaldehyde and ethanol have been reported. Even so, a few studies have purified membrane-bound ADHs from several acetic acid bacteria and examined substrate specificity of these enzymes with respect to ethanol and formaldehyde (Tayama *et al*., 1989; Shinagawa *et al*., 2006). Tayama *et al*. (1989) reported that the ADH in *A. polyoxogenes* sp. nov. showed a stronger activity toward ethanol than toward formaldehyde (62% relative to ethanol specific activity). Similarly, the ADHs purified from *Acetobacter sp.* SKU 14, *A. aceti* IFO 3284 and *G. suboxydans* IFO 12528 also had a higher activity toward ethanol than toward formaldehyde (50% relative to ethanol specific activity). If an enzyme like ADH in the binary substrate system was capable of ethanol and formaldehyde degradation, then competition for the catalytic enzyme between the two substrates would be possible.

Degradation of Formaldehyde and Ethanol

Based on the results of the binary substrate experiments that paired formaldehyde with acetaldehyde or acetate, it is possible that ethanol might have some negative impacts on formaldehyde degradation. Therefore, formaldehyde and ethanol were examined as binary substrates to clarify the impact of ethanol on formaldehyde degradation. Two different binary substrate experiments were conducted. In Experiment BS-FE-1, a ratio of S_0/X_0 of 0.08 mg/mg VSS for formaldehyde and 0.03 mg/mg VSS for ethanol along with an X_0 of 126 mg VSS/L were used to examine formaldehyde and ethanol degradation. As shown in Figure 3.15, both substrates were completely degraded within 60 minutes; the substrate mixtures under the conditions tested seemed to have no significant impacts on each other.

For Experiment BS-FE-2, higher S_0/X_0 values of 0.14 mg/mg VSS for formaldehyde and 0.25 mg/mg VSS for ethanol at a lower X_0 of 38 mg VSS/L were used. The degradation profiles of formaldehyde and ethanol in the binary substrate system during Experiment BS-FE-2 are also plotted in Figure 3.15. The results indicate that both formaldehyde and ethanol degradation rates were impaired under the test conditions; in particular, the ethanol removal ceased after 30 minutes. The DO concentration of 1.3 mg/L remaining in the system after 120 minutes in this experiment indicates oxygen limitation should not have been the reason for the observed inhibition. As discussed in the results section of Experiment BS-FA-4, it is possible that competitive inhibition occurred between formaldehyde and ethanol due to the higher S_0/X_0 values for both substrates in Experiment BS-FE-2, when compared with Experiment BS-FE-1. Another possible explanation is that degradation byproduct(s) of the substrate mixtures exerted a toxic/negative effect on microbial activity on the consortium that led to the decreased degradation rates for both formaldehyde and ethanol.

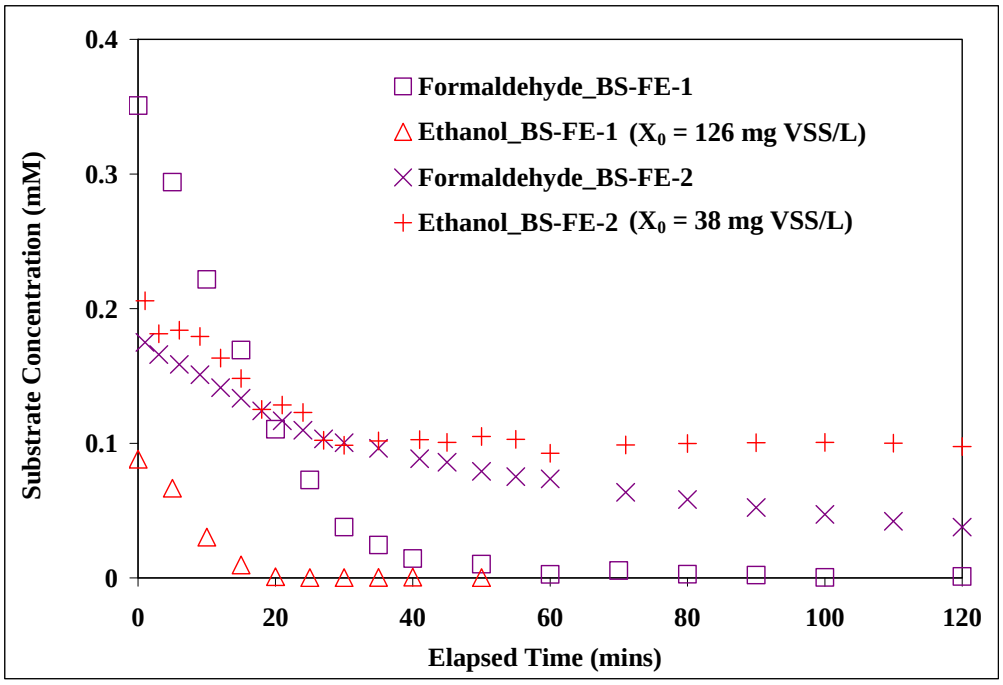

Figure 3.15. Concentration profiles for formaldehyde and ethanol degradation in the binary substrate systems (Experiments BS-FE-1 and BS-FE-2).

Based on the data obtained from Experiments BS-FE-1 and BS-FE-2, one can conclude that the mixtures of formaldehyde and ethanol can affect both ethanol and formaldehyde degradation rates in the consortium, and the inhibition becomes more significant with increasing S_0/X_0 for both substrates. Kinetic modeling using the experimental data can be used to quantify how the substrate mixtures affected formaldehyde and ethanol degradation and provide further insight into potential mechanisms. This modeling is presented and discussed in the next Chapter.

Degradation of Formaldehyde and Acetate

As seen in the single acetaldehyde experiment, the formation of acetate and ethanol was observed during acetaldehyde degradation. Therefore, it is also important to investigate if the presence of acetate would affect formaldehyde degradation and to determine whether ethanol was the only substrate that impacted formaldehyde degradation in the binary substrate system containing formaldehyde and acetaldehyde (Experiment BS-FA-4). Therefore, Experiment BS-FAc was conducted to examine formaldehyde degradation in the presence of acetate. The concentration profiles for formaldehyde, acetate and formate (formaldehyde degradation byproduct) are shown in Figure 3.16. Based on the experimental data, 0.18 mM of formaldehyde was completely eliminated within 80 minutes, and formate accumulation reached a peak concentration of 0.03 mM but decreased to non-detectable concentrations by 70 minutes. These results suggest that the presence of acetate did not have an obvious impact on formaldehyde and/or formate degradation. Acetate degradation, on the other hand, only occurred during the first 30 minutes of the experiment, leaving 25% of the acetate (~0.04 mM) remaining in the system. Since a similar degradation pattern has been observed previously for acetate in the single acetate degradation in Experiments SS-Ac-4 and SS-Ac-5, it does not appear that either formaldehyde or its degradation byproduct formate led to incomplete removal of acetate in this experiment.

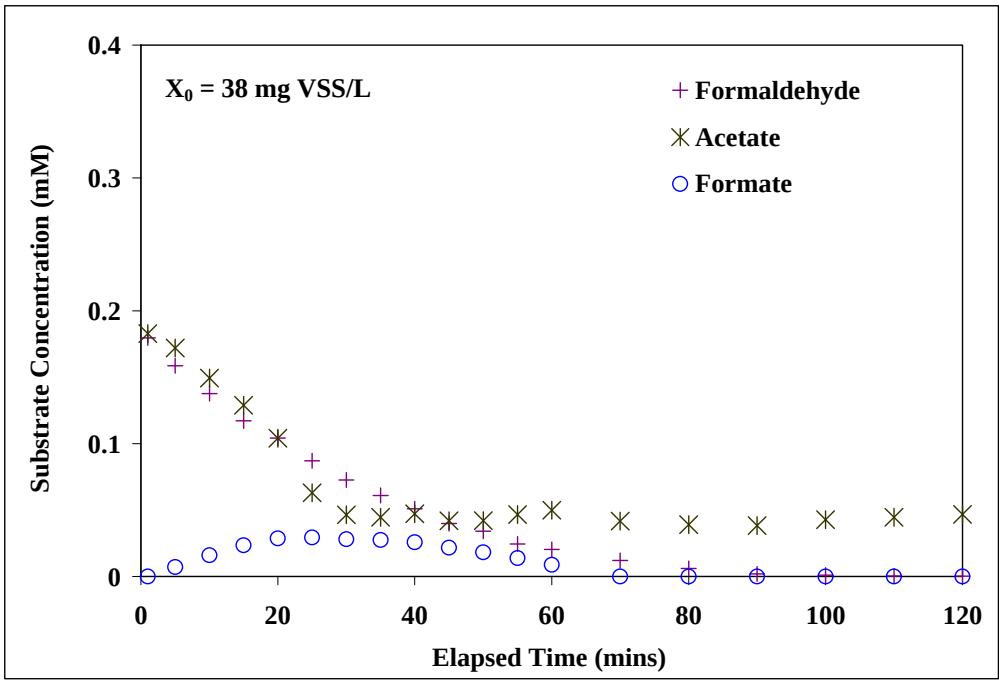

Figure 3.16. Concentration profiles for formaldehyde and acetate degradation in the binary substrate system (Experiment BS-FAc). The concentration profile for formate, a formaldehyde degradation byproduct, is also included.

3.3. SUMMARY

The first stage of experimentation was conducted to assess the effect of key parameters on substrate degradation kinetics, and the results indicate the following:

- Neither duel substrate limitations at low oxygen concentrations nor oxygen toxicity at high concentrations in the headspace-free batch systems were confounding substrate degradation kinetics.
- System pH affected aldehyde degradation; a negative impact on removal of formaldehyde and acetaldehyde was observed at pH 3.9 and 5.8, respectively.
- Enrichment conditions for the aldehyde-degrading consortium affected ethanol and acetate degradation during batch experiments; acetate degradation would not occur unless acetate was supplied as a carbon source during enrichment, while an enhanced ethanol degradation rate was observed when ethanol was used as the sole enrichment carbon source.

The results of single substrate kinetic degradation experiments showed that the enriched aldehyde-degrading consortium was capable of complete degradation of formaldehyde, acetaldehyde and ethanol under the test conditions. However, the consortium was unable to completely remove acetate from the batch reactors. The experimental data yielded consistent results in which 1-2 mg/L of acetate remained by the end of the experiments. The degradation byproducts observed during the single substrate degradation experiments using formaldehyde, acetaldehyde and ethanol are summarized in Table 3.9.

Table 3.9. Degradation byproduct(s) observed during single substrate degradation

Substrate	Byproduct(s)
Formaldehyde	Methanol; Formate
Acetaldehyde	Ethanol; Acetate
Ethanol	Acetate

The binary substrate experiments were carried out to examine substrate mixture effects on substrate degradation, and the results indicate the following:

- Acetaldehyde degradation was not affected by the presence of formaldehyde or ethanol in the binary substrate systems.
- Formaldehyde degradation was detrimentally impacted when either acetaldehyde or ethanol was supplied as a second substrate in the binary substrate systems, while the presence of acetate was not found to have a significant effect on formaldehyde removal.
- Accumulation of ethanol from acetaldehyde elimination and inhibition of ethanol degradation were observed in the binary substrate system containing acetaldehyde and ethanol.
- Inhibition of ethanol degradation in the presence of formaldehyde became significant with increasing S_0/X_0 for both substrates.

Chapter 4: Evaluation of Monod Kinetics for Ethanol Plant Pollutants

This chapter presents the biodegradation kinetic parameters determined for the selected ethanol plant pollutants in the absence and presence of a second substrate. The experimental data from the single substrate systems (Section 3.2.2) were evaluated using Monod kinetics to determine single substrate kinetic parameters. In addition, several inhibition models were applied to the experimental data from the binary substrate systems (Section 3.2.3) to assess whether the impact of co-substrates or intermediate byproducts could be quantitatively described in these systems.

4.1. METHODS

4.1.1. Determination of Monod Kinetic Parameters for Single Substrate

The experimental data from the batch kinetic experiments of formaldehyde, acetaldehyde and ethanol degradation using the enriched consortium (Section 3.2.2) were utilized to determine single substrate degradation kinetics. No kinetic parameters for acetate degradation were determined due to the incomplete degradation observed in all the acetate degradation experiments. Monod kinetics was used to model substrate degradation observed in the batch experiments, and the kinetic parameters for each substrate were estimated. Biomass concentration was treated as a constant in the Monod model equation (i.e., $X=X_0$) since the increase in biomass concentration did not exceed 10% during any of the batch experiments. Thus, substrate degradation for each substrate of interest in this research was considered as no growth Monod kinetics (Simkins and Alexander, 1984).

Nonlinear regression analysis of the experimental kinetic data was performed to determine K_s and k for each substrate of interest in this research. A fourth-order Runge-Kutta iteration method was used to calculate a series of time-based substrate concentrations using initial guessed values of K_s and k. The normalized residual sum of squares ($NRSS = \Sigma (S_{calculation}-S_{experiment})^2 / S_{experiment}^2$) between the calculated substrate concentration ($S_{calculation}$) and experimental substrate concentration ($S_{experiment}$) was then determined, and then it was minimized using the Solver routine in Microsoft Excel to solve for the best-fit values of k and K_s (Wahman, 2006). The uncertainty of the best-fit k and K_s parameters was evaluated using the approximate method described by Smith *et al*. (1998). Estimation of 95% joint confidence limits involving k and K_s was adapted from the technique described by Wahman (2006).

4.1.2. Evaluation of Substrate Interactions Using Monod Inhibition Models

To identify substrate mixture effects observed in the binary substrate systems, the Monod model describing no inhibition and three inhibition models describing competitive, noncompetitive and uncompetitive inhibition were utilized. Evaluation of Model fitting was performed on four binary substrate systems examined in Section 3.2.3, including acetaldehyde and ethanol (Experiment BS-AE), formaldehyde and ethanol (Experiment BS-FE-1), formaldehyde and acetaldehyde (Experiment BS-FA-4), and formaldehyde and acetate (Experiment BS-FAc). The equations that represent the degradation of substrate i in the presence of substrate j for the Monod model and the three inhibition models are presented in Table 4.1; all the parameters have been defined in Section 2.3.1. In addition, mean values and 95% joint confidence limits of k and K_s determined from the single substrate systems were utilized as known parameters for these models.

Table 4.1. Kinetic models used to identify substrate degradation scenarios for *i* and *j* in a binary substrate system

Scenario	Kinetic Model
Substrate *i* described by Monod model (Not inhibited by *j*)	$\frac{dC_i}{dt} = -\frac{k_i \cdot X \cdot C_i}{K_{s,i} + C_i}$
Substrate *i* competitively inhibited by *j*	$\frac{dC_i}{dt} = -\frac{k_i \cdot X \cdot C_i}{K_{s,i}\left(1 + \frac{C_j}{K_{I,j}}\right) + C_i}$
Substrate *i* noncompetitively inhibited by *j*	$\frac{dC_i}{dt} = -\frac{k_i \cdot X \cdot C_i}{\left(K_{s,i} + C_i\right)\left(1 + \frac{C}{K_{I,j}}\right)}$
Substrate *i* uncompetitively inhibited by *j*	$\frac{dC_i}{dt} = -\frac{k_i \cdot X \cdot C_i}{\left(K_{s,i}\left(1 + \frac{C_j}{K_{I,1,j}}\right) + C_E\right)\left(1 + \frac{C_j}{K_{I,2,j}}\right)}$

To perform this task, AQUASIM was utilized as the computer modeling tool. Each of the binary substrate experiments was established as an independent *System* in AQUASIM. For each system, experimental conditions such as initial biomass concentration and substrate concentration profile, as well as single kinetic parameters such as k and K_s, were provided to the program component titled *Variables*. Then, the potential kinetic models (shown in Table 4.1) were integrated into each of the program components titled *Process*, and all the processes associated with both substrates were then included in the program component titled *Mixed Reactor Compartment*. Model fitting to the experimental data through a series of nonlinear regression analyses for three inhibition scenarios were performed. The sum of the squares of the weighted deviations ($\chi^2 = \Sigma\ (S_{experiment}\text{-}S_{fit})^2\ /\sigma^2$) between experimental data ($S_{experimental}$) and the model fit (S_{fit})

was minimized to generate an estimated K_I value(s) for each of the inhibition scenarios. The scenario that yielded the lowest χ^2 value was selected as the best model to describe substrate mixture effects in the binary substrate systems. To evaluate a scenario that degradation of one substrate was not inhibited by the presence of a second substrate, Monod model predictions using single kinetic parameters for the substrates of interest were carried out in AQUASIM. Experimental data were then compared with model predictions for agreement.

4.2. RESULTS AND DISCUSSION

4.2.1. Monod Kinetic Parameters for Single Substrates

The single substrate data from Experiments SS-F-7 (formaldehyde), SS-E-4/SS-E-6 (ethanol) and SS-A-8 (acetaldehyde) were used to determine the single substrate Monod kinetic parameters using nonlinear regression analysis. The main difference between Experiments SS-E-4 and SS-E-6 is that ethanol was used as the sole carbon source during biomass enrichment for Experiment SS-E-6, while ethanol and two aldehydes were supplied as the carbon sources during the enrichment period for Experiment SS-E-4.

The experimental data for the single substrate degradation experiments and the concentration profiles simulated by the Monod model for formaldehyde, ethanol and acetaldehyde are shown in Figures 4.1 to 4.3. As evident in Figures 4.1 and 4.2, single substrate formaldehyde and ethanol degradation can be described by the Monod model. However, the fitted curve for single acetaldehyde degradation, shown in Figure 4.3, predicted a slightly faster elimination between 5 to 25 minutes than was observed in the results of Experiment SS-A-8. However, it is difficult to conclude only based on this

model fit if the disagreement was analytical, was the result of acetaldehyde production from ethanol degradation via Pathway C, or the inadequacy of the model. Additional analysis will be required to confirm if acetaldehyde is produced in a batch system where ethanol is supplied to the enriched consortium as the sole carbon source. If the scenario does occur, acetaldehyde production kinetics, as a result of ethanol degradation, can be established and utilized to evaluate the acetaldehyde concentration profile derived in Experiment SS-A-8. The model fit to the ethanol concentration profile, shown in Figure 4.3, is discussed further in Section 4.2.2.

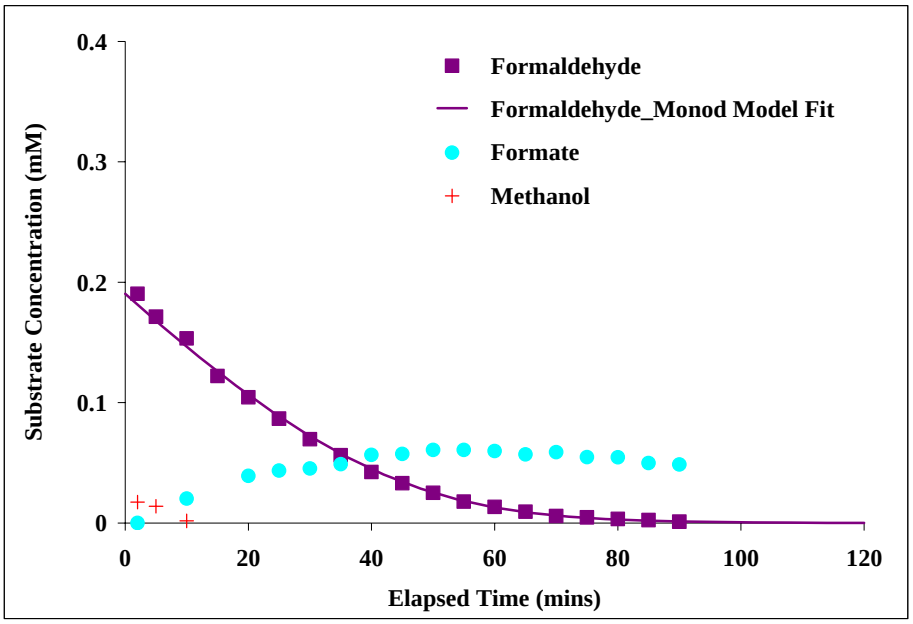

Figure 4.1. Experimental data (symbols) and Monod model fit (line) for single formaldehyde degradation in Experiment SS-F-7. Data of formate and methanol, the degradation products of formaldehyde, are also included.

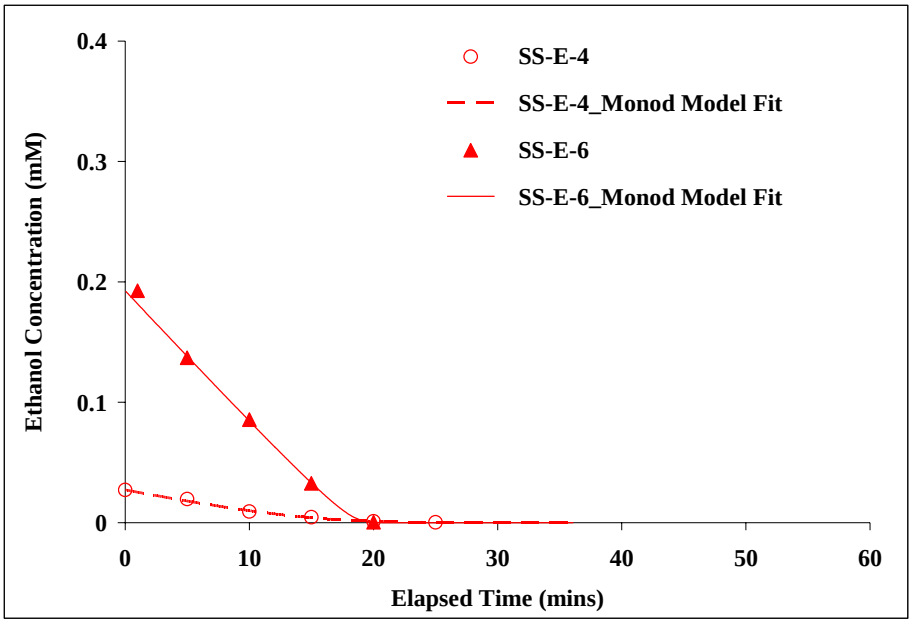

Figure 4.2. Experimental data (symbols) and Monod model fit (lines) for single ethanol degradation in Experiments SS-E-4 and SS-E-6.

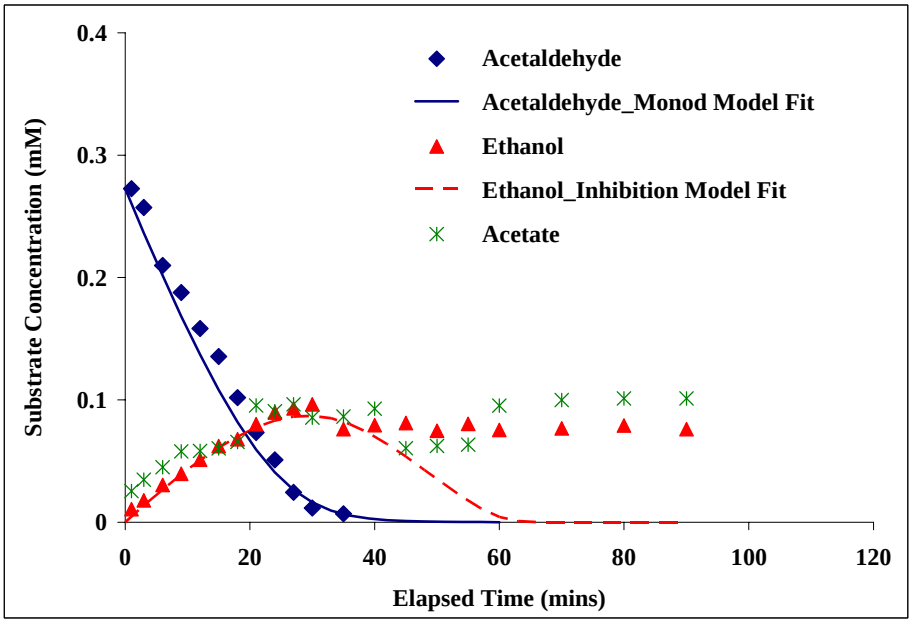

Figure 4.3. Experimental data (symbols) and Monod model fit/prediction (lines) for single acetaldehyde degradation in Experiment SS-A-8. Data of ethanol and acetate, the degradation products of acetaldehyde, are also included.

The Monod parameters K_s and k values estimated along with their 95% joint confidence limits for formaldehyde, acetaldehyde and ethanol are also listed in Table 4.2. The K_s values are affected more by carbon oxidation state then by carbon content as the values increase in the order ethanol < formaldehyde ≈ acetaldehyde. The K_s value for ethanol (0.007~0.008 mM) is one order of magnitude smaller than the K_s values for either formaldehyde (0.07 mM) or acetaldehyde (0.08 mM), implying that ethanol is the most biodegradable of the substrates. Compared with the K_s value of ethanol determined in this research, Lovanh *et al*. (2002) reported a slightly lower K_s value of 0.088 mg/L (0.002 mM) for aerobic ethanol degradation using *Pseudomonas putida* F1. A similar K_s value (2±1 mg/L) for aerobic acetaldehyde degradation was determined by Rajagopalan *et al.* (1998).

Table 4.2. Summary of 95% joint confidence limits for single substrate Monod kinetic parameters of K_s and k determined during the batch experiments

Substrate (Experiment)	k (mg/mg VSS/hr)			K_s (mM) (K_s (mg/L))		
	Lower 95%	Mean	Upper 95%	Lower 95%	Mean	Upper 95%
Formaldehyde (SS-F-7)	0.23	0.27	0.31	0.05 (1.60)	0.07 (2.12)	0.09 (2.64)
Acetaldehyde (SS-A-8)	0.54	0.85	1.16	0.02 (0.72)	0.08 (3.50)	0.14 (6.29)
Ethanol (SS-E-4)	0.16	0.23	0.30	0.003 (0.14)	0.007 (0.32)	0.011 (0.50)
Ethanol (SS-E-6)	0.90	0.95	1.00	0.006 (0.29)	0.008 (0.38)	0.010 (0.46)

No values of K_s for formaldehyde degradation under aerobic conditions were found in previous research for comparison. A few studies have reported Monod kinetic parameters for anaerobic formaldehyde degradation. For instance, Qu *et al*. (1997) estimated Monod kinetic parameters by examining anaerobic formaldehyde degradation by a methanogenic culture in serum bottles. They reported K_s values of 2.1-2.4 mg/L with k values of 0.35-0.46 day^{-1} derived from the culture prior to acetate acclimation, and K_s values of 0.8-3.7 mg/L with 0.35-0.42 day^{-1} after the culture was acclimated to acetate.

As shown in Table 4.2, the estimated k value (in mg/mg VSS/L) for acetaldehyde (0.85±0.31) is higher than the value for formaldehyde (0.27±0.04). Since the K_s values for the aldehydes are similar, the consortium should have a higher utilization rate of acetaldehyde than formaldehyde for similar aldehyde concentrations. In addition, the k value for single ethanol degradation in Experiment SS-E-6 (0.95±0.05) is higher that that in Experiment SS-E-4 (0.23±0.07). The difference in k indeed reflects differences in the carbon sources used during biomass enrichment (i.e., two aldehydes and ethanol for Experiment SS-E-4 and only ethanol for Experiment SS-E-6). Given that the consortium used in the binary substrate kinetic experiments was enriched under conditions similar to that in Experiment SS-E-4, the ethanol kinetic parameters derived based on Experiment SS-E-4 were utilized in the following evaluation of the binary substrate experiments.

4.2.2. Binary Substrate Degradation Kinetics

Acetaldehyde and Ethanol

As discussed in Section 3.2.3, the enriched consortium in this research preferred acetaldehyde reduction to ethanol oxidation when both acetaldehyde and ethanol were present in the batch reactor. As a result, acetaldehyde was eliminated as ethanol accumulated in the system, and even after the acetaldehyde was removed from the system, ethanol degradation was virtually non-existent (Figure 4.4). To account for this observation in Experiment BS-AE, two mass balance equations with respect to both substrates in the system were written as follows.

Rate of change of acetaldehyde mass in a batch reactor = ***Degradation of acetaldehyde mass per unit time in a batch reactor***

$$\frac{d}{dt}\left(C_A \cdot V\right) = r_A \cdot V \qquad \text{(Equation 4.1)}$$

Rate of change of ethanol mass in a batch reactor = ***Formation of ethanol mass per unit time in a batch reactor*** - ***Degradation of ethanol mass per unit time in a batch reactor***

$$\frac{d}{dt}\left(C_E \cdot V\right) = -\alpha \cdot r_A \cdot V + r_E \cdot V \qquad \text{(Equation 4.2)}$$

where V = liquid volume in a batch reactor (L);

C_A, C_E = acetaldehyde and ethanol concentrations (mg/L);

r_A, r_E = biodegradation rates of acetaldehyde and ethanol (mg/L/hr);

α = stoichiometric coefficient (determined experimentally).

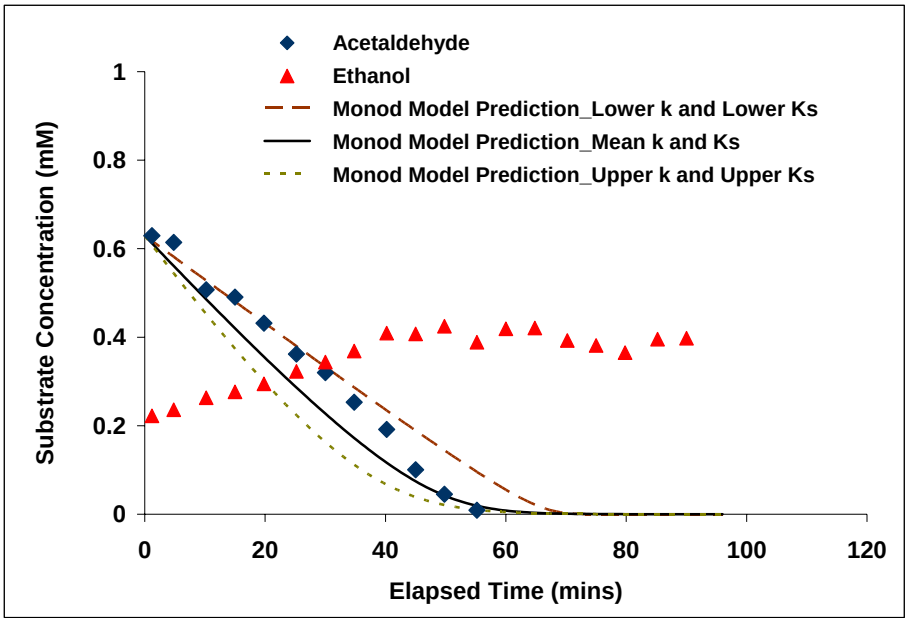

Figure 4.4. Experimental data (symbols) and Monod model predictions (lines) for acetaldehyde degradation in the presence of ethanol (Experiment BS-AE).

First, to assess whether acetaldehyde degradation was affected by the addition of ethanol at the beginning of the binary substrate experiment, the Monod model was utilized to predict acetaldehyde degradation without inhibition. The initial acetaldehyde and biomass concentrations, along with the single acetaldehyde kinetic parameters determined in the previous section, were applied to the Monod model. Three different Monod model predictions using mean values and lower and upper 95% joint confident limits for k and K_s (Table 4.2) were generated and compared to the acetaldehyde experimental data (Figure 4.4). The first prediction used the mean values of k and K_s. The second prediction used the lower 95% joint confident limits of k and K_s and finally, the third used the upper 95% joint confident limits of k and K_s.

Figure 4.4 indicates that the experimental data are within the range predicted by the lower and upper 95% joint confident limits of k and K_s. However, the actual Monod

model prediction underpredicts acetaldehyde degradation especially in the middle of the experiment from 15 to 45 minutes. The degradation pattern, evident in Figure 4.4, is similar to the pattern observed for the single-substrate acetaldehyde data (Figure 4.3). This implies that there could be another contributing factor to the observed acetaldehyde kinetics. According to the discussion in Chapter 3, it is possible that acetaldehyde- and ethanol-degrading microbial communities were present in the enriched consortium. Therefore, this difference between the experimental data and the model simulations could be a result of acetaldehyde production by the ethanol-degrading community. If this assumption is correct then the acetaldehyde Monod parameters estimated from the single substrate data reflect apparent degradation rates in which both degradation and production are incorporated into the Monod parameters. Nevertheless, since the estimated Monod kinetic parameters predict acetaldehyde concentration variation in the batch systems, the acetaldehyde kinetics were still utilized to examine its effects on degradation of other substrates in the following sections.

Next, to understand how acetaldehyde influenced ethanol removal in the binary system, ethanol degradation was evaluated under four scenarios corresponding to four different kinetic expressions (Table 4.3) for the rate of substrate utilization $r_{E,}$ in Equation 4.2. It is important to note that the α term in Equation 4.2 was a stoichiometric coefficient (0.4), which was calculated based on the elimination rate of acetaldehyde divided by the formation rate of ethanol during the first 30 minutes of both Experiments SS-A-8 and BS-AE. It should be noted that the uncompetitive inhibition model fit was identical to that of the noncompetitive inhibition model (see the following discussion). As a result, the simulations for the Monod, competitive inhibition and noncompetitive inhibition models along with the experimental data are shown in Figure 4.5.

Table 4.3. Summary of kinetic expressions evaluated in the mass balance equations for acetaldehyde and ethanol degradation in Experiment BS-AE

Substrate	Scenario	Expression	Parameters
Acetaldehyde (A)	No Inhibition by E	$r_A = -\frac{k_A \cdot X \cdot C_A}{K_{s,A} + C_A}$	-
Ethanol (E)	No Inhibition by A	$r_E = -\frac{k_E \cdot X \cdot C_E}{K_{s,E} + C_E}$	-
	Competitive Inhibition by A	$r_E = -\frac{k_E \cdot X \cdot C_E}{K_{s,E}\left(1 + \frac{C_A}{K_{I,A}}\right) + C_E}$	$K_{I,A}$
	Noncompetitive Inhibition by A	$r_E = -\frac{k_E \cdot X \cdot C_E}{\left(K_{s,E} + C_E\right)\left(1 + \frac{C_A}{K_{I,A}}\right)}$	$K_{I,A}$
	Uncompetitive Inhibition by A	$r_E = -\frac{k_E \cdot X \cdot C_E}{\left(K_{s,E}\left(1 + \frac{C_A}{K_{I,A,1}}\right) + C_E\right)\left(1 + \frac{C_A}{K_{I,A,2}}\right)}$	$K_{I,A,1}$ $K_{I,A,2}$

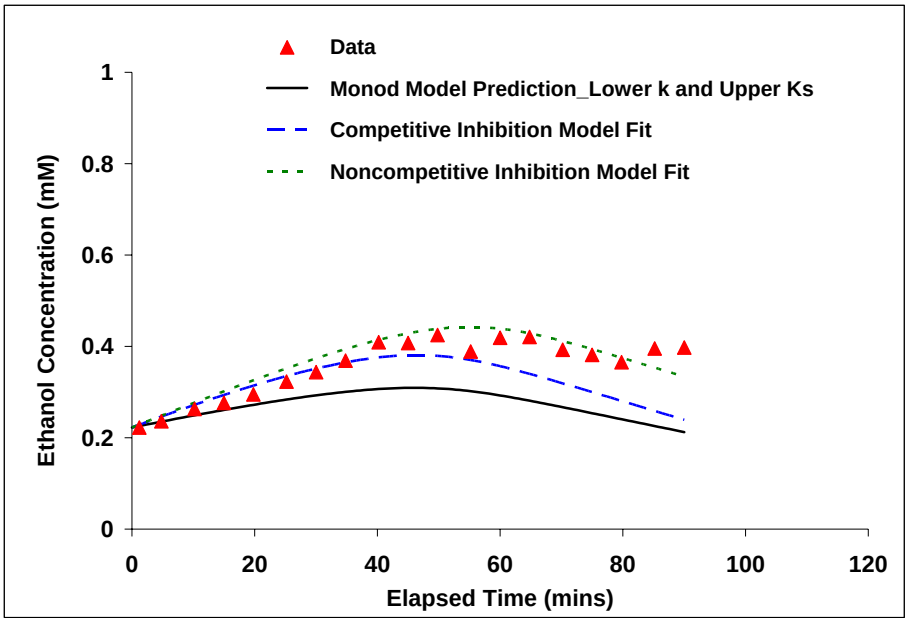

Figure 4.5. Experimental data (triangles) and model predition/fit (lines) for ethanol degradation in the presence of acetaldehyde (Experiment BS-AE).

Ethanol degradation was inhibited in the binary substrate system as the Monod model prediction using the joint 95% confident limits of lower k and upper K_s did not agree with the experimental data. The Monod prediction shown in Figure 4.5 underpredicts the experimental data except at the beginning of the experiment. The experimental data can be described by either noncompetitive or uncompetitive inhibition; however, the fitted $K_{I,A,1}$ value in the noncompetitive inhibition model reduced the $(1+C_A/K_{I,A,1})$ term to 1, and forced uncompetitive inhibition to converge to noncompetitive inhibition. Based on the modeling results, it appears that ethanol degradation was noncompetitively inhibited by acetaldehyde and an inhibition constant of acetaldehyde ($K_{I,A}$) of 0.36 mg/L was estimated from this inhibition model based on the fitting results.

The kinetic parameters derived from single substrate degradation (Experiment SS-E-4) and binary substrate degradation (Experiment BS-AE) were utilized to predict ethanol concentrations for Experiment SS-A-8 in which acetaldehyde degradation produced ethanol as an intermediate. As shown in Figure 4.3, the predicted ethanol profile only agrees with the experimental data for the first 40 minutes of the experiment. It should be noted that the model prediction was based on inhibition of ethanol degradation in the presence of acetaldehyde. The fact that ethanol degradation remained inhibited after acetaldehyde was completely eliminated indicates another mechanism was involved. It has been reported that ADHs in acetic acid bacteria are sensitive to acetic acid (Park *et al*., 1989). Therefore, increasing acetic acid concentrations observed in the experiment could result in lower ADH activity and reduced ethanol oxidation. Since the consortium was incapable of complete acetate degradation, acetate from ethanol oxidation accumulated and appeared to have negatively impacted the ethanol-catalyzing enzymes, leading to further inhibition of ethanol degradation.

Formaldehyde and Ethanol

The data from the binary substrate systems containing formaldehyde and ethanol (Section 3.2.3) suggest that removal of both substrates was dependent on S_0/X_0 for both substrates. Although complete removal of formaldehyde and ethanol was observed during Experiment BS-FE-1, formaldehyde degradation slowed and ethanol degradation completely stopped during the course of Experiment BS-FE-2. Since the selected inhibition models can only evaluate interactions between substrates and toxicity effects on microbial activity are not considered in the models, only data from Experiment BS-FE-1 were used to evaluate substrate interactions between formaldehyde and ethanol.

Prior to identifying potential inhibition between the binary substrates, the Monod model was utilized to predict formaldehyde and ethanol degradation without inhibition. Mean values and 95% joint confidence limits of k and K_s for two substrates (Table 4.2) were used in the Monod model for prediction. The data for formaldehyde degradation in the presence of ethanol, as well as the Monod model predictions based on three pairs of k and K_s. are presented in Figure 4.6. The Monod model prediction using the k and K_s values estimated from the single substrate data appears to underestimate the concentrations of formaldehyde throughout the experiment. However, the Monod model prediction using the lower bound of k and the upper bound of K_s from the 95% joint confidence limits on these parameters does fit the experimental data. Single ethanol kinetic parameters of k and K_s (Table 4.2) were also applied to the Monod model to predict ethanol degradation without inhibition. The experimental data and Monod model predictions for ethanol degradation during Experiment BS-FE-1 are shown in Figure 4.7. Similarly, the Monod model prediction based on the 95% joint confidence limits for lower k and upper K_s barely capture the experimental data. Nonetheless, the results imply that the binary substrate mixtures did not have significant impacts on either formaldehyde or ethanol degradation under the test conditions of Experiment BS-FE-1.

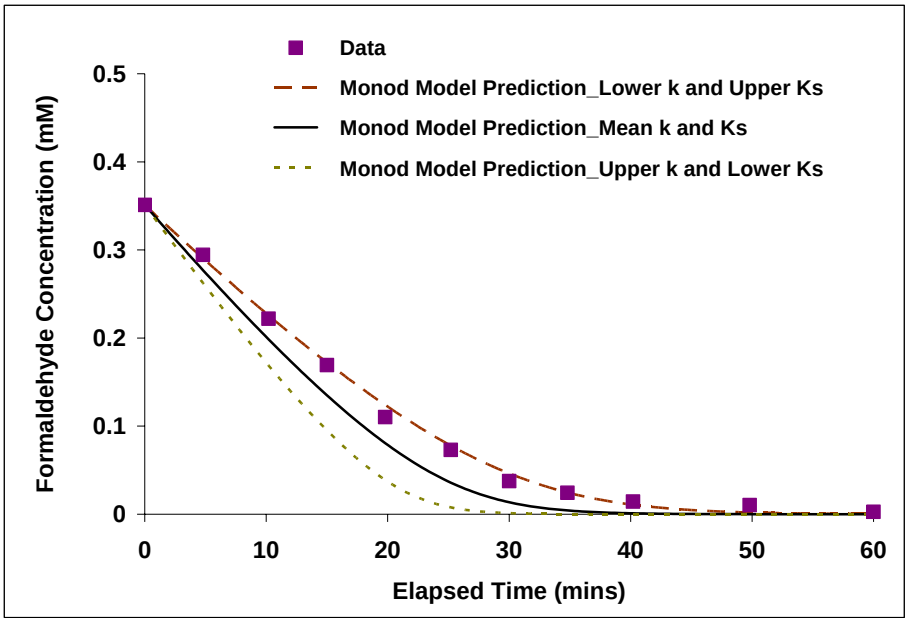

Figure 4.6. Experimental data and Monod model predictions for formaldehyde degradation in the presence of ethanol (Experiment BS-FE-1).

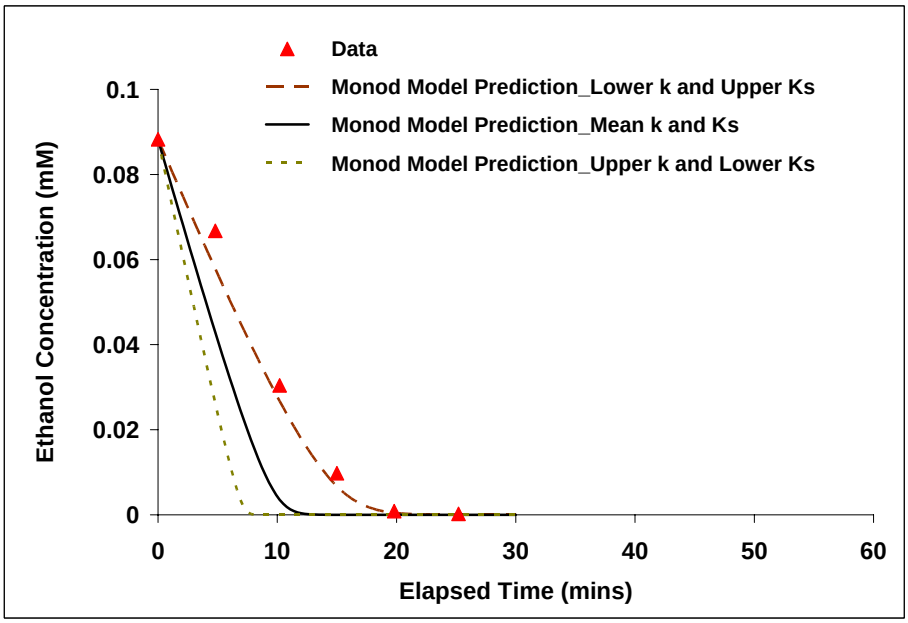

Figure 4.7. Experimental data and Monod model prediction for ethanol degradation in the presence of formaldehyde (Experiment BS-FE-1).

Although no inhibition of substrate degradation in the mixture containing formaldehyde and ethanol during Experiment BS-FE-1 can be inferred from the comparison of Monod model predictions to the data, an inhibition scenario was considered. Competitive and noncompetitive inhibition models were utilized to evaluate the potential for inhibition. Equations 4.3 and 4.4 were respectively written for formaldehyde and ethanol degradation in the batch system, where r_E and r_F were replaced with the corresponding expression to reflect either competitive inhibition (Equation 4.5) or noncompetitive inhibition (Equation 4.6). The K_I term was the only fitting parameter, and AQUASIM was used to determine a best value for each inhibition model.

Rate of change of formaldehyde mass in a batch reactor = ***Degradation of formaldehyde mass per unit time in a batch reactor***

$$\frac{d}{dt}\left(C_F \cdot V\right) = r_F \cdot V \qquad \text{(Equation 4.3)}$$

Rate of change of ethanol mass in a batch reactor = ***Degradation of ethanol mass per unit time in a batch reactor***

$$\frac{d}{dt}\left(C_E \cdot V\right) = r_E \cdot V \qquad \text{(Equation 4.4)}$$

$$r_i = -\frac{k_i \cdot X \cdot C_i}{K_{s,i}\left(1 + \frac{C_j}{K_{I,j}}\right) + C_i} \qquad \text{(Equation 4.5; competitive inhibition)}$$

$$r_i = -\frac{k_i \cdot X \cdot C_i}{\left(K_{s,i} + C_i\right)\left(1 + \frac{C_j}{K_{I,j}}\right)}$$ (Equation 4.6; noncompetitive inhibition)

As seen in Figure 4.8, the competitive and noncompetitive inhibition model fits for formaldehyde degradation overlapped, yielding a χ^2 value of 2.9 in each case. The modeling results imply that the presence of ethanol might have negatively affected formaldehyde degradation in the binary substrate system; however, the inhibition does not appear to be sufficient enough to allow for it to be distinguished as either competitive or noncompetitive inhibition by the models.

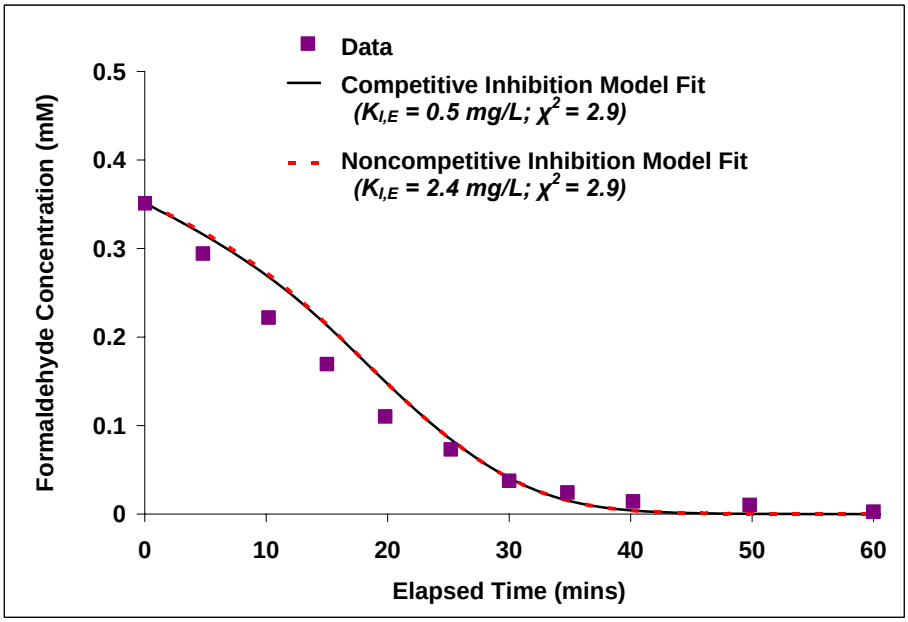

Figure 4.8. Inhibition model fits for formaldehyde degradation in the presence of ethanol in Experiment BS-FE-1.

The potential inhibition effect of formaldehyde on ethanol degradation was also evaluated using the competitive and noncompetitive inhibition models, and the model results are shown in Figure 4.9. The fit from the competitive inhibition model provided a slightly lower χ^2 value, when compared to the noncompetitive inhibition model. In other words, if substrate inhibition did occur during Experiment BS-FE-1, it is more likely that formaldehyde competitively inhibited ethanol degradation in the binary substrate system. A formaldehyde inhibition constant ($K_{I,F}$) of 2.0 mg/L was estimated based on the competitive inhibition model fit by AQUASIM.

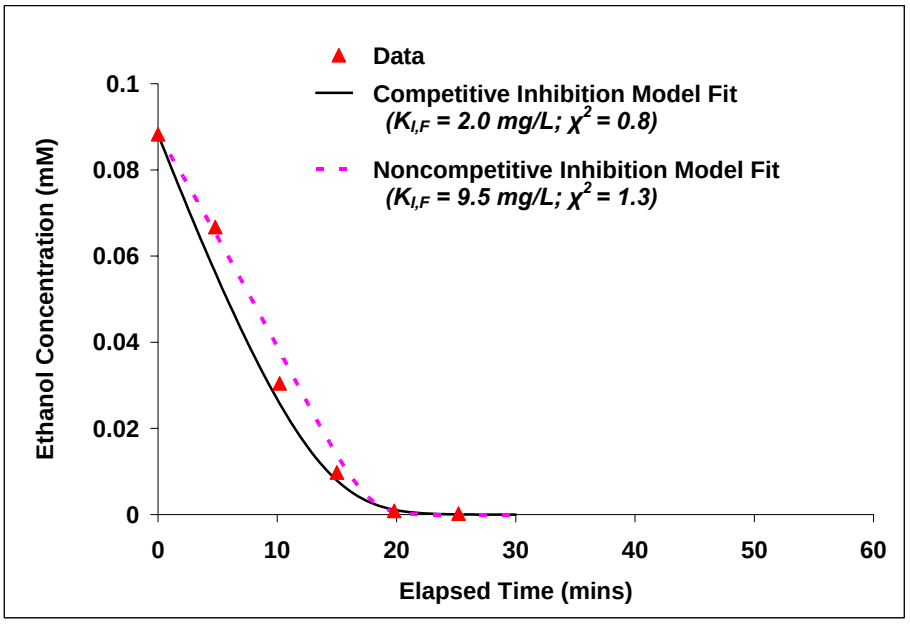

Figure 4.9. Results of inhibition model fit for ethanol degradation in the presence of formaldehyde in Experiment BS-FE-1.

Formaldehyde and Acetaldehyde

For the binary substrate system containing two aldehydes (Experiment BS-FA-4), acetaldehyde degradation in the presence of formaldehyde was evaluated first. To determine if acetaldehyde degradation was affected by formaldehyde, the Monod model prediction curves using single acetaldehyde kinetic parameters (Table 4.2) were generated. As seen in Figure 4.10, the acetaldehyde experimental data fall between the Monod model predictions obtained using 95% joint confidence limits for k and K_s, regardless of the presence of formaldehyde in the binary substrate system. Alternatively, the Monod model was used to fit the experimental data, yielding a k value of 1.1 mg/mg VSS/hr. By examining the Monod model fit and the experimental data for acetaldehyde degradation shown in Figure 4.10, a slight decrease in the rate of acetaldehyde removal was observed as ethanol was produced from acetaldehyde between 8 to 18 minutes, again suggesting the potential for ethanol oxidation to acetaldehyde by an ethanol-degrading microbial community (see the results section for Experiment BS-AE).

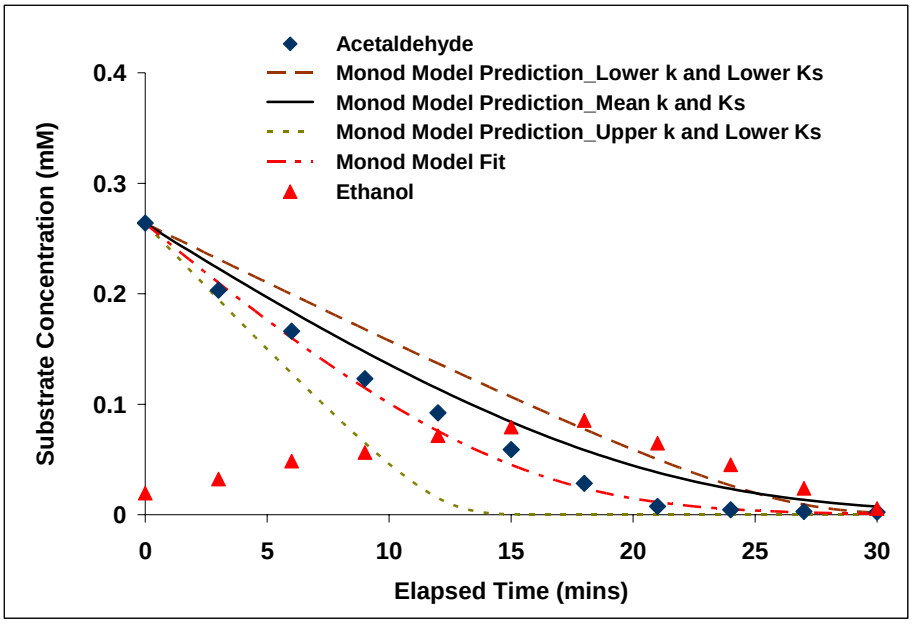

Figure 4.10. Experimental data (diamonds) and Monod model prediction/fit (lines) for acetaldehyde degradation in the presence of formaldehyde in Experiment BS-FA-4. Ethanol data (triangles) are also shown for evaluation.

As discussed earlier, noncompetitive inhibition of ethanol degradation in the presence of acetaldehyde was confirmed in Experiment BS-AE. In addition, the previous evaluation for Experiment BS-FE-1 indicates that the presence of formaldehyde did not show a significant impact on ethanol degradation. Therefore, the models that best described substrate interactions between acetaldehyde and ethanol in Experiment BS-AE were also checked for applicability in this binary experiment. A new value for the inhibition parameter was determined for ethanol using this data. Figure 4.11 shows the experimental data and the model simulation for ethanol degradation in the binary aldehyde system. As is evident in this figure, the model fit and the experimental ethanol data are in good agreement. The inhibition constant of acetaldehyde ($K_{I,A}$) on ethanol degradation was estimated as 0.93±0.63 mg/L for this experiment, which is similar to the

value of 0.36 mg/L estimated for Experiment BS-AE. These results also confirm that the presence of formaldehyde in the binary aldehyde systems did not inhibit ethanol degradation.

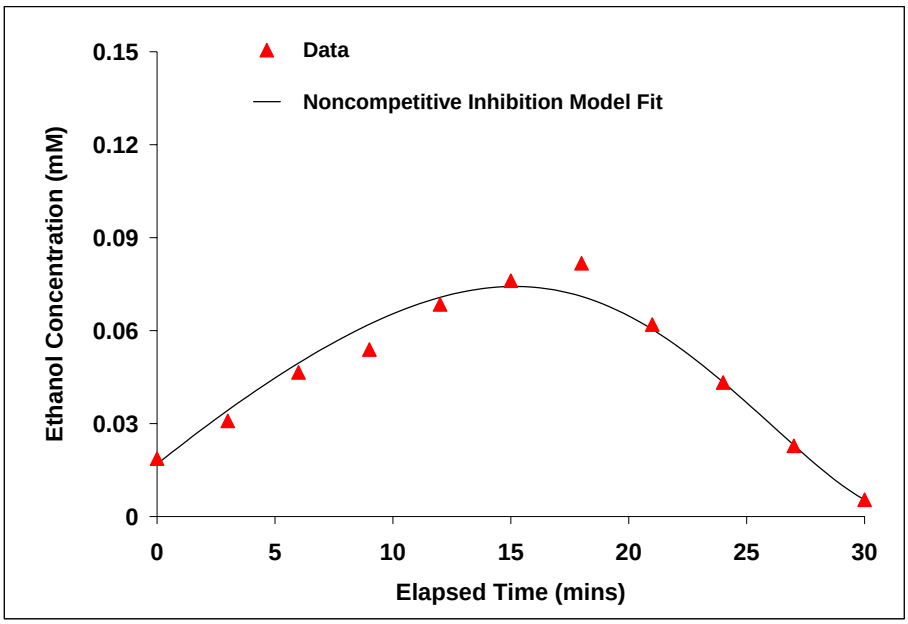

Figure 4.11. Experimental data and noncompetitive inhibition model fit for ethanol degradation in the presence of acetaldehyde and formaldehyde (Experiment BS-FA-4)

Formaldehyde degradation in Experiment BS-FA-4 was evaluated to determine if either acetaldehyde or ethanol potentially inhibited formaldehyde elimination. It is important to note that only the data observed between 0 and 30 minutes were used in modeling since acetaldehyde and ethanol were not present in the system after 30 minutes of Experiment-FA-4. Formaldehyde degradation was examined using the Monod model without inhibition. As shown in Figure 4.12, the Monod model prediction again appeared to overestimate the rate of formaldehyde degradation in the binary substrate experiment but the model prediction using the lower bound k and the upper bound K_s

values from the the 95% joint confidence limits provided a good fit to the experimental formaldehyde data within the first 30 minutes of the experiment. The formaldehyde concentration profile started to deviate from the Monod model prediction as the ethanol concentration decreased between 20 and 30 minutes. However, it is difficult to conclude what led to the observed inhibition of formaldehyde degradation based on the existing results. Therefore, future examination is necessary to clarify if the inhibition was due to depletion of an essential nutrient or cofactor, or was due to the production of a toxic degradation byproducts that was not identified in this research.

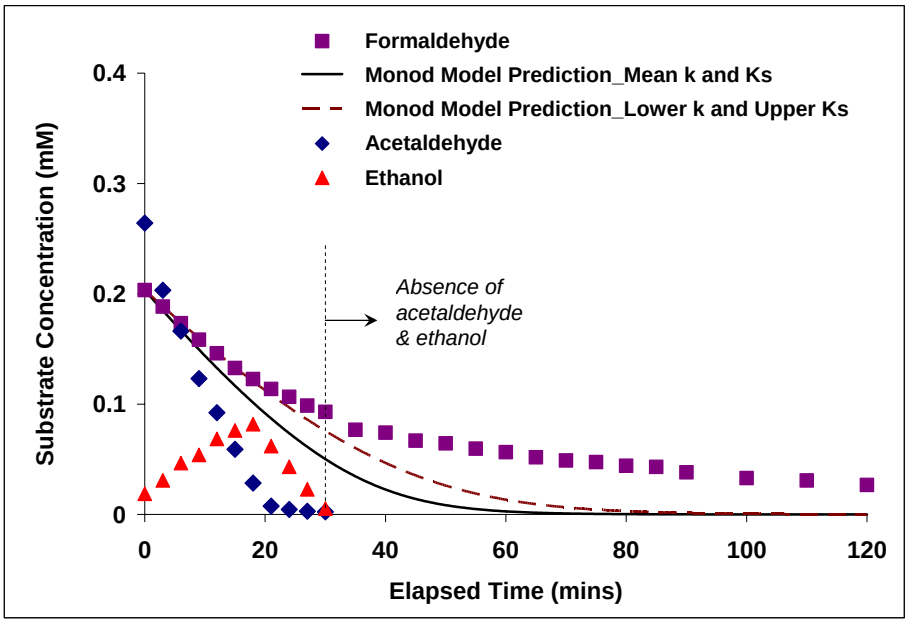

Figure 4.12. Experimental data (squares) and Monod model fit (lines) for formaldehyde degradation in the presence of acetaldehyde and ethanol (Experiment BS-FA-4). Data of acetaldehyde (diamonds) and ethanol (triangles) are also shown.

Formaldehyde and Acetate

In Experiment BS-FAc, formaldehyde was paired with acetate, and their degradation profiles in the binary substrate system were monitored. As discussed earlier in Section 3.2.3, formaldehyde was completely eliminated in the presence of acetate while a portion of acetate remained in the system. Therefore, the Monod model using the mean values and 95% joint confidence limits of k and K_s was used to generate three predictions for formaldehyde degradation. As shown in Figure 4.13, formaldehyde degradation in the presence of acetate was described well by the Monod model suggesting that acetate did not affect formaldehyde degradation under the test conditions of Experiment BS-FAc.

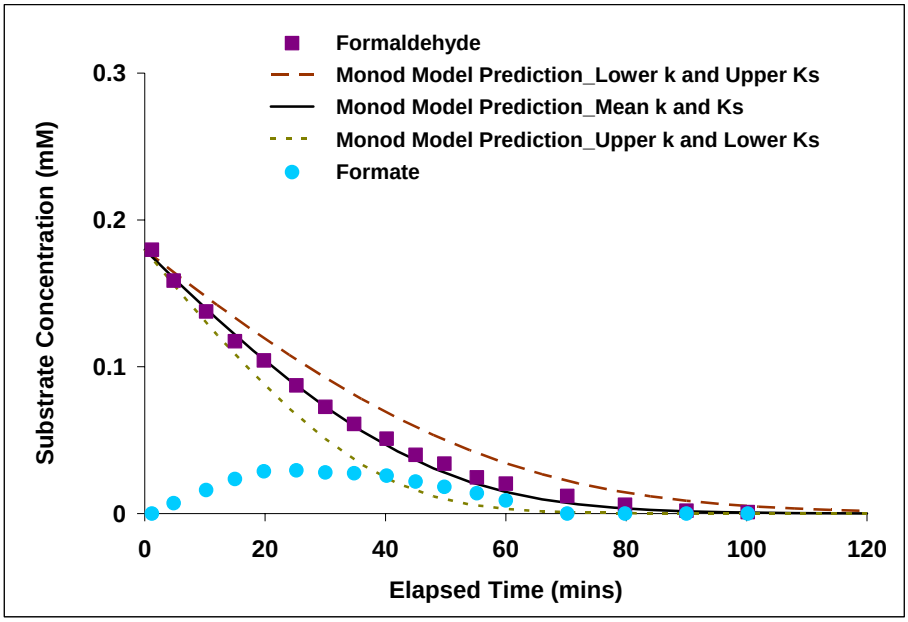

Figure 4.13. Experimental data and Monod model prediction for formaldehyde degradation in the presence of acetate (Experiment BS-FAc). Formate (formaldehyde degradation byproduct) data are also shown.

4.3. SUMMARY

The kinetic parameters for single substrate degradation using formaldehyde, acetaldehyde and ethanol have been determined by fitting the Monod model to the experimental data. Based on the evaluation of substrate degradation kinetics, ethanol had the smallest half-saturation constant ($K_{s,E}$=0.3±0.2 mg/L) followed by formaldehyde ($K_{s,F}$=2.1±0.5 mg/L) and acetaldehyde ($K_{s,A}$=3.5±2.8 mg/L). These estimated K_s values suggest that ethanol was the most biodegradable among the three substrates.

In addition, the results of this evaluation suggest that k (mg/mg VSS/hr) for ethanol degradation in a single substrate system changed with biomass enrichment conditions. The k for single ethanol degradation varied from 0.95±0.05 (with ethanol as the sole enrichment carbon source) to 0.23±0.07 (with ethanol and two aldehydes as the enrichment carbon sources). In addition, the consortium had a higher utilization rate for acetaldehyde (k_A=0.85±0.31 mg/mg VSS/hr) than for either ethanol (k_E=0.23±0.07 mg/mg VSS/hr) or for formaldehyde (k_F=0.27±0.04 mg/mg VSS/hr) when formaldehyde and acetaldehyde were used as the carbon sources during biomass enrichment.

The effects of binary substrate mixtures on the removal of formaldehyde, acetaldehyde and ethanol using the consortium were also evaluated through the Monod model and selected inhibition models. Several conclusions can be made as follows:

- Degradation of acetaldehyde in the presence of either ethanol or formaldehyde in the binary substrate systems can be predicted by the Monod model describing single substrate degradation.
- Ethanol was produced from acetaldehyde degradation, and acetaldehyde concurrently inhibited ethanol degradation noncompetitively ($K_{I,A}$ of 0.93±0.63 mg/L); this is believed to be due to an acetaldehyde-degrading microbial community in the consortium.

- Acetaldehyde production from ethanol may have impacted the rate of acetaldehyde removal in these systems; however, the quality of the data was not sufficient to quantitatively incorporate the production of acetaldehyde.
- Both ethanol and formaldehyde degradation observed in the binary system can be described by the Monod model with the lower k and upper K_s of the 95% joint confidence limits determined from the single substrate systems. This result suggests that no significant inhibition of substrate degradation occurred in the binary substrate system under the test conditions.
- Formaldehyde degradation was not affected by the presence of acetate (an ethanol degradation byproduct) and can be described by the Monod model. Although inhibition of formaldehyde degradation occurred in the binary aldehyde system in the presence of acetaldehyde and its degradation byproducts (ethanol and acetate), additional analysis will be required to clarify what actually caused this inhibition.

Chapter 5: Biofilter Study of Ethanol Plant Pollutants

Although biofiltration is commonly used in many industries to control air pollution, it has yet to be utilized at ethanol production facilities to treat VOC and HAP emissions. As described in Chapters 3 and 4, a simplified batch reactor system was used to delineate the biodegradation kinetics for the two major HAPs present in ethanol production emissions - formaldehyde and acetaldehyde. The objective of the research described in this chapter was to assess the capability of a biofilter to degrade these aldehydes over a range of loading rates and in the presence of ethanol and acetic acid, two representative VOCs that are also typically present in ethanol plant emissions. Preliminary experiments using a compost-based biofilter were conducted to examine formaldehyde elimination capacity over the range of loading rates typically found at ethanol production facilities. Then, a biofilter packed with inorganic silicate pellets was used to treat a series of simulated waste gas streams that progressed in complexity from a single aldehyde component (Phase I) to a four component mixture of formaldehyde, acetaldehyde, ethanol and acetic acid (Phase IV).

5.1. METHODS

Preliminary biofitlration experiments were conducted using a compost biofiter to establish the formaldehyde elimination capacity at different resident times of the biofilter. A Celite® biofilter was subsequently utilized to address the importance of several key scenarios that can potentially occur during treatment of ethanol plant emissions.

5.1.1. Biofilter Setup

The nutrient retention capacity and low cost of compost make it an attractive option for use as a packing material in biofilters. For this reason, a compost-based material was utilized during preliminary biofilter experiments to determine the elimination capacity of formaldehyde over the range of loading rates expected at ethanol production facilities. During this initial evaluation, it was determined that the compost-based packing material interfered with the analytical method for formaldehyde (see discussion in Section 5.2.1); in addition, the unidentified mixture of organics present in the compost would make it more difficult to interpret the effect of substrate mixtures on biofilter performance. Thus, inert silicate pellets (Celite®) were selected as the packing material for the subsequent biofilter experiments investigating the removal of VOC mixtures. The experimental setup for both the compost biofilter and Celite® biofilter columns are described below.

Compost Biofilter

A mixture of 60% compost, 36.5% perlite and 3.5% crushed oyster shell (v/v) was used as the packing material in the preliminary experiments to examine formaldehyde removals in the biofilter. The compost was sieved to remove particles less than 2 mm before being mixed with the other components. Perlite was included in the compost mixture to reduce compaction of the packing material and oyster shell was used to provide buffer capacity. Throughout the compost biofilter study, the moisture content of the packing material was maintained between 41% to 55% on a wet basis.

The stainless steel biofilter column consisted of five sections, each with a height of 36 cm and an inner diameter of 16.2 cm. The middle three sections were each packed to a height of 18 cm with packing material, providing a total packed bed height of 54 cm.

To ensure an adequate nitrogen supply in the packing material, a mixture of phosphorous and nitrogen sources (2.72 g KH_2PO_4, 1.42 g Na_2HPO_4, 3.96 g $(NH_4)_2SO_4$, and 10.1 g KNO_3) was added to 1 L of the inoculum solution before being mixed with the packing material (Kwon, 2007). An aqueous solution ranging from 3.7% to 37% by weight of formaldehyde was injected into one air stream using a syringe pump (kd Scientific, Model KDS220) to achieve the desired formaldehyde concentrations in the gas phase. This air stream was then mixed with a humidified air stream in a mixing chamber prior to being supplied to the biofilter.

During the startup period of the biofilter, several problems associated with generating a steady formaldehyde supply in the gas phase were encountered; as a result, the experimental setup and operating conditions were modified accordingly. First, it was determined that when the concentration of formaldehyde in the syringe pump was higher than 3.7% (w/w), polymerization of formaldehyde onto the surface of the Teflon® tubing connecting the syringe pump to the biofilter became severe after only a few hours of operation. Formaldehyde polymerization was also observed by Andrawes (1984) when they used a water solution containing 3 to 37% of formaldehyde to generate formaldehyde vapor. To solve this problem, a range of formaldehyde stock solution concentrations were tested in the experimental biofilter to determine if polymerization could be avoided by lowering the concentration of formaldehyde in the syringe pump feed system. The results of these experiments indicate that using a 1% formaldehyde solution in water in the syringe pump led to minimal losses of formaldehyde in the tubing connecting the syringe pump to the biofilter. For this reason, a 1% formaldehyde solution in water was chosen for the formaldehyde elimination capacity experiments. At this concentration, the maximum concentration of formaldehyde that can be volatilized into an air stream is limited to 70 ppm_v at ambient temperatures. To ensure

that the formaldehyde would exit the biofilter at detectable concentrations, the biofilter column was reduced from three packed bed sections to one packed bed section as shown in Figure 5.1. This section was packed to a bed height of 9 cm which is equivalent to 2L of packed volume.

It was also determined during the initial experiments that when an external mixing chamber was used to mix the formaldehyde-containing air stream with a humidified air stream, most of the gaseous formaldehyde dissolved into the condensed liquid phase inside the mixing chamber and never reached the biofilter. To overcome this problem, the external mixing chamber was removed and the compost biofilter setup was reconfigured as shown in Figure 5.1. In this final configuration, 4 L/min of humidified air and 8 L/min of the gas stream containing formaldehyde were mixed directly in the empty 8L top section of the biofilter.

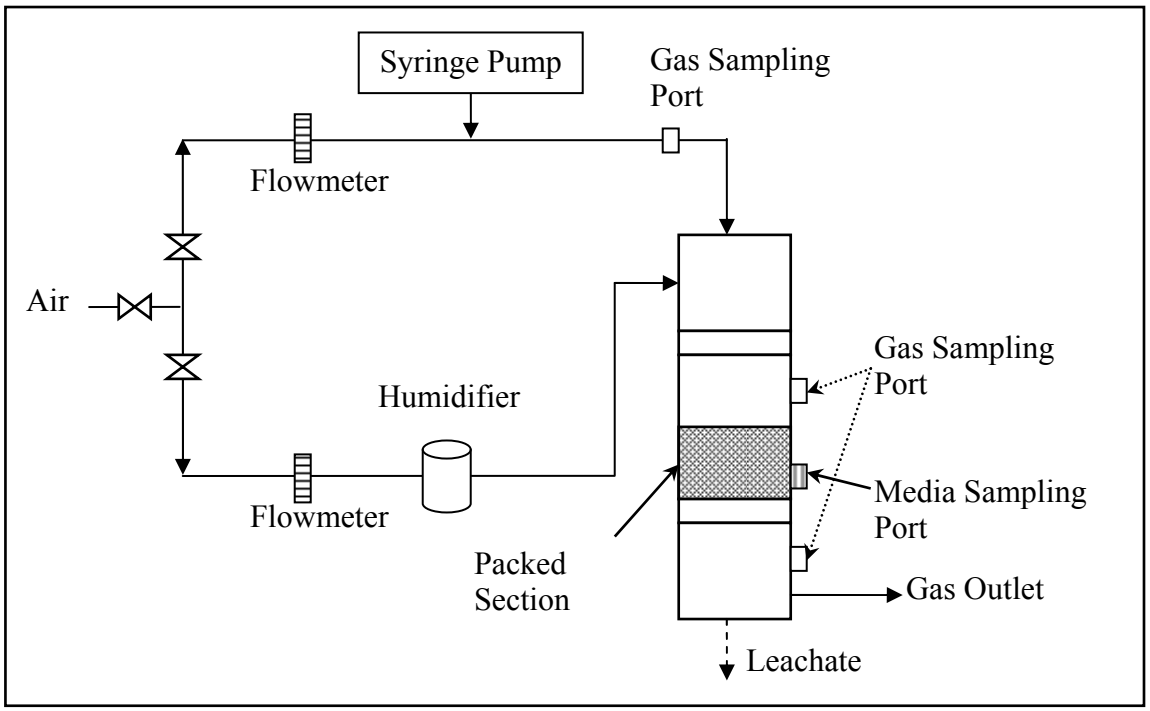

Figure 5.1. Schematic diagram of the compost biofilter system.

Celite® Biofilter

The Celite® biofilter consisted of four stainless steel sections, each with a height of 36 cm and an inner diameter of 16.2 cm (see Figure 5.2). The biofilter column was equipped with three gas sampling ports and two media sampling ports. The middle two sections of the biofilter were packed with 2L of inert, porous silicate pellets (Celite® R-635, Lompoc, CA) to provide an overall packed bed volume of 4L. Prior to biofilter inoculation, the Celite® pellets were sterilized through autoclaving before being placed in the two packed sections of the biofilter. In addition, to prevent biomass detachment from the surfaces of the top packing material, a layer of fine steel wool was placed on top of the first packed section (Kwon, 2007). The packing material was then soaked in 16 L of a concentrated nutrient solution (1.36 g/L KH_2PO_4, 5.68 g/L Na_2HPO_4, 3.96 g/L $(NH_4)_2SO_4$ and 10.1 g/L KNO_3) overnight. After the nutrient solution was drained, 4L of biomass solution containing the enriched aldehyde-degrading consortium and sterile PBS was recirculated through the biofilter overnight at a rate of 0.5 L/min to allow for biofilm development (Song and Kinney, 2000). A peristaltic pump (Cole-Parmer, Masterflex L/S) and a high pressure spray system consisting of a nozzle (BETE, TF type) located at the top of the packing material were used to recirculate the inoculum solution that collected in the sump at the base of the biofilter back through the packed bed. During operation of the biofilter, this system was also used to recirculate 4L of the previously described concentrated nutrient solution through the packed bed for a period of one hour for every 3 days of biofilter operation.

To provide a synthetic waste gas stream to the biofilter, filtered compressed air was split into two streams: the first stream was fed into a humidifier, while the other stream was supplied with target substrate(s) through the injection of liquid solutions via two syringe pumps (kd Scientific, Model KDS220). The two gas streams were fed

directly into the empty 8L top section of the biofilter where they mixed prior to entering the packed biofilter sections. During the first two weeks of biofilter operation (Phases I and II), 16 ppm_v of formaldehyde and/or 20 ppm_v of acetaldehyde were supplied continuously to the biofilter.

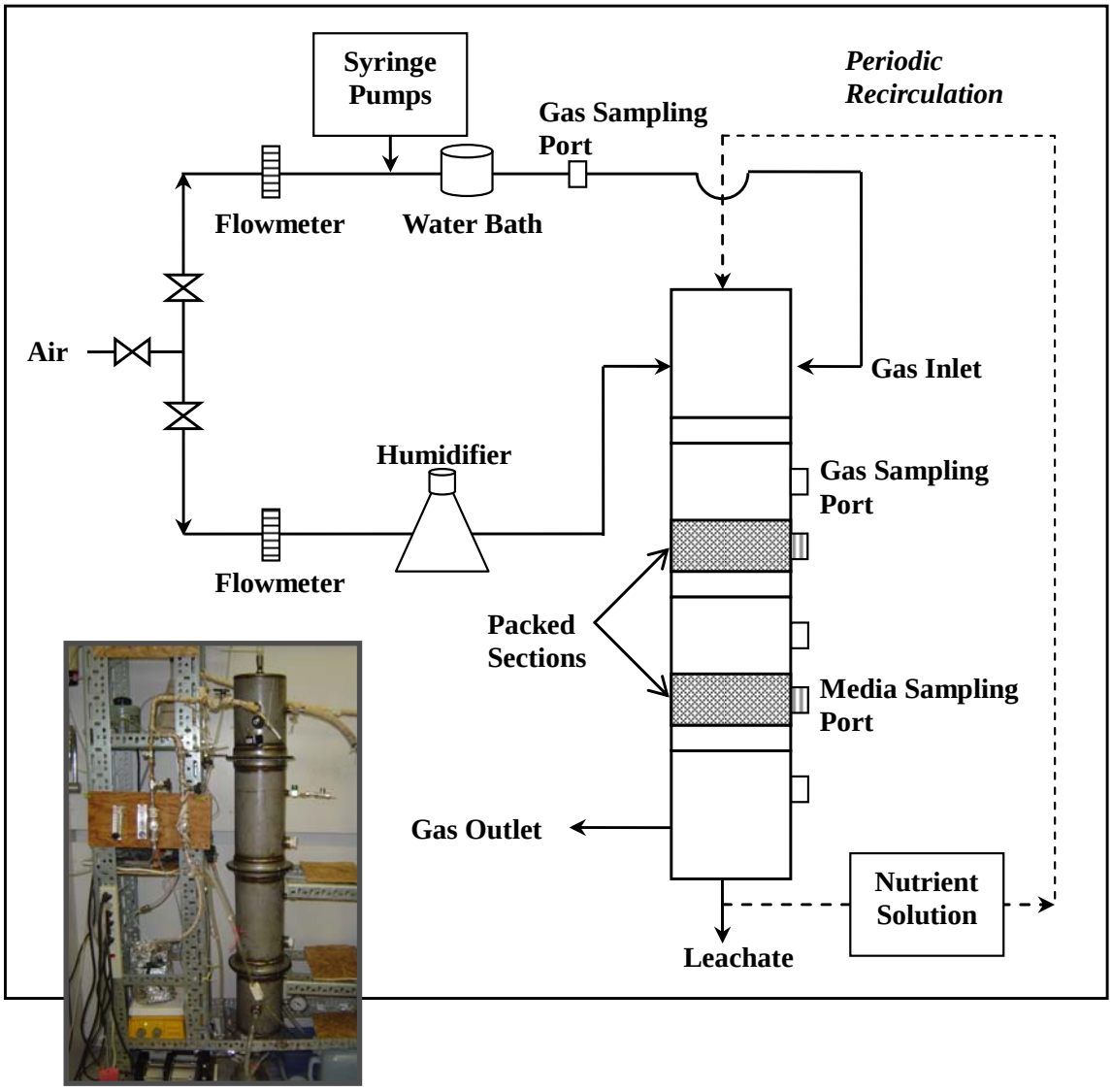

Figure 5.2. Schematic diagram and picture of the Celite® biofilter system.

5.1.2. Compost Biofilter Study

To investigate the removal of formaldehyde in the compost biofilter, the elimination capacity (EC; Equation 5.1) of formaldehyde as a function of loading was examined.

$$EC\,(g\ pollutant / m^3 / hr) = \frac{Q \times (C_{in} - C_{out})}{V} \qquad \text{(Equation 5.1)}$$

where C_{in} = pollutant inlet concentration (g/m^3);

C_{out} = pollutant outlet concentration (g/m^3);

Q = gas flow rate (m^3/hr);

V = packed volume of the biofilter (m^3).

Prior to initiating the elimination capacity experiments, a baseline formaldehyde concentration of 8 ppm_v was supplied to the inlet of the compost biofilter for a period of 12 days. Except for the periods that the inlet concentration was increased for a given elimination capacity experiment, this baseline concentration was maintained throughout the compost biofilter study.

Empty bed contact times (EBCTs) ranging from 8 to 90 seconds have been reported in the literature for biofilters degrading formaldehyde (Ferranti and Conca, 2000; Garner, 2002; Prado *et al*., 2004 & 2006). In this research study, EBCTs of 10, 15 and 20 seconds were evaluated, which represent the lower range of those reported in the literature. For each EC experiment conducted at a given EBCT, the inlet formaldehyde concentration was increased in a stepwise manner. Each inlet concentration was held constant for a period of 8 hours, then returned to the baseline concentration, which was maintained overnight prior to increasing the inlet concentration

to the next higher level. The operating conditions for the biofilter EC experiments are summarized in Table 5.1.

Table 5.1. Operating conditions for the EC experiments in the compost biofilter system

EBCT (Seconds)	Packed Volume(L)	Flowrate (L/min)	Loading Range ($g/m^3/hr$)	Conc. Range (ppm_v)	Operating Period
20	4	12	1.0-3.9	4.3-17.3	Day 12-49
10	2	12	4.2-14.7	9.3-32.7	Day 60-68
15	2	8	1.6-3.1	5.4-10.2	Day 70-91

5.1.3. Celite® Biofilter Study

Four phases of study were conducted with the Celite® biofilter to evaluate the effects of substrate mixtures and low pH on biofilter performance. Between the experiments in each phase, the Celite® biofilter was fed a gas stream containing the pollutant(s) to be examined in the following experiment. The pollutant loading was set equal to the baseline level of the next experiment. Table 5.2 summarizes the operating conditions used in each experiment during the four phases of the biofilter study. Each phase of study is described in more detail in the sections that follow.

It is worth noting that formaldehyde did not breakthrough the second packed section of the Celite® biofilter during operation in this research. Therefore, pollutant mass loading rates in each experiment during the Celite® biofilter study (Table 5.2) were reported with respect to the first packed section (i.e., a packed volume of 2L).

Table 5.2. Operating conditions of the Celite® biofilter during different experimental phases

Experiment	Substrate	Flowrate (L/min)	Loading* ($g/m^3/hr$)	Conc. (ppm_v)	System pH	Operating period
Phase I: Single-Component Aldehyde Experiments						
I-1	Formaldehyde	12	7.5-27.1	17.3-62.7	7.1~7.3	Day 2-6
I-2	Acetaldehyde	12	32.0-66.5	48.7-101.3	7.1	Day 10
I-3	Acetaldehyde	12	6.2-101.6	9.4-154.6	6.9	Day 21-23
I-4	Formaldehyde	24	1.5-32.5	1.8-37.4	7.2~7.3	Day 28-29
I-5	Acetaldehyde	24	25.4-77.7	19.5-57.0	7.6	Day 174
Phase II: Dual-Component Aldehyde Experiments						
II	Formaldehyde Acetaldehyde	12	7.2-27.1 30.6	16.1-60.9 47.0	7.2~7.3	Day 8-9
Phase III: Three-Component Mixture Experiments						
III-1	Formaldehyde Acetaldehyde Ethanol	24	7.3 16.9-67.2 80.7-242.4	8.4 12.8-51.2 58.8-176.4	7.1~7.2	Day 129-132
III-2	Formaldehyde Acetaldehyde Ethanol	12	7.3 11.7-52.0 34.2-107.0	16.8 17.8-79.2 49.8-155.7	7.1~7.3	Day 134-136
Phase IV: Four-Component Mixture Experiments						
IV-1	Formaldehyde Acetaldehyde Ethanol Acetic Acid	12	7.3 37.5 52.5 40.7	16.8 57.1 75.9 91.4	6.4~7.3	Day 153-164
IV-2	Formaldehyde Acetaldehyde Ethanol Acetic Acid	12	13.6 28.2 57.3 39.3	31.4 42.9 83.4 88.2	2.8~3.5	Day 177-185

* Based on the first packed section (2L)

Phase I: Single-Component Aldehyde Experiments

During Phase I, single aldehyde (formaldehyde or acetaldehyde) EC as a function of loading rate was evaluated in the Celite® biofilter. Formaldehyde removal examined during Experiment I-1 was conducted from Day 2 to 6 of operation period, followed by Experiment I-2 evaluating acetaldehyde removal after 10 days of operation.

In addition to the EC experiments described above, Experiment I-3 was conducted to examine the effect of nutrient supply on acetaldehyde removal in the biofilter. Given every 3 days as the routine recirculation frequency of nutrient solutions through the biofilter, no nutrient solution was recirculated for 12 days prior to Experiment I-3. A range of acetaldehyde loadings (6.2 to 101.6 $g/m^3/hr$) was evaluated in the biofilter during Experiment I-3, and the EC data were then compared to Experiment I-2 that was conducted immediately after nutrient solution recirculation.

To evaluate the effect of a shorter EBCT on the removal of a single aldehyde during Phase I, the total flow rate of the biofilter system was adjusted to 24 L/min during Experiments I-4 and I-5, yielding an EBCT of 5 seconds. Experiment I-4 was conducted to examine formaldehyde EC as a function of loading rate (1.5 to 32.5 $g/m^3/hr$), while acetaldehyde removal over a loading range of 25.4 to 77.7 $g/m^3/hr$ was evaluated during Experiment I-5.

Phase II: Dual-Component Aldehyde Experiments

The kinetic data derived from the binary aldehyde batch experiments indicate that an uncharacterized acetaldehyde degradation byproduct(s) inhibited formaldehyde degradation when the aldehyde-degrading consortium was utilized in the batch reactor. To determine if a similar effect would occur in the biofilter, formaldehyde and acetaldehyde were fed simultaneously to the biofilter during Phase II. For these

experiments, the acetaldehyde loading was held constant while two different formaldehyde loadings were tested during Experiment II.

Phase III: Three-Component Mixture Experiments

Formaldehyde, acetaldehyde and ethanol were supplied to the biofilter during Phase III to evaluate the effect of three component mixtures on pollutant removals in the biofilter over a range of loading rates. The performance of the biofilter system was evaluated at two flow rates: 24 L/min during Experiment III-1 and 12 L/min for Experiment III-2. In both experiments, a range of ethanol and acetaldehyde loadings was applied to the biofilter while the formaldehyde loading was held constant (Table 5.2).

Phase IV: Four-Component Mixture Experiments

Based on the batch experimental results shown in Chapter 3, degradation of formaldehyde and acetaldehyde was inhibited when the pH of the batch reactor dropped to 3.9 and 5.8, respectively. To determine how pH may affect the removals of pollutants in the biofilter, acetic acid was added to the simulated gas stream during Phase IV. A mixture of four air pollutants (formaldehyde, acetaldehyde, ethanol and acetic acid) at loadings representative of ethanol plant emissions were supplied to the Celite® biofilter in this phase. The constant pollutant loadings, selected based on their highest concentrations reported in the DDGS process emissions in Table 2.1, were maintained throughout Phase IV.

Experiments IV-1 and IV-2 were conducted over testing periods of 11 and 9 days, respectively, to examine the effect of the four-component mixtures on pollutant removals

in the biofilter at two different pH conditions. To decrease the pH of the biofilter system from neutral to acidic conditions within a reasonable time frame, a pH 4.7 nutrient solution (0.01 M KH_2PO_4, 0.03 M $(NH_4)SO_4$, 0.06 M KNO_3) was recirculated through the packed bed 2 hours per day for 3 days prior to initiating Experiment IV-1. To further drop the pH of the biofilter system before Experiment IV-2 began, a 0.01N HCl solution was recirculated through the biofilter system for 2 hours per day for 2 days.

5.1.4. Sampling and Analytical Methods

Formaldehyde

Gas samples containing formaldehyde were collected in the biofilter experiments using the sampling technique described in USEPA Method 0011 (USEPA, 1996). The samples were taken from the gas sampling ports of the biofilter using a sampling train (shown in Figure 5.3) consisting of two 25-mL midget impingers (SKC, model 225-36-2) in an ice bath, an impinger trap (SKC, model 225-22), and a sampling pump (Buck, Basic-1). Each impinger contained 20 mL of Millipore water, and the impinger trap was filled with a charcoal/silica gel sorbent and glass wool to prevent water and organic vapors from entering the sampling pump. The inlet and outlet gas samples from the biofilter were collected at an air sampling rate of 400 mL/min for 15 minutes and 60 minutes, respectively. The liquid in the two midget impingers were combined into a 40-mL vial and analyzed using the colorimetric method described earlier in Section 3.1.3. Leachate samples were filtered through 0.2 μm syringe filters before being analyzed for formaldehyde concentrations, also using the colorimetric method.

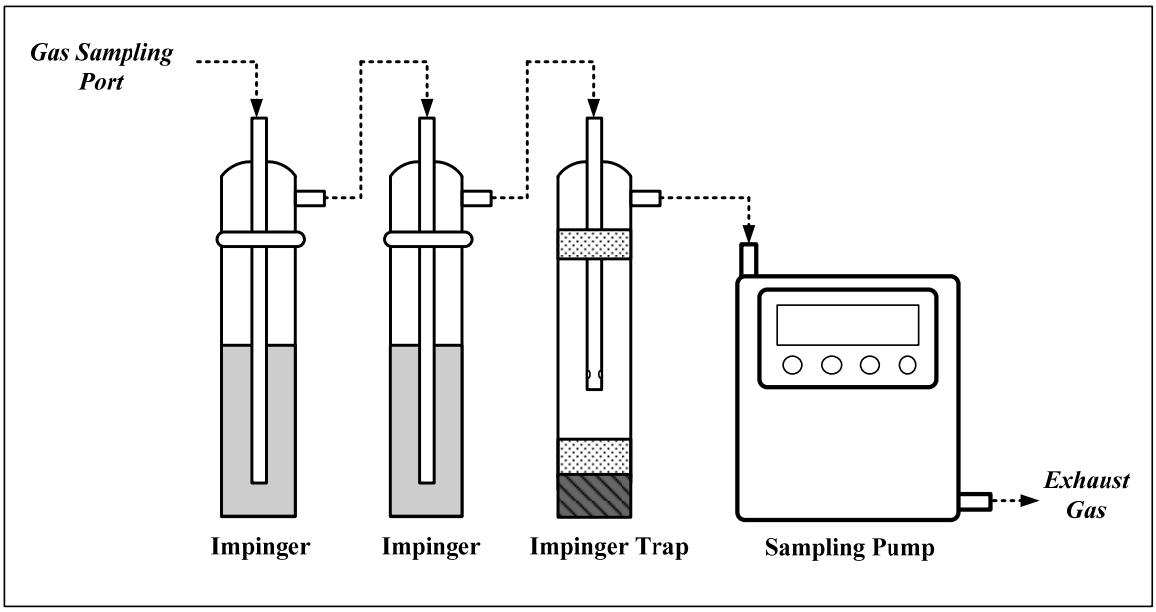

Figure 5.3. Schematic diagram of an impinger sampling train for formaldehyde.

Acetic Acid

The sampling technique employed to determine gaseous formaldehyde concentrations was also used to determine acetic acid concentrations present in the gas phase during the biofilter experiments. The sampling method was the same as described earlier, except that each midget impinger contained 20 mL of a solution consisting of 1.0 mM $NaHCO_3$ and 3.2 mM Na_2CO_3. The concentration of acetic acid trapped in the impinger liquid was analyzed using the same IC method described earlier in Section 3.1.3.

Acetaldehyde and Ethanol

Gas samples containing acetaldehyde and/or ethanol were taken directly from the gas sampling ports of the Celite® biofilter using a 0.5 mL gastight syringe (VICI, Series

A-2). The samples were then injected into a 5890 II Plus GC-FID for determination of acetaldehyde and ethanol concentrations in the gas phase. Mulitpoint gas standards containing acetaldehyde and/or ethanol were prepared every day for calibration. The operating conditions of the GC were the same as described in Section 3.1.3.

Moisture Content and Volatile Solids

The moisture content of packing material samples collected from the sampling ports of the compost and Celite® biofilters was determined gravimetrically. Prior to each measurement, a ceramic crucible was washed, dried in a 105°C oven overnight, and then cooled in a desiccator until use. The packing samples were then collected and placed in the ceramic crucible; the weights of the empty crucible and the crucible containing samples were recorded accordingly. The crucible, along with the collected samples, was then placed in a 105°C oven and dried overnight. After drying, the samples were allowed to cool to room temperature in a desiccator before being reweighed. In addition, the amount of volatile solids on the Celite® packing was determined by taking the difference between the weight of a crucible containing packing samples after drying at 105°C and after drying at 550°C.

pH of Leachate and Packing Samples

The pH of leachate samples collected from the bottom of the biofilters was monitored using an Orion pH meter (Model 520A) equipped with a VWR Scientific pH probe (No.34105-148). Occasionally, pH of the Celite® packing material was estimated by directly placing pH test paper directly on the surface of packing samples.

5.2. RESULTS AND DISCUSSION

5.2.1. Formaldehyde Elimination Capacity in the Compost Biofilter

The elimination capacity of formaldehyde as a function of loading at three EBCTs of 10, 15, and 20 seconds in the compost biofilter are shown in Figure 5.4. The results indicate that formaldehyde was readily degraded in the biofilter with greater than 96% formaldehyde removal observed for the loading range (1.0-14.7 g/m^3/hr) and EBCTs evaluated. The experimental results also suggest that biofiltration can be effective in removing formaldehyde at dry mill ethanol production facilities since formaldehyde emitted from several processes such as DDGS dryers and fermentation tanks at dry mill ethanol production facilities is usually in the loading range of 0.5 to 15 g/m^3/hr.

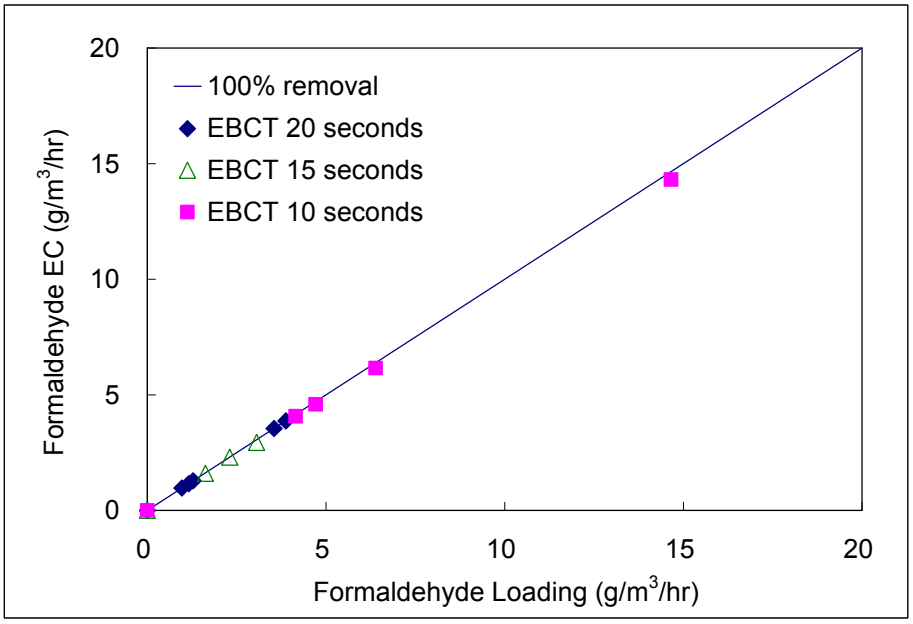

Figure 5.4. Formaldehyde EC curves at different EBCTs in the compost biofilter.

During the operation of the compost biofilter, certain substances in the compost packing were found to be carried over to the leachate samples. The substances reacted with the reagents that were used in formaldehyde analysis and caused color interferences in the absorbance measurements. As a result, mass balance closure for formaldehyde around the compost biofilter could not be completed since it could not be confirmed if formaldehyde was present in the leachate that collected in the bottom of the biofilter. To correct this issue, inert Celite® was selected as the packing material for the subsequent biofiltration experiments. The use of Celite® instead of compost for the substrate mixture tests in the biofilter also reduced the possibility of experimental interference from the complex organic matter present in the compost.

5.2.2. Celite® Biofilter Experiments

Phase I: Single-Component Aldehyde Experiments

The formaldehyde EC curves derived from the single formaldehyde biofiltraion Experiments I-1 and I-4 are shown in Figure 5.5. Although the biofilter system was operated at two different EBCTs during the experiments, formaldehyde removal across the biofilter was nearly 100% at both EBCTs. These results from the Celite biofilter were similar to the observations in the compost biofilter in Section 5.2.1. The high removal efficiencies observed in both the compost and Celite® biofilter systems indicate that packing material did not have an impact on formaldehyde removals for the loading ranges investigated. This is also confirmed by Prado *et al.* (2004), who studied formaldehyde removals in three biofilters packed with either lava rocks, perlite or activated carbon. Approximately 15 $g/m^3/hr$ of formaldehyde in the presence of 0.5-26 $g/m^3/hr$ methanol was readily degraded in each biofilter at an EBCT of 80 seconds, with

reported formaldehyde removals ranging from 41 to 71%. Their results show that formaldehyde removal efficiency depended more on the loadings of a second substrate methanol than on packing material in their biofilters. Compared to the study conducted by Prado *et al.* (2004), both the compost and Celite biofilter systems examined in this research achieved higher formaldehyde removals at a shorter EBCT, even in the presence of a secondary substrate (see discussion of Phase II experiments below).

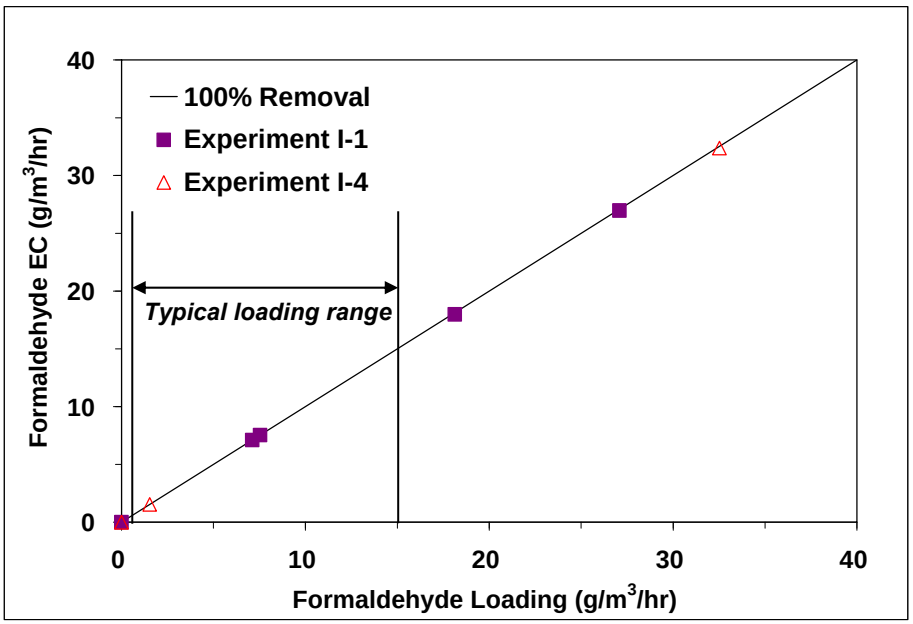

Figure 5.5. Formaldehyde EC curves derived in the Celite® biofilter during Experiment I-1 (EBCT 10 seconds; Day 2-6) and Experiment I-4 (EBCT 5 seconds; Day 28-29).

The similarity between the formaldehyde EC data at an EBCT of 10 seconds collected after 60-68 days of operation in the compost biofilter and after only 2 to 6 days of operation in the Celite® biofilter suggests that high formaldehyde removals are possible in a biofilter following a relatively short startup period. A relatively short startup period was also observed by Ferranti and Conca (2000) who studied a pilot-scale

biofilter packed with inert spherical pellets treating approximately 18 $g/m^3/hr$ of formaldehyde at an EBCT of 8 seconds. Their data show that formaldehyde removal in the biofilter was about 60% initially but increased to greater than 95% after two weeks of operation. It is worth noting that the Celite® biofilter was inoculated with an aldehyde-degrading consortium; however, Ferranti and Conca did not provide details about the inoculum used in their biofilter.

The EC data from the single acetaldehyde biofiltration Experiment I-2 at an EBCT of 10 seconds are shown in Figure 5.6. As seen in Figure 5.6, the maximum EC in Experiment I-2 was less than 40 $g/m^3/hr$ with increasing acetaldehyde loading. Approximately 60% removal efficiency was observed at the highest acetaldehyde loading of 66.5 $g/m^3/hr$. Since this EC experiment was conducted after only 10 days of biofilter operation, the biomass responsible for acetaldehyde removal may not have been well developed at this point in the operation. A similar EC curve for acetaldehyde was observed in a compost biofilter as reported by Bangs (2005). The biofilter in Bangs study had been used to treat a mixture of benzene, toluene, ethyl benzene and xylenes for eight months prior to switching the biofilter over to an acetaldehyde feed of 18 ppm_v for four hours prior to beginning the acetaldehyde EC experiments.

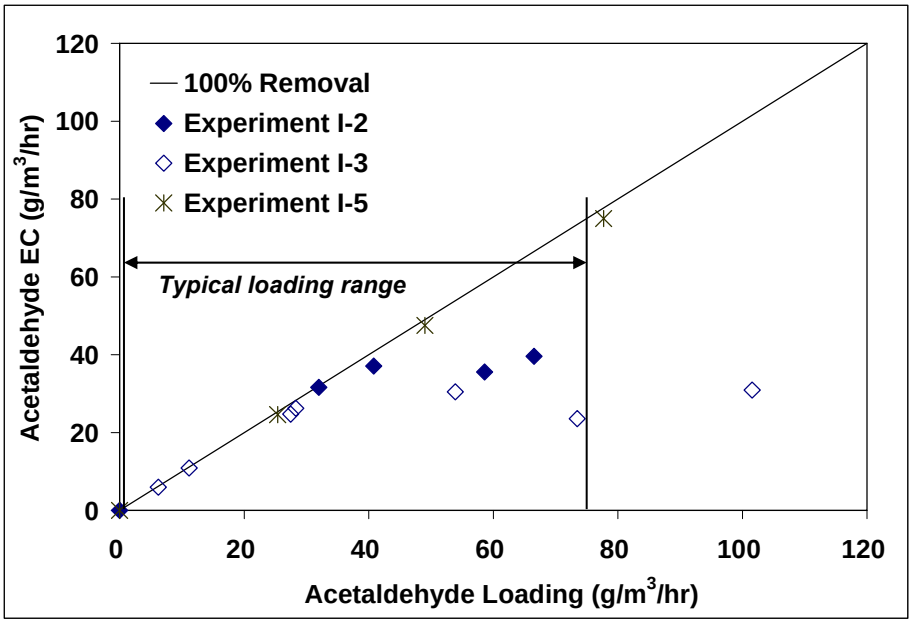

Figure 5.6. Acetaldehyde EC curves derived in the Celite® biofilter during Experiment I-2 (EBCT 10 seconds; Day 10), Experiment I-3 (EBCT 10 seconds; Day 21-23) and Experiment I-5 (EBCT 5 seconds; Day 174).

Experiment I-5 was conducted to determine if acetaldehyde removal would improve with operating time. The EC data from Experiment I-5, shown in Figure 5.6, indicate that the acetaldehyde EC improved greatly compared to the results obtained during Experiment I-2 which was conducted after 10 days of operation, even though the EBCT was reduced to half of the normal operating value. Since formaldehyde removal seemed insensitive to start up period, these acetaldehyde results suggest that the required startup period for a biofilter system simultaneously treating formaldehyde and acetaldehyde will be dependent on the desired acetaldehyde ECs for a given waste gas stream. Some research studies have also shown that startup periods for biofiltration systems are highly dependent upon pollutant characteristics and operating conditions, and startup periods from a few days to several months may be required for a system to reach

target pollutant removal efficiencies (Deshusses *et al*., 1996; Zhou *et al*., 1998; Fortin and Deshusses, 1999). For instance, Deshusses *et al*. (1996) observed that less than 5 days of startup time was possible for complete removals of methyl ethyl ketone and methyl isobutyl ketone in their biofilter, which they attributed to effective inoculation. However, Fortin and Deshusses (1999) observed that a startup phase of nearly two months for a biotrickling filter packed with lava rocks was required to achieve approximately 95% removal efficiency for methyl *tert*-butyl ether.

Experiment I-3 was conducted to evaluate if discontinuing the periodic recirculation of the nutrient buffer solutions for nearly two weeks would affect acetaldehyde removals in the Celite® biofilter. Also shown in Figure 5.6, the EC curves from Experiments I-2 and I-3 are not significantly different and the pH of the biofilter remained neutral (6.9~7.0) without the recirculation of the buffer solution. These results suggest that nutrients were not limiting at least over a nearly two week period of operation and that pH adjustment in the biofilter was not necessary to maintain a stable acetaldehyde EC over approximately a two-week period.

Phase II: Dual-Component Aldehyde Experiments

The EC data for formaldehyde both in the absence of acetaldehyde and in the presence of 30.6 g/m^3/hr acetaldehyde during Phase II are shown in Figure 5.7. The results indicate that both aldehydes were removed simultaneously in the biofilter under the test conditions. In addition, formaldehyde was not detected either in the effluent gas stream or in the leachate over the aldehyde loadings examined during Phase II. The results suggest that formaldehyde removal was not affected by the presence of acetaldehyde in the biofilter, even though the presence of acetaldehyde negatively impacted formaldehyde degradation in the batch reactors. Nevertheless, it is difficult to conclude if formaldehyde degradation was inhibited by acetaldehyde in the biofilter since breakthrough of formaldehyde in either the gas phase or in the leachate was not observed.

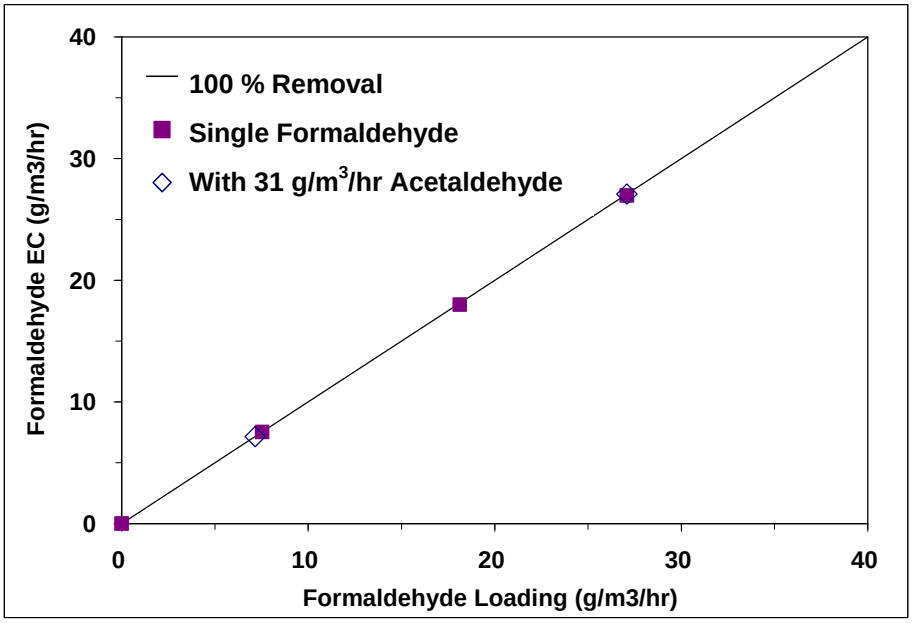

Figure 5.7. Formaldehyde EC curves in the absence of acetaldehyde (filled squares) and in the presence of 31 g/m^3/hr acetaldehyde (open diamonds) in the Celite® biofilter during Experiment II (EBCT 10 seconds; Day 8-9).

Figure 5.8 presents the acetaldehyde EC results obtained in the biofilter when either 7 g m^3/hr or 27 g/m^3/hr formaldehyde were present (Phase II experiments). The experimental data indicate that even a formaldehyde loading of 27 g/m^3/hr did not have an adverse impact on acetaldehyde removal in the biofilter, which is in good agreement with the lack of acetaldehyde inhibition observed in the presence of formaldehyde in the batch experiments.

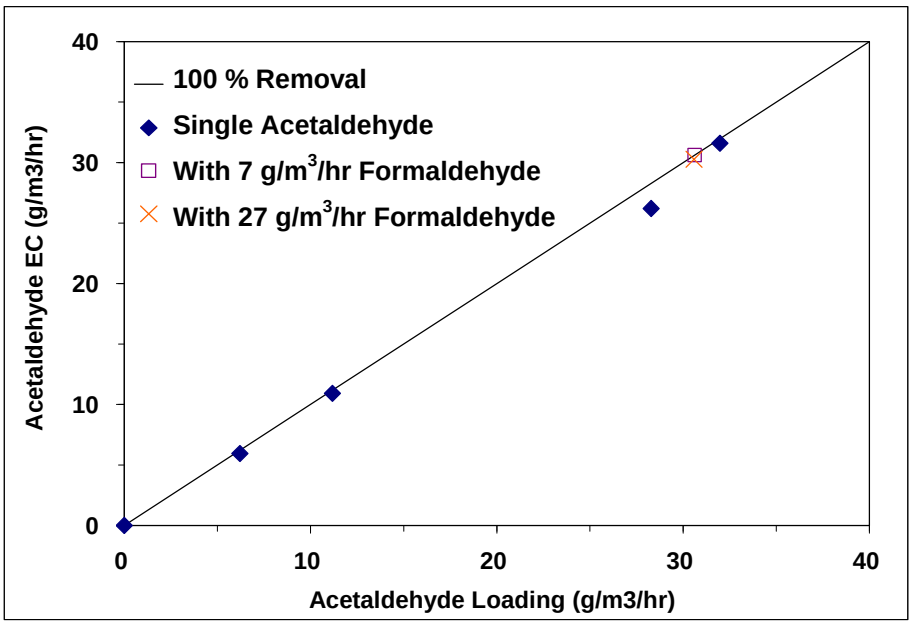

Figure 5.8. Acetaldehyde EC curves derived in the Celite® biofilter in the absence of formaldehyde (filled diamonds), and in the presence of formaldehyde at a loading of 7 g/m^3/hr (open square) and 27 g/m^3/hr (cross) during Experiment II (EBCT 10 seconds; Day 8-9).

Phase III: Three-Component Mixture Experiments

Formaldehyde, acetaldehyde and ethanol were supplied simultaneously to the Celite® biofilter during Phase III. Experiments III-1 and III-2 were performed 10 days after ethanol was added to the aldehyde mixture in the inlet gas stream. The EBCT in the biofilter was 5 seconds for Experiment III-1 and 10 seconds for Experiment III-2. The EC data for ethanol observed during the Phase III experiments are shown in Figure 5.9, suggesting that high ethanol removals are possible in the presence of formaldehyde and acetaldehyde in the biofilter. Under the highest ethanol loadings of 242.4 g/m^3/hr in Experiment III-1 and 107.0 g/m^3/hr in Experiment III-2, 87.8% and 90.7% removal efficiencies were obtained in the Celite® biofilter respectively.

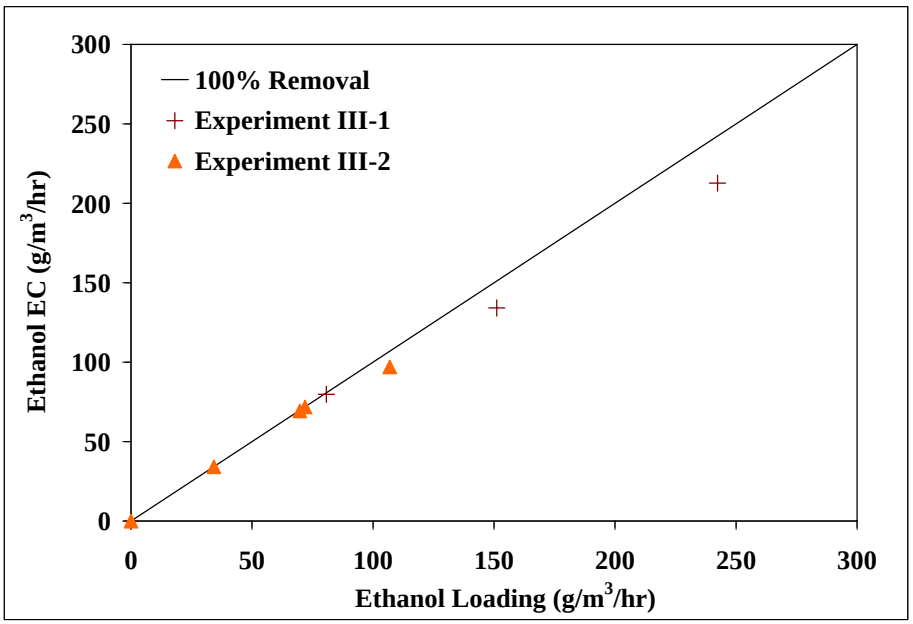

Figure 5.9. Ethanol EC curves in the Celite® biofilter during Experiment III-1 (EBCT 5 seconds; Day 129-132) and Experiment III-2 (EBCT 10 seconds; Day 134-136) in the presence of formaldehyde and acetaldehyde.

Although it was observed that acetaldehyde inhibited ethanol elimination in the batch reactor systems, the biofilter achieved high ethanol removal efficiencies in the presence of acetaldehyde. It should be noted that the operating conditions of the biofilter system can lead to development of a diverse microbial community, whereas the conditions of the batch systems might provide a greater likelihood for growth of a more uniform community. Moreover, the biofilter rapidly acclimated to ethanol even though it had been treating formaldehyde and acetaldehyde for nearly 4 months. This fast adaptation could be due to the relatively low K_s value of ethanol as compared to formaldehyde and acetaldehyde. Given the fact that several processes like fermentation and distillation at ethanol production facilities generate fair amounts of ethanol, it is very beneficial for a biofilter system to quickly adapt to changes in the composition of waste gas streams.

Studies using bacteria or fungi-based biofiltration systems to treat waste gas streams containing ethanol have been performed extensively (Devinny and Hodge, 1995; Arulneyam and Swaminathan, 2000; Christen *et al*., 2002; Terán Pérez *et al*., 2002). Although the maximum ethanol EC values reported in the literature ranges from 100 to 250 $g/m^3/hr$, it has been reported that biofiltration of high ethanol loadings frequently leads to a deterioration in system performance. For instance, Devinny and Hodge (1995) investigated ethanol removals at a constant loading of 156 $g/m^3/hr$ in three biofilters operated at an EBCT of 3.1 minutes. The biofilters were packed with GAC and the main difference among them was the amount of inoculated biomass. The authors reported that high ethanol loading eventually led to breakthroughs of ethanol as well as occurrence of toxic and/or acidic intermediates (acetaldehyde, acetic acid and ethyl acetate) in the effluent gas streams of the biofilter with the highest biomass concentration. The highest ethanol loading (212.7 $g/m^3/hr$) in Experiment III-1 of this

research was only tested for a few hours. Further testing would be required to determine whether a negative impact on pollutant removals in the biofilter would result from long term exposure to high ethanol loading.

Removal efficiencies of acetaldehyde with increasing loading in the biofilter were also investigated during Experiments III-1 and III-2 and the EC data for acetaldehyde are plotted in Figure 5.10. Greater than 88% acetaldehyde removal was achieved in the biofilter when the inlet gas stream contained a mixture of 242.4 g/m^3/hr ethanol, 67.2 g/m^3/hr acetaldehyde and 7.3 g/m^3/hr formaldehyde. As seen in Figure 5.10, it appears that the highest acetaldehyde EC achieved in Experiment III-1 was similar to that obtained in the single acetaldehyde biofiltration study during Experiment I-5. These results imply that there were no substantial substrate interactions affecting the acetaldehyde ECs in Experiment III-1, confirming the conclusion from the batch experiments that acetaldehyde degradation was not inhibited by the presence of the other substrates.

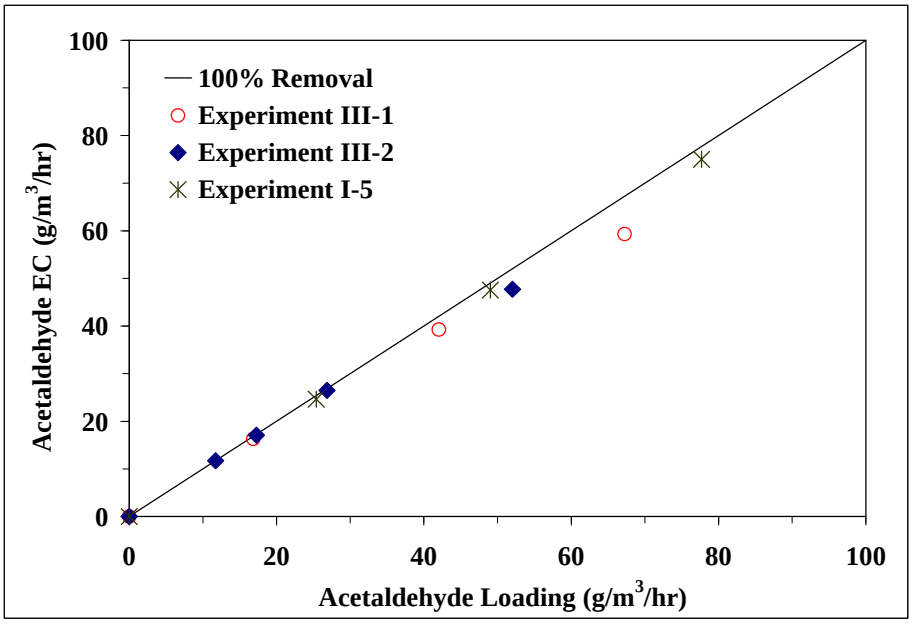

Figure 5.10. Acetaldehyde EC curves derived in the Celite® biofilter during Experiment III-1 (EBCT 5 seconds; Day 129-132), Experiment III-2 (EBCT 10 seconds; Day 134-136) and Experiment I-5 (EBCT 5 seconds; Day 174).

Phase IV: Four-Component Mixture Experiments

Recirculation of a pH 4.7 nutrient solution through the biofilter was performed several times to deplete the buffer capacity of the system prior to the beginning of Experiment IV-1 when acetic acid was to be introduced into the biofilter feed mixture. The leachate samples collected before and after recirculation indicated that the pH of the biofilter system dropped from 7.2 to 6.3. Experiment IV-1 was conducted immediately following recirculation to examine the effect of a four component substrate mixture (17 ppm_v formaldehyde, 57 ppm_v acetaldehyde, 76 ppm_v ethanol and 91 ppm_v acetic acid) on biofilter performance. Removal efficiencies of acetaldehyde and ethanol as a function of time are plotted in Figure 5.11. The results show that removal efficiencies of acetaldehyde and ethanol decreased from 99% to 87% and from 97% to 81% respectively

by the end of Experiment IV-1. While the biofilter leachate pH dropped from 7.3 to 6.4, no breakthrough of formaldehyde was detected in the effluent gas stream or in the biofilter leachate during Experiment IV-1. Although the concentration profiles of acetic acid in the gas phase suggest that acetic acid was readily removed in the biofilter with removal efficiencies approaching 100%, approximately 1% breakthrough was observed at the end of Experiment IV-1. Nonetheless, formate (formaldehyde degradation byproduct) and acetate (ethanol degradation byproduct) were not detected in the leachate samples collected during this experiment.

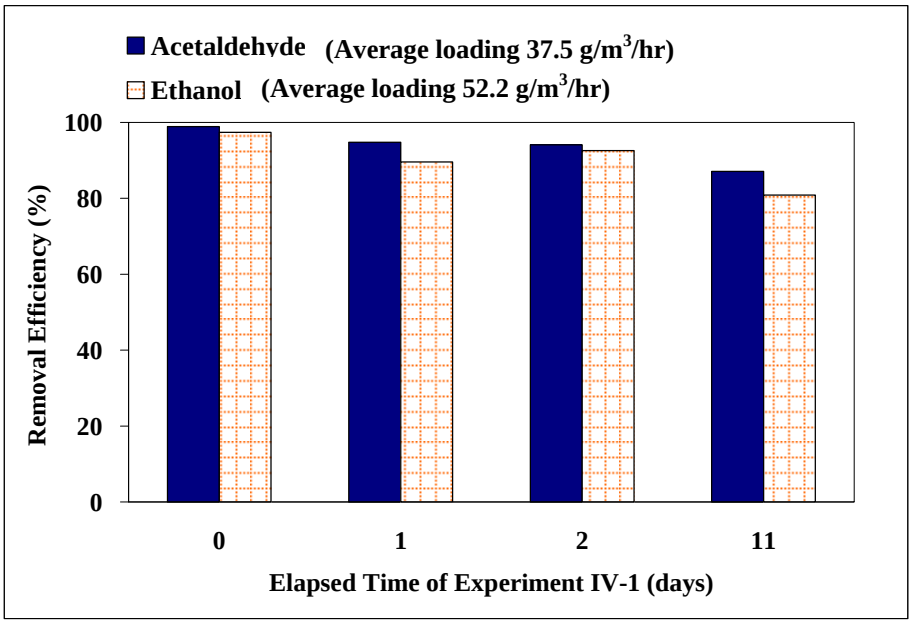

Figure 5.11. Removal efficiencies of acetaldehyde and ethanol during Experiment IV-1 (EBCT 10 seconds; Day 153-164) when the Celite® biofilter pH dropped from 7.3 to 6.4.

The results obtained in Experiment IV-1 indicates that loading a substrate mixture containing formaldehyde, acetaldehyde, ethanol and acetic acid to the biofilter for a period of 11 days gradually impaired the microbial activity in the biofilter and led to a

decrease in the overall pollutant removal efficiency. One possible explanation for this decline in performance was that continuous exposure of the biofilter to acetic acid reduced the residual buffer capacity of the biofilm. However, the leachate pH in the biofilter remained above 6 during Experiment IV-1, so it was unclear whether a reduction in the biofilm buffer capacity led to the gradual decline in biofilter performance observed.

To determine whether a significant decline in biofilter pH would affect biofilter performance, a 0.01N HCl solution was recirculated several times through the biofilter packing material until the pH of the packing in the top biofilter packed section reached a value below 4. Once the pH condition of the biofilter packing was confirmed, a gas stream containing 31 ppm_v formaldehyde, 43 ppm_v acetaldehyde, 83 ppm_v ethanol and 88 ppm_v acetic acid was supplied to the biofilter continuously for a period of 9 days during Experiment IV-2. The EC data for acetaldehyde and ethanol were examined on the 1^{st}, 2^{nd}, 8^{th} and 9^{th} day of the experiment. As seen in Figure 5.12, the low pH conditions significantly impaired the removal efficiencies of acetaldehyde and ethanol, which dropped to 30% and 33% by the end of Experiment IV-2. These results are consistent with the significant inhibition of acetaldehyde degradation observed in the batch systems when the aqueous phase pH dropped below 6.

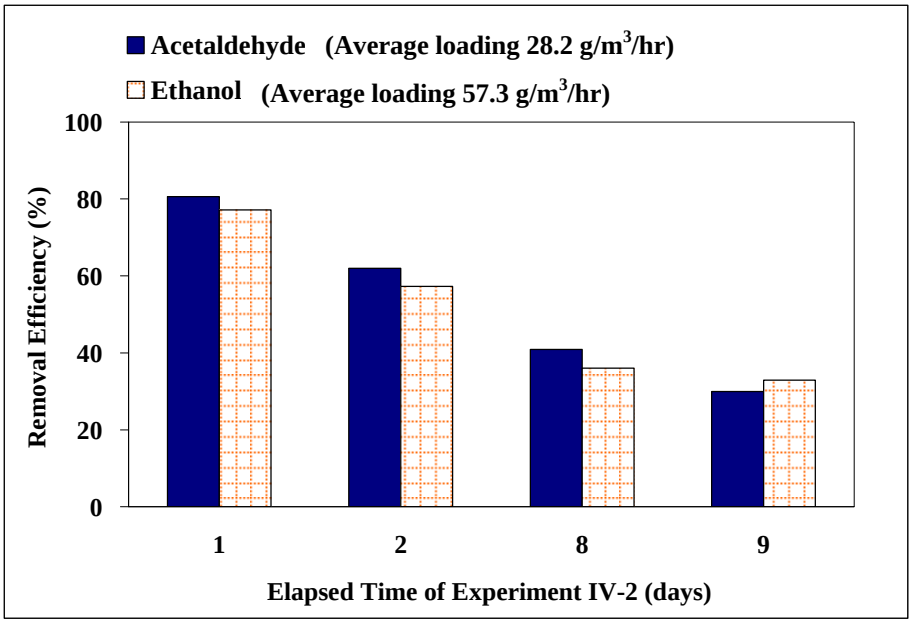

Figure 5.12. Removal efficiencies of acetaldehyde and ethanol during Experiment IV-2 (EBCT 10 seconds; Day 177-185) when the Celite® biofilter pH dropped below 4.

Formaldehyde breakthrough was also observed both in the effluent gas stream from the first packed section and in the leachate by the end of Experiment IV-2. The removal efficiency of formaldehyde in the gas phase of the biofilter dropped to 97% (equivalent to 0.9 ppm_v of breakthrough), and a maximum formaldehyde concentration of 0.4 mg/L was also detected in the leachate. This finding is significant to this research in two ways. First, while formaldehyde removal was not affected by the presence of the other substrates even at short EBCTs, low pH conditions did lead to formaldehyde breakthrough. Second, the inhibition of formaldehyde degradation at pH values below 4 is consistent with the results observed in the batch systems in which the formaldehyde degradation rate began to decrease at pH 3.9. A similar effect of acidic pH on formaldehyde removal in a biotrickling filter has also been reported by Prado *et al*. (2004,

2006). The authors reported that removal of formaldehyde decreased to 50-60% in their biotrickling filters when the pH of the systems was approximately 3.9-4.2.

Under acidic conditions examined in Experiment IV-2, the removal efficiency of acetic acid also declined to approximately 95%, resulting in effluent concentrations of 4.4 ppm_v from the first packed section of the biofilter. While formate and acetate are relatively soluble they were not identified in leachate samples during Experiment IV-2 due to analytical interferences from other anions in the leachate.

Excess loading of acidic air pollutants or accumulation of acidic byproducts could lead to a decline in biofilter pH and, as the results of Experiment IV indicate, pollutant breakthrough. These results further demonstrate the importance of maintaining pH control in biofilter systems treating gas streams emitted from ethanol production facilities. This can be accomplished by a number of methods. For instance, a pretreatment system, such as a wet scrubber, can effectively remove soluble acidic components before entering a biofilter system (Bangs, 2005). In addition, a biotrickling filter which allows continuous recirculation of pH buffer solutions can also be used to control and maintain system pH (Prado *et al*., 2004 & 2006).

5.3. SUMMARY

The objective of the biofilter study presented in this chapter was to evaluate the potential of biofiltration to treat waste gas streams emitted from ethanol production facilities. The pollutants studied in these experiments included two major HAPs, acetaldehyde and formaldehyde, and two typical non-HAPs, ethanol and acetic acid.

The results from biofiltration of formaldehyde in the compost and Celite® biofilters both show that nearly 100% formaldehyde removal was possible (up to 27 g/m^3/hr at an EBCT of 10 seconds, and 33 g/m^3/hr at an EBCT of 5 seconds). The data also suggest that formaldehyde was readily biodegradable in the biofilter systems and its removal was not affected by the choice of packing materials. In addition, the results of the single acetaldehyde biofiltration experiments indicate that greater than 97% removal efficiency was achieved when a loading up to 78 g/m^3/hr was tested in the Celite® biofilter at an EBCT of 5 seconds. Also, a longer startup period was required to achieve desired removals of acetaldehyde than formaldehyde in the Celite® biofilter when treating loadings typically found in ethanol plant emissions.

The results of the substrate mixture experiments investigated in the Celite® biofilter indicate that the applied formaldehyde loadings (7 g/m^3/hr at an EBCT of 10 seconds) did not appear to affect the removal efficiencies of the other pollutants including acetaldehyde, ethanol and acetic acid. It was also confirmed that neither high loadings of acetaldehyde (up to 67 g/m^3/hr at an EBCT of 5 seconds) nor ethanol (up to 242 g/m^3/hr at an EBCT of 5 seconds) caused formaldehyde breakthrough in the biofilter under neutral pH conditions. The Celite® biofilter performance was severely hindered after the pH of the biofilter system was purposely adjusted below 4. Extended feeding of acetic acid to the biofilter along with the aldehydes and ethanol gradually depleted the buffer capacity of the packing and further worsened the overall system performance

under the existing low pH conditions. Acetaldehyde and ethanol removal efficiencies, in particular, decreased much more dramatically than formaldehyde and acetic acid.

In conclusion, the results of the biofilter study indicate a biofilter system is capable of treating simulated air pollutants at loading rates that are greater than those found in ethanol plant emissions, even with a relatively short EBCT of 5 to 10 seconds. However, it is necessary to properly control the pH of the biofilter; this pH control may require continuous addition of buffering agents or removal of acidic components such as acetic acid from the waste gas stream prior to biofiltration treatment.

Chapter 6: Biofilter Modeling

This chapter discusses the results obtained from a model developed to aid in the interpretation of the experimental biofilter results (Chapter 5) and to better understand the parameters including substrate degradation and inhibition that can affect pollutant removals in the biofilter system. The numerical model was written in Matlab® and was used to develop substrate concentration profiles through the biofilter for a range of experimental scenarios.

6.1. MODEL DEVELOPMENT

6.1.1. Model Description

To develop a mathematical model for a biofilter system, three phases including gas, biofilm and solids are typically used to describe key processes occurring in the system. The biofilm model shown in Figure 6.1 was utilized in this research to determine if the experimental results obtained during the biofilter study were consistent with the substrate mixture effects observed in the batch system. The model has been applied extensively in bioreactor studies, particularly biofilter systems, and has produced model predictions that correlate well with experimental observations (Ottengraf & van den Oever, 1983; Zarook *et al*., 1993; Deshusses *et al*., 1995a & 1995b; Hodge and Devinny, 1995; Mohseni & Allen, 2000; Dupasquier *et al*., 2002).

The model considers the gas phase moving through a bioreactor in plug flow, so transport of substrates by advection is the dominant mechanism. Moreover, it assumes transfer of substrates from the gas phase to the biofilm phase is limited by diffusion resistance in the biofilm. This assumption is based on the fact that molecular diffusion

coefficients in air are approximately four orders of magnitude larger than those found in water (Ottengraf & van den Oever, 1983; Devinny and Ramesh, 2005). Therefore, it is reasonable to assume that gas-phase interfacial resistance is negligible relative to diffusion resistance in the biofilm at the surface. Based on this assumption, substrate concentrations at the gas/biofilm interface are in equilibrium with the bulk gas phase. Once in the biofilm phase, substrates are degraded by microbial cultures as they diffuse across the biofilm. For this research, the solids phase was not considered in model development since VOC adsorption capacity of Celite® observed in previous biofiltration research was determined to be insignificant when compared to biodegradation (Woertz *et al*., 2000).

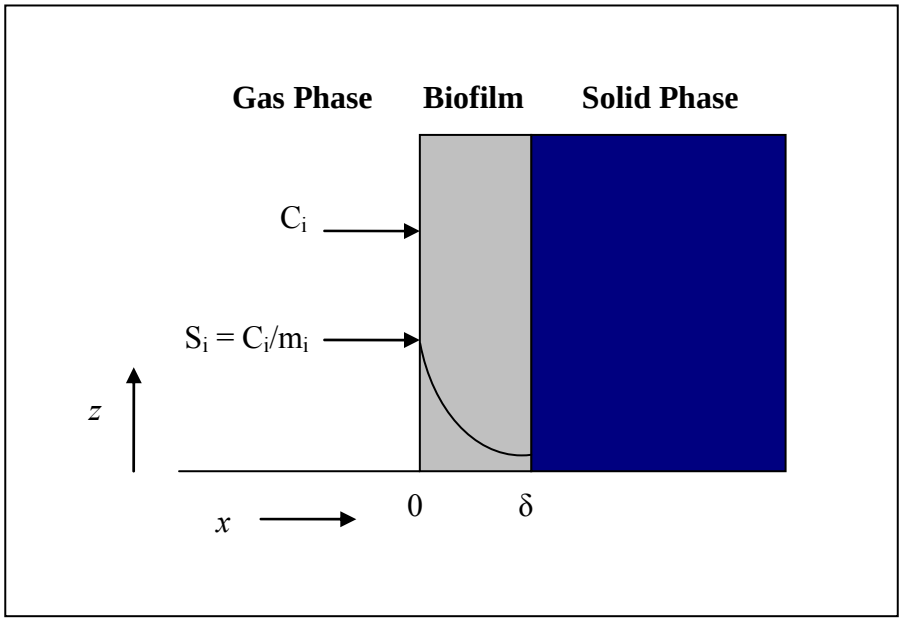

Figure 6.1. Schematic diagram of the steady-state biofilter model (Ottengraf and van den Oever, 1983). The parameters are defined in Table 6.1.

Table 6.1. Parameters used in the biofilter model

Parameter	Description	Unit
x	Distance in the biofilm	m
z	Biofilter height	m
S	Substrate concentration in the biofilm	$g/m^3_{(l)}$
C	Substrate concentration in the gas phase	$g/m^3_{(g)}$
m	Henry's Law constant of substrate	$m^3_{(l)}/m^3_{(g)}$
δ	Biofilm thickness	m
D_e	Diffusion coefficient of substrate in the biofilm	m^2/hr
U_g	Superficial gas velocity	$m^3/m^2/hr$
A_s	Biofilm specific surface area	m^2/m^3 packing
r_s	Substrate utilization rate	$g/m^3/hr$
k	Max. specific utilization rate of substrate	g/g/hr
K_s	Half-saturation constant of substrate	g/m^3
K_I	Inhibition constant of inhibitor	g/m^3
X_t	Total biofilm density	g/m^3
X_a	Active biofilm density	g/m^3
f_a	Active biomass fraction	%

In addition, several assumptions about the operation of the biofilter were made for the application of the model in this research, listed as follows.

- The biofilm grows on the outer surface of Celite® pellets, and the biofilm density is constant throughout the biofilter.
- The biofilm consists of active and inactive fractions of biomass, and only the active biomass fraction is able to degrade the substrates. An active biofilm density (X_a) is equal to a total biofilm density (X_t) multiplied by an active biomass fraction (f_a).
- In the biofilm, the diffusion of substrates is described by Fick's Law, and biodegradation of substrates is described by substrate degradation kinetics determined in the batch systems of this research.

- Substrate concentrations at the gas/biofilm interface are calculated using their Henry's Law constants.

6.1.2. Governing Mass Balance Equations

Based on the previous assumptions, a substrate (*i*) in the gas phase of the biofilter at steady state is described by the mass balance Equation 6.1. In this equation the change of substrate concentration as it travels through the biofilter is equal to its diffusive flux into the biofilm phase.

$$U_g \frac{dC_i}{dz} = A_s D_{e,i} \left[\frac{dS_i}{dx} \right]_{x=0} \qquad \text{(Equation 6.1)}$$

(with the boundary condition: $C_i = C_{i,in}$ at z = 0)

As for the mass balance in the biofilm phase, the biodegradation rate of the substrate is equal to its diffusive flux across the biofilm thickness. This relationship is described by the following equation.

$$D_{e,i} \frac{d^2 S_i}{dx^2} = r_{s,i} \qquad \text{(Equation 6.2)}$$

(with the boundary conditions: $S_i = \frac{C_i}{m_i}$ at x = 0;

$\frac{dS_i}{dx} = 0$ at x = δ)

It is worth noting that the $r_{s,i}$ term in Equation 6.2 is substrate-dependent. If there was no inhibition observed during degradation of a specific substrate (e.g. acetaldehyde) in the presence of other substrates in the batch system, then $r_{s,i}$ shown in Equation 6.3 was substituted into Equation 6.2 to model the biofilter. Similarly, an expression describing either competitive inhibition (Equation 6.4) or noncompetitive inhibition (Equation 6.5) replaced the $r_{s,i}$ term in Equation 6.2 to properly reflect any inhibition observed in the batch systems.

No Inhibition: $$r_{s,i} = -\frac{k_i \cdot X_a \cdot S_i}{K_{s,i} + S_i} \qquad \text{(Equation 6.3)}$$

Competitive Inhibition by j: $$r_{s,i} = -\frac{k_i \cdot X_a \cdot S_i}{\left(K_{s,i}\left(1 + \frac{S_j}{K_{I,j}}\right) + S_i\right)} \qquad \text{(Equation 6.4)}$$

Noncompetitive Inhibition by j: $$r_{s,i} = -\frac{k_i \cdot X_a \cdot S_i}{\left(K_{s,i} + S_i\right)\left(1 + \frac{S_j}{K_{I,j}}\right)} \qquad \text{(Equation 6.5)}$$

6.2. METHODS

6.2.1. Biofilter Data for Model Evaluation

The results from Phases III-1, III-2 and I-5 of the biofilter study were evaluated using the biofilter model. Acetaldehyde, formaldehyde and ethanol were fed to the biofilter during Phases III-1 and III-2 at an EBCT of 5 and 10 seconds, respectively. Biofiltration of acetaldehyde alone was evaluated at an EBCT of 5 seconds during Phase I-5. As discussed in Chapter 5, the Celite® biofilter system examined in this research successfully treated the gas stream deigned to mimic typical loading ranges of ethanol plant pollutants, and contaminant breakthroughs occurred only after the first 2L packed section. Therefore, evaluation of the biofilter model for substrate removal profiles was only performed with respect to the first packed section which corresponds to a biofilter bed height of 10 cm and a packed bed volume of 2L.

6.2.2. Model Evaluation

To calibrate the biofilter model to the results of the biofilter study, X_a was varied while the remaining parameters were held constant. The values of X_t determined for Phases III and I-5 were used as an initial guess of X_a for model fitting, and the ratio of X_a/X_t was reported as the active biomass fraction.

The previous batch experimental data and modeling results suggest that acetaldehyde degradation by the enriched consortium was carried out via one pathway that led to ethanol formation while a second pathway was utilized to convert ethanol to acetate. These results suggest the possibility that two separate microbial communities present in the enriched consortium were responsible for the conversions of acetaldehyde

and ethanol. To reflect this, X_a was utilized as a fitting parameter for each pollutant degrading community in the biofilter modeling.

No inhibition of acetaldehyde degradation due to the presence of either ethanol or formaldehyde was observed in the batch experiments. Therefore, no inhibition was assumed for acetaldehyde degradation in the biofilter during Phases III-1 and III-2. For this reason, Monod kinetics (Equation 6.6) were utilized to model acetaldehyde degradation for both the Phase III (three component mixture) and the Phase I-5 (single acetaldehyde) biofilter experiments:

Acetaldehyde: $$r_{s,A} = -\frac{k_A \cdot X_a \cdot S_A}{K_{s,A} + S_A}$$ (Equation 6.6)

Based on the high ethanol EC observed in the biofilter, it is difficult to conclude if acetaldehyde had the same effect on ethanol degradation in the biofilter as it did in the batch experiments (Section 4.2.2). As a result, two scenarios were considered for modeling ethanol degradation in the biofilter during Phases III-1 and III-2. In the first scenario, acetaldehyde is reduced to ethanol and also noncompetitively inhibits ethanol degradation. This scenario had occurred during the batch Experiment BS-AE, so the equation describing the interactions between these two substrates developed in Section 4.2.2 (Equation 6.7) was therefore used to model this scenario. In the second scenario, acetaldehyde is not reduced to ethanol and does not inhibit ethanol degradation (Equation 6.8). In this scenario, Monod kinetics were used to describe ethanol degradation. In a similar manner, Monod kinetics (Equation 6.9) were used to describe formaldehyde degradation in the biofilm of the biofilter. Although no breakthrough of formaldehyde was observed in Phases III-1 and III-2 of the biofilter experiments, the model was used to

determine if the experimental data were consistent with the concentration profiles developed by the model.

Ethanol: $$r_{s.E} = 0.4\frac{k_A \cdot X_a \cdot S_A}{K_{s,A} + S_A} - \frac{k_E \cdot X_a \cdot S_E}{\left(K_{s,E} + S_E\right)\left(1 + \frac{S_A}{K_{I,A}}\right)}$$ (Equation 6.7)

$$r_{s,E} = -\frac{k_E \cdot X_a \cdot S_E}{K_{s,E} + S_E}$$ (Equation 6.8)

Formaldehyde: $$r_{s,F} = -\frac{k_F \cdot X_a \cdot S_F}{K_{s,F} + S_F}$$ (Equation 6.9)

6.2.3. Determination of Model Input Parameters

The parameters of biofilter, packing and biofilm characteristics, substrate characteristics and biodegradation kinetics that were used in the model are summarized in Table 6.2. The following sections describe how the model parameters were determined or estimated.

Table 6.2. Summary of the model input parameters

	Parameter	Value	Unit	Sources
Biofilter, Packing & Biofilm Characteristics				
U_g	Superficial gas velocity	70 (Phases III-1 &I-5) 35 (Phase III-2)	$m^3/m^2/hr$	This study
z	Packed bed height	0.1	m	This study
ε	Clean packing porosity	0.34	-	Alonso *et al*., 1997
ϕ	Packing sphericity	0.857	-	Alonso *et al*., 1997
ρ	Bulk packing density	5.1×10^5	g/m^3	Song, 2001
δ	Biofilm thickness	3×10^{-4}	m	Estimated
A_s	Biofilm specific surface area	425	m^2/m^3	Alonso *et al*., 1997
X_{bulk}	Bulk packing biomass density	1.1×10^3 (Phases III-1&2) 2.2×10^3 (Phase I-5)	g/m^3	This study
X_t	Total biofilm density	88×10^3 (Phases III-1&2) 172×10^3 (Phase I-5)	g/m^3	This study
Substrate Characteristics				
m_A	Henry's Law constant, acetaldehyde	2.73×10^{-3}	$m^3_{(l)}/m^3_{(g)}$	Gaffney *et al*., 1987
m_F	Henry's Law constant, formaldehyde	1.38×10^{-5}	$m^3_{(l)}/m^3_{(g)}$	Betterton & Hoffmann, 1988
m_E	Henry's Law constant, ethanol	2.05×10^{-4}	$m^3_{(l)}/m^3_{(g)}$	Gaffney *et al*., 1987
$D_{e,A}$	Diffusion coefficient, acetaldehyde	5.08×10^{-6}	m^2/hr	USEPA, 1994b
$D_{e,F}$	Diffusion coefficient, formaldehyde	7.13×10^{-6}	m^2/hr	USEPA, 1994b
$D_{e,E}$	Diffusion coefficient, ethanol	4.68×10^{-6}	m^2/hr	USEPA, 1994b
Biodegradation Kinetics				
k_A	Max. specific utilization rate for acetaldehyde	0.85±0.31	g/g/hr	This study
k_F	Max. specific utilization rate for formaldehyde	0.27±0.04	g/g/hr	This study
k_E	Max. specific utilization rate for ethanol	0.23±0.07	g/g/hr	This study
$K_{s,A}$	Half-saturation constant for acetaldehyde	3.50±2.76	g/m^3	This study
$K_{s,F}$	Half-saturation constant for formaldehyde	2.12±0.52	g/m^3	This study
$K_{s,E}$	Half-saturation constant for ethanol	0.32±0.18	g/m^3	This study
$K_{I,A}$*	Inhibition constant of acetaldehyde for ethanol degradation	0.93±0.63	g/m^3	This study

* Shown with its standard deviation estimated by AQUASIM from batch kinetic modeling.

Packing & Biofilm Characteristics

Biofilm specific surface area (A_s), biofilm thickness (δ) and total biofilm density (X_t) values have been reported in the literature for biofilter systems similar to the one utilized in this research: A_s 25-1000 m^{-1}, δ 30-600 μm and X_t 20-220 kg/m^3 (Cox *et al*., 1997; Fortin and Deshusses, 1999; Pineda *et al*., 2000; Dupasquier *et al*., 2002). In this research, A_s and δ are assumed to be inter-dependent according to the methods described by Alonso *et al.* (1997). In the Alonso paper, the authors examined the same size of Celite® packing and concluded that an increase in δ resulted in a decrease in A_s. As seen in Equation 6.10, A_s is a function of δ and several packing parameters including the number of spheres in contact with a given packing sphere (n). For the Celite® R-635 packing, n was calculated to be 10 using Equation 6.11, which describes the relationship between packing bed porosity (ε) and n. In the current study, this approach was followed to calculate A_s as a function of δ.

$$A_s = \frac{3(1-\varepsilon)}{2R}\left(1+\frac{\delta}{R}\right)\left((2-n)\frac{\delta}{R}+2\right) \qquad \text{(Equation 6.10)}$$

$$\varepsilon = 1.072 - 0.1193n + 0.004312n^2 \qquad \text{(Equation 6.11)}$$

where A_s = Surface area per unit volume under biofilm growth conditions (m^{-1});

δ = Biofilm thickness (m);

ε = Clean bed porosity (0.34 for Celite® R-635);

R = Characteristic packing sphere radius (3×10^{-3} m for Celite® R-635);

n = Number of characteristic packing spheres in contact with a given sphere (10 for Celite® R-635).

The biofilter model requires an estimate of the total biofilm density and the active biomass density as described earlier. The bulk biomass density on the packing was determined in this study by measuring the volatile solids (VS) content (C_{vs}) of duplicate samples of packing material during Phases I-5 and III. Equation 6.12 below was then used to convert the volatile solids concentration to the bulk biomass density on the packing. The average concentrations of 22×10^{-3} and 43×10^{-3} g VS /g dry packing (C_{vs}) for Phase III and Phase I-5 were used to calculate X_{bulk} in Equation 6.12. In order to determine the total biomass density in the biofilm, X_t, the biofilm surface area, A_s, and thickness, δ, must be estimated per Equation 6.13 below. Since A_s is a function of δ (Equation 6.10), the actual parameter that must be estimated is δ.

$$X_{bulk} = C_{VS} \cdot \rho \qquad \text{(Equation 6.12)}$$

$$X_t = X_{bulk} / \left(A_s \cdot \delta\right) \qquad \text{(Equation 6.13)}$$

The biofilm thickness, δ, was not explicitly measured in this research; therefore a series of model runs were required to estimate the biofilm thickness value that provided a reasonable fit to the Phases III-1 acetaldehyde removal data. In this analysis, three sets of δ (150, 300 and 450 μm) which resulted in calculated A_s of 530, 425 and 308 m^{-1}, respectively were evaluated. The measured X_{bulk} (1.1×10^3 g/m^3) value and the active biomass fraction in the biofilm, f_a, of 3.2%. were held constant throughout these model runs. The results of the model for each δ value are reported in Figure 6.2 along with the experimental acetaldehyde concentration profile during Phase III-1 when the influent acetaldehyde concentration was 0.093 g/m^3. It is important to note that since the bulk biofilm density on the packing X_{bulk} is held constant, the total biomass density in the

biofilm, X_t (and thus $X_a = f_a X_t$) is a function of δ as shown in the figure. The results of these modeling runs indicate that for the active biomass fraction evaluated, the biofilm thickness value of 300 µm provides the best fit to the experimental data. However, as evident in the figure, the predicted removal is relatively insensitive to biofilm thickness at least within the range evaluated. The δ value of 300 µm provided the best fit to the experimental data and is well within the biofilm thickness values reported in the literature; for these reasons this biofilm thickness was selected for use in the biofilter model.

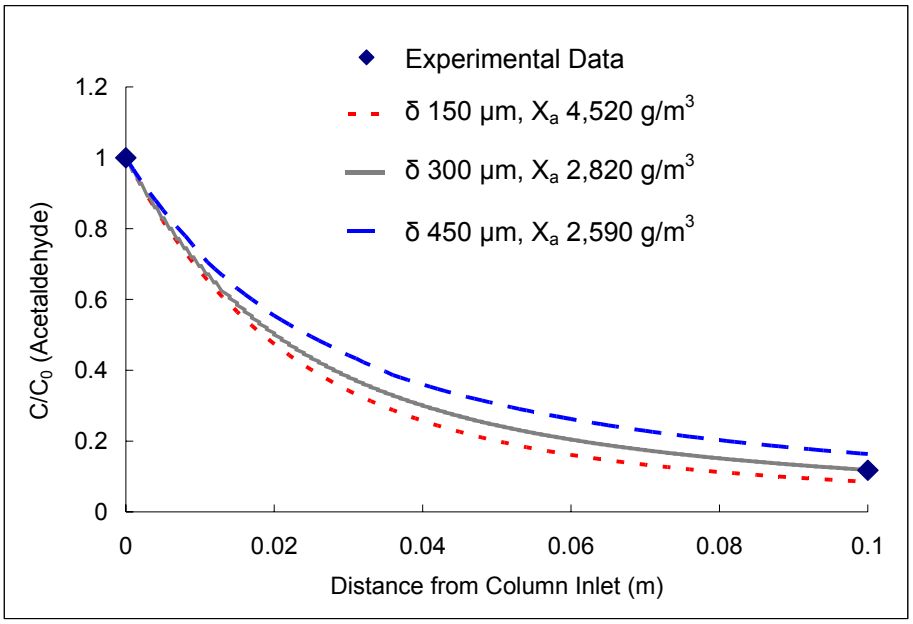

Figure 6.2. The experimental and predicted acetaldehyde removal profiles in the model using a range of δ and X_a.

As mentioned in Section 6.2.2, X_a was used as the fitting parameter to reflect different pollutant-degrading communities in the biofilter modeling. To determine the response of the model to changes in X_a, ±50% variation of 2,820 g/m^3 was evaluated for a constant biofilm thickness of δ (300 μm). Figure 6.3 shows the predicted acetaldehyde removal for each of the three X_a values; the predicted C/C_0 at the biofilter exit ranged from 0.09 to 0.21 when X_a decreased from 4,230 to 1,410 g/m^3, suggesting that the model was sensitive to changes in X_a.

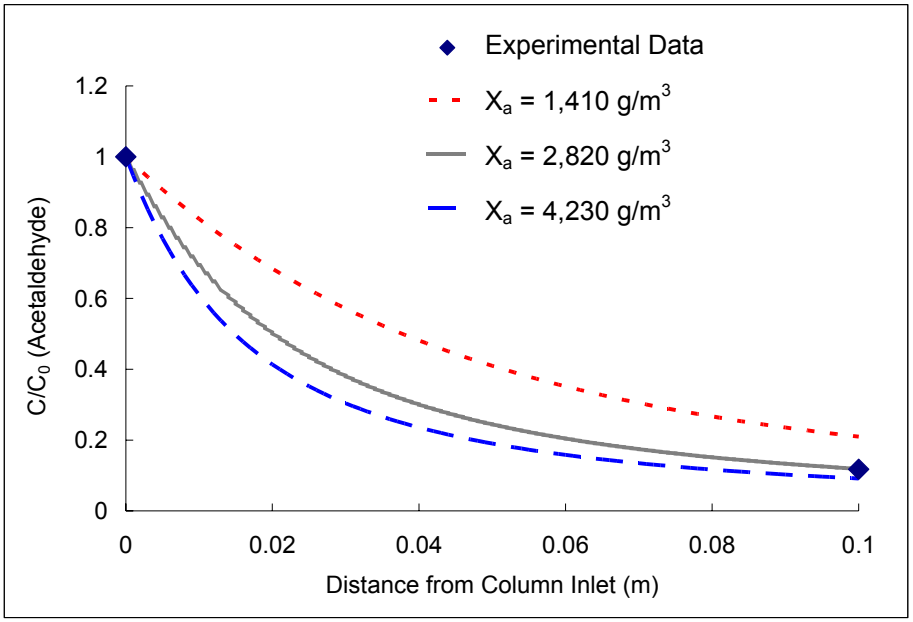

Figure 6.3. The experimental and predicted acetaldehyde removal profiles in the model using three X_a values for a constant δ (300 μm).

As expected, the model predicted less pollutant degradation across the biofilter column height as the active biofilm density declined. The importance of X_a in the Monod equation can also be seen by examining the mass balance equations used in this model; a higher X_a means faster pollutant degradation rates in the biofilm. It has also

been concluded in other studies that biomass density has a high impact on biofilter model predictions (Alonso *et al*., 1997; Arcangeli and Arvin, 1997; Song, 2001). These results further suggest that care should be taken when estimating a representative X_a value for biofilter model applications.

Substrate Characteristics

The biofilm that developed on the biofilter packing consisted of 94~98% by weight water. Thus, the diffusion coefficients for the substrates in water were assumed to reflect their diffusion in the biofilm. Also, Henry's Law was used to determine the substrate concentrations at the gas/biofilm interface. The chemical properties listed in Table 6.2 were applied in the biofilm model.

Biodegradation Kinetics

The kinetic parameters for substrate degradation were determined previously in the batch experiments as described in Chapters 3 and 4. For convenience, the values of k and K_s and their 95% joint confidence limits for acetaldehyde, formaldehyde and ethanol are reported in Table 6.2.

6.2.4. Numerical Approach

The nonlinear differential mass balance equations described in Section 6.1.2 were solved numerically to create a concentration profile of the substrate in the gas phase along the height of the biofilter. A computer code integrating the *bvp4c* solver in Matlab® was written to solve for substrate removal along the biofilter; the Matlab® code is presented in Appendix A. The *bvp4c* solver is a finite difference code that

implements the three-stage Lobatto IIIa formula for solving boundary value problems with fourth-order accuracy.

The biofilter model in Matlab® was initiated by inputting an initial guess of active biofilm density to solve for the value of dS/dx at the gas-biofilm interface in Equation 6.2. Next, this value was utilized in Equation 6.1 to calculate dC/dz at that point along the biofilter height, which was used to determine the change in the gas phase concentration of the substrate for the next height interval. This process was repeated over equal intervals of height from the inlet to the outlet of the biofilter. A substrate concentration profile over the height of the biofilter was returned from modeling and the effluent concentration was then compared to the experimental data from the biofilter study.

6.3. RESULTS AND DISCUSSION

6.3.1. Acetaldehyde Removal

Degradation of acetaldehyde in the biofilm of the biofilter was modeled utilizing the Monod model without inhibition (Equation 6.6). Although three different acetaldehyde loadings were examined in the biofilter in each of the experimental phases, it was observed that only the highest loadings provided an effluent concentration significantly above the method detection limit (MDL) of 0.002 g/m^3. Therefore, the highest acetaldehyde influent concentrations in Phase III-1 (C_{in} 0.093 g/m^3) and Phase III-2 (C_{in} 0.145 g/m^3) were introduced into the model, and their corresponding effluent concentration (Phase III-1 C_{out} 0.011 g/m^3 and Phase III-2 C_{out} 0.012 g/m^3) were set as the fitting targets.

Model fitting was initiated using 88,000 g/m^3 (the calculated X_t value of the biofilter during Phase III experiments) as the initial guess. It was concluded that a X_a value of 2,820 g/m^3 provided a good fit to the data at both EBCTs of 5 and 10 seconds. The ratio of this best-fit X_a to the X_t was approximately 3.2%; this active biomass fraction was held constant in the model which was then used to predict the effluent concentrations at the two other acetaldehyde loadings for each EBCT. The experimental data and model predictions for different inlet acetaldehyde concentrations at an EBCT of 5 and 10 seconds are shown in Figures 6.4 and 6.5, respectively.

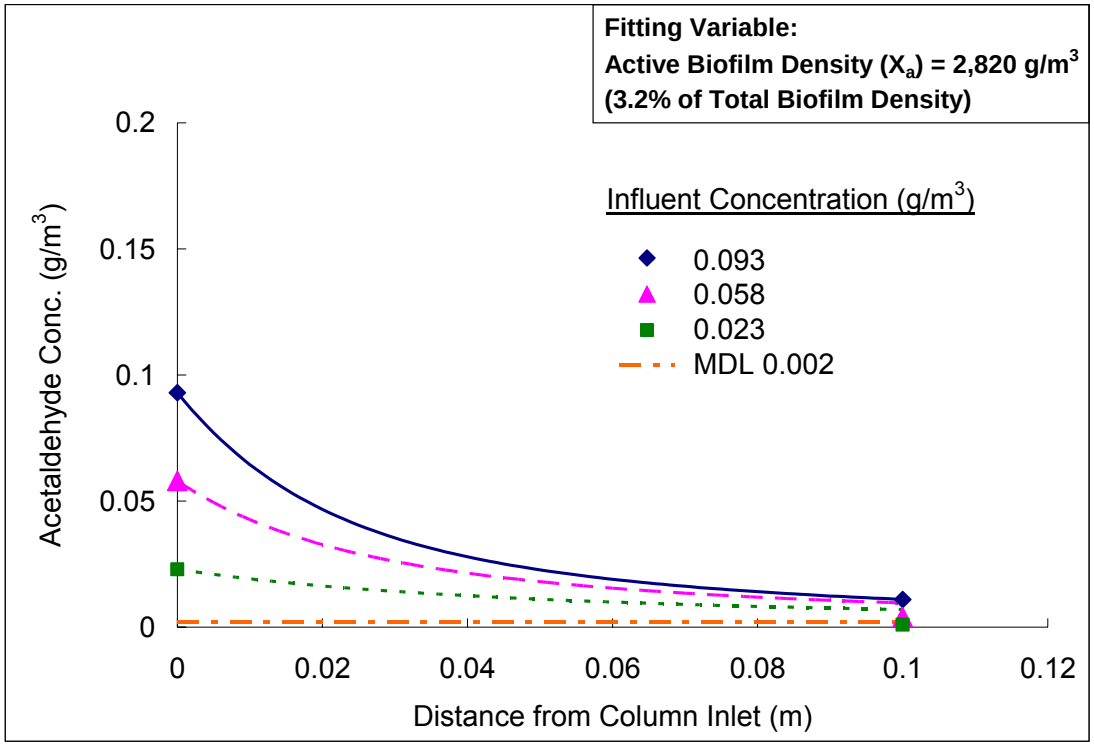

Figure 6.4. Comparison of the experimental data (symbols) and model predictions (lines) for the influent acetaldehyde concentrations of 0.023, 0.058 and 0.093 g/m^3 in the biofilter at an EBCT of 5 seconds during Phase III-1.

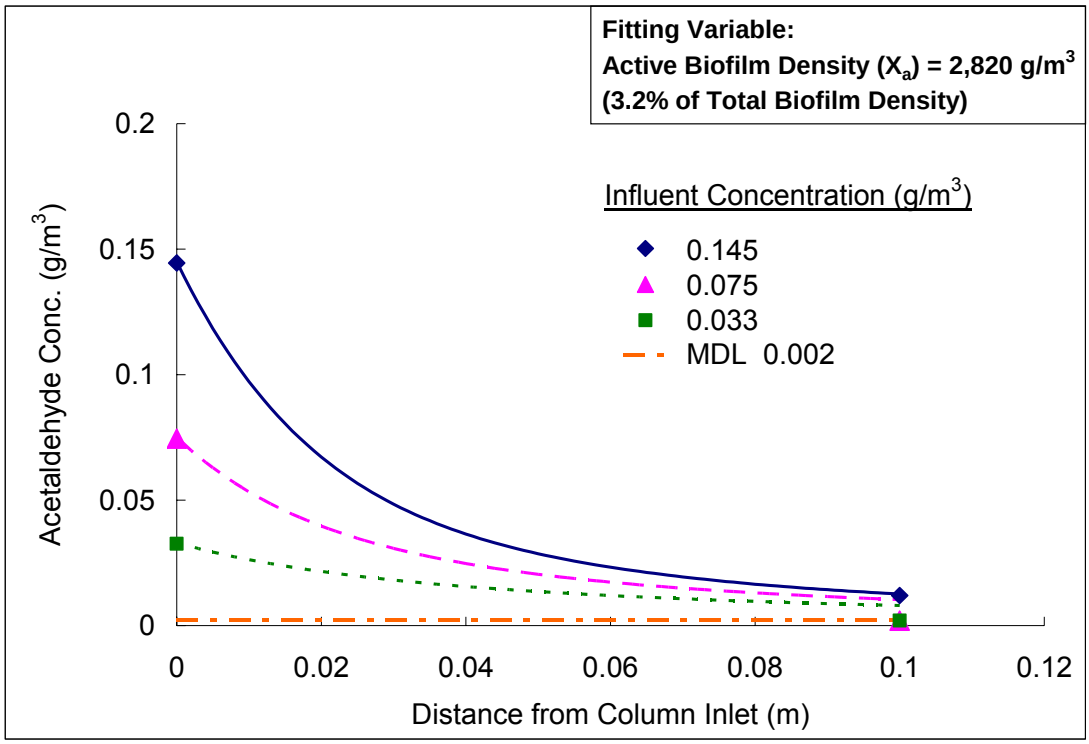

Figure 6.5. Comparison of the experimental data (symbols) and model predictions (lines) for the influent acetaldehyde concentrations of 0.023, 0.075 and 0.145 g/m^3 in the biofilter at an EBCT of 10 seconds during Phase III-2.

Using Equations 6.12 and 6.13, the X_t value of the biofilter during the Phase I-5 experiments was calculated as 172,000 g/m^3. This value was nearly double that of Phase III since the Phase I-5 experiments were conducted 45 days after Phase III. To account for the increase in biofilm density in Phase I-5, the X_a value (5,500 g/m^3) was determined by assuming that the active biomass fraction was the same (3.2%) as used in the previous model runs. Prediction of the acetaldehyde concentration profiles for three inlet concentrations was performed, and the results are present in Figure 6.6. These results indicate that the active biomass fraction of 3.2% that best described acetaldehyde degradation was fairly constant throughout the phases of the biofilter study.

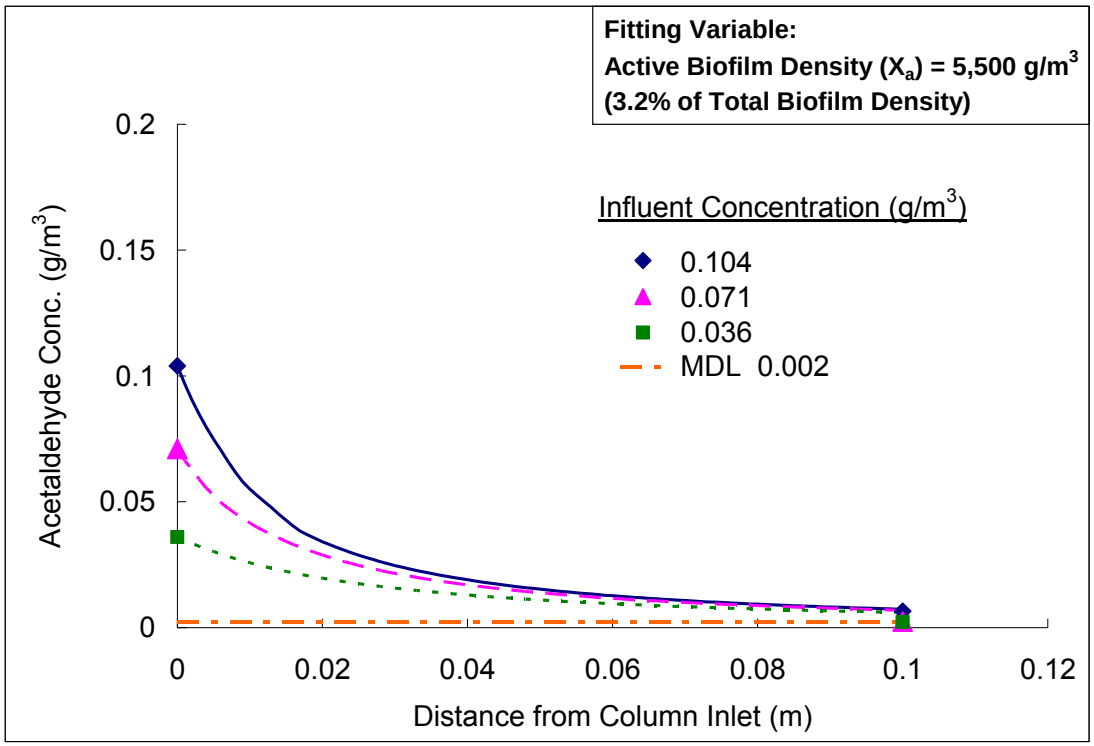

Figure 6.6. Comparison of the experimental data (symbols) and model predictions (lines) for the influent acetaldehyde concentrations of 0.036, 0.071 and 0.104 g/m^3 in the biofilter at an EBCT of 5 seconds during Phase I-5.

Although it is generally accepted that the biofilm in biofiltration systems consists of active and inactive biomass, most biofilter models do not explicitly differentiate X_t from X_a during modeling. In addition, it is a common practice to lump biomass density with other parameter(s) as a single fitting parameter (Hodge and Devinny, 1995; Deshusses *et al*., 1995a; Mohseni and Allen, 2000; Sologar *et al*., 2003; Zhang *et al*., 2008) in order to simplify modeling. Some biofilter studies used a hypothetical X_a that was either adapted from the literature or assumed based on the range reported in the literature (Zarook *et al*., 1993; Tang *et al*., 1996; Dirk-Faitakis and Allen, 2005). Only a few studies have used measured X_t to model X_a (Arcangeli and Arvin, 1997; Dupasquier

et al., 2002), or estimated an effective δ to reflect active biomass in their biofilter models (Tang *et al*., 1996; Arcangeli and Arvin, 1997; Sologar *et al*., 2003). Even though the active biomass fraction of 3.2% for the acetaldehyde-degrading community appears to be low, active biomass fractions of 5 to 10% yielding X_a values of 2,200 to 6,300 g/m^3 have been reported for biofiltration systems treating other VOCs such as toluene, trichloroethylene, methyl tert butyl ether and styrene (Arcangeli and Arvin, 1992; Cox *et al*., 1997; Arcangeli and Arvin, 1997; Pineda *et al*., 2000; Dupasquier *et al*., 2002). To further explore the impact of X_a on model predictions, a sensitivity analysis was performed as discussed below in Section 6.3.2. The results of this analysis suggest that other active biomass fractions do not fit the experimental results as well as the 3.2% value.

6.3.2. Ethanol Removal

Although acetaldehyde degradation resulted in ethanol accumulation and also noncompetitively inhibited ethanol degradation in the batch systems, high ethanol removal in the presence of acetaldehyde was observed in the biofilter. To explore the potential kinetics that were involved in ethanol degradation during Phase III of biofilter study, two scenarios describing ethanol degradation with and without substrate mixture effects were evaluated. Each of these scenarios is discussed below.

Inhibition of Ethanol Degradation by Acetaldehyde

In this scenario, ethanol formation as a result of acetaldehyde degradation was coupled with noncompetitive inhibition of ethanol degradation by acetaldehyde as described by Equation 6.7. Since the model predictions are dependent on the inhibition

constant, $K_{I,A}$, the response of the model to the values of $K_{I,A}$ determined in the batch kinetic studies (see Chapter 4) was evaluated. To perform this evaluation, the best-fit $K_{I,A}$ value (0.93 g/m^3) as well as the lower and upper bounds of $K_{I,A}$ (0.30 g/m^3 and 1.56 g/m^3) determined in the batch kinetic studies were examined in the model. It is important to note that the higher the value of $K_{I,A}$, the less that acetaldehyde inhibits ethanol degradation and the lower the active ethanol-degrading biomass, X_a, required to achieve a given pollutant removal. The highest ethanol influent concentration of 0.34 g/m^3 in the presence of 0.093 g/m^3 acetaldehyde (Phase III-1) was used in the model. The X_a required in the model to produce the observed ethanol effluent concentration was determined for each $K_{I,A}$ value. During these model runs, all model parameters except for X_a were held constant and X_a was changed until the effluent concentration of the model matched the experimental result.

The results, plotted in Figure 6.7, show that the model was able to match the experimental effluent concentration with $K_{I,A}$ values of 0.93 and 1.56 g/m^3 using active biomass fractions of 59% and 38% respectively. However, the model was not able to match the experimental effluent concentration using a $K_{I,A}$ value of 0.30 g/m^3(the lower bound of $K_{I,A}$ determined in the batch kinetic experiments) even when the active biomass fraction was set to 100%. These results indicate that the lower bound of the $K_{I,A}$ developed from the batch kinetic experimental results is not representative of the ethanol inhibition that was potentially present within the biofilter during the Phase III-1 experiments. However, the other values of $K_{I,A}$ (mid and upper bound) do provide a reasonable fit to the Phase III-1 experimental biofilter results but they require a much higher active ethanol-degrading biomass fraction than was predicted for the acetaldehyde-degrading community.

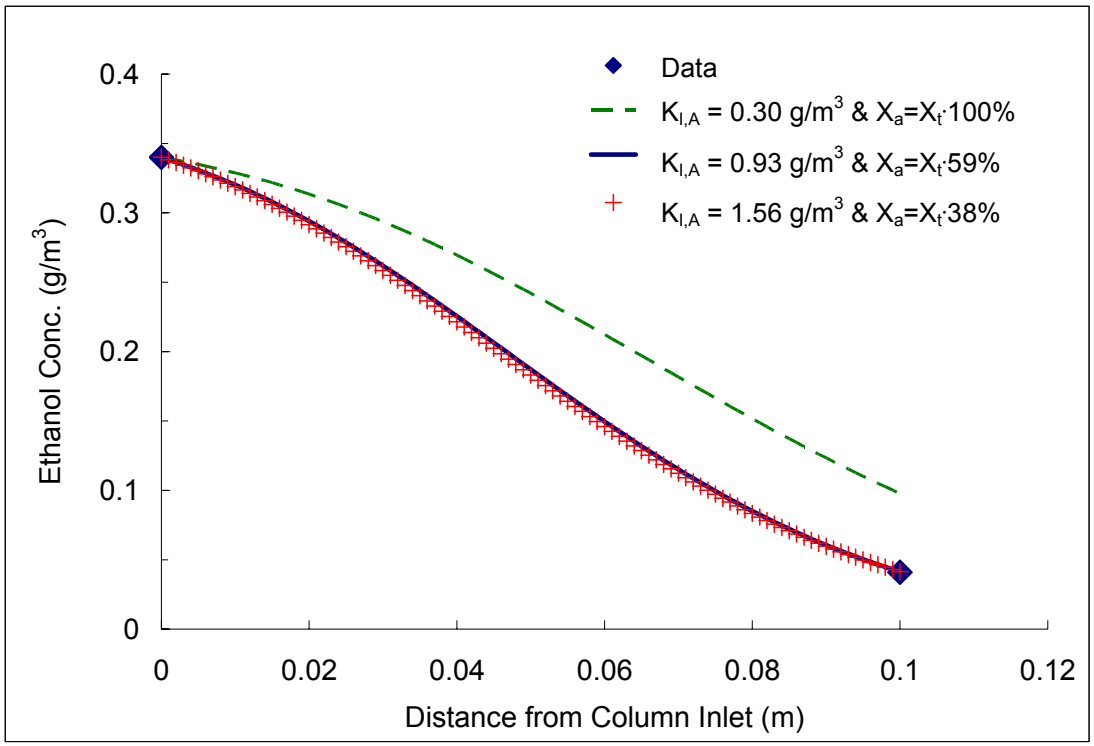

Figure 6.7. Predicted ethanol concentration profiles in the biofilter during Phase III-1 at an EBCT of 5 seconds for a range of inhibition constants ($K_{I,A}$) and active biomass fractions for the case that considers acetaldehyde inhibition of ethanol degradation.

To further examine the impact of $K_{I,A}$ values on the biofilter model predictions, the active biomass fractions determined above were used to predict the ethanol removal in the biofilter during the Phase III-2 experiments. In these model runs, the highest ethanol influent concentration of 0.3 g/m^3 in the presence of 0.145 g/m^3 acetaldehyde (Phase III-2) was used in the model. As seen in Figure 6.8, for all the $K_{I,A}$ and X_a evaluated, the model predicts complete removal of ethanol even though the ethanol was actually observed to breakthrough in the biofilter experiments (C_{out} = 0.025 g/m^3). These results suggests that a lower active biomass fraction is required for any of the selected $K_{I,A}$ values for data fitting for Phase III-2.

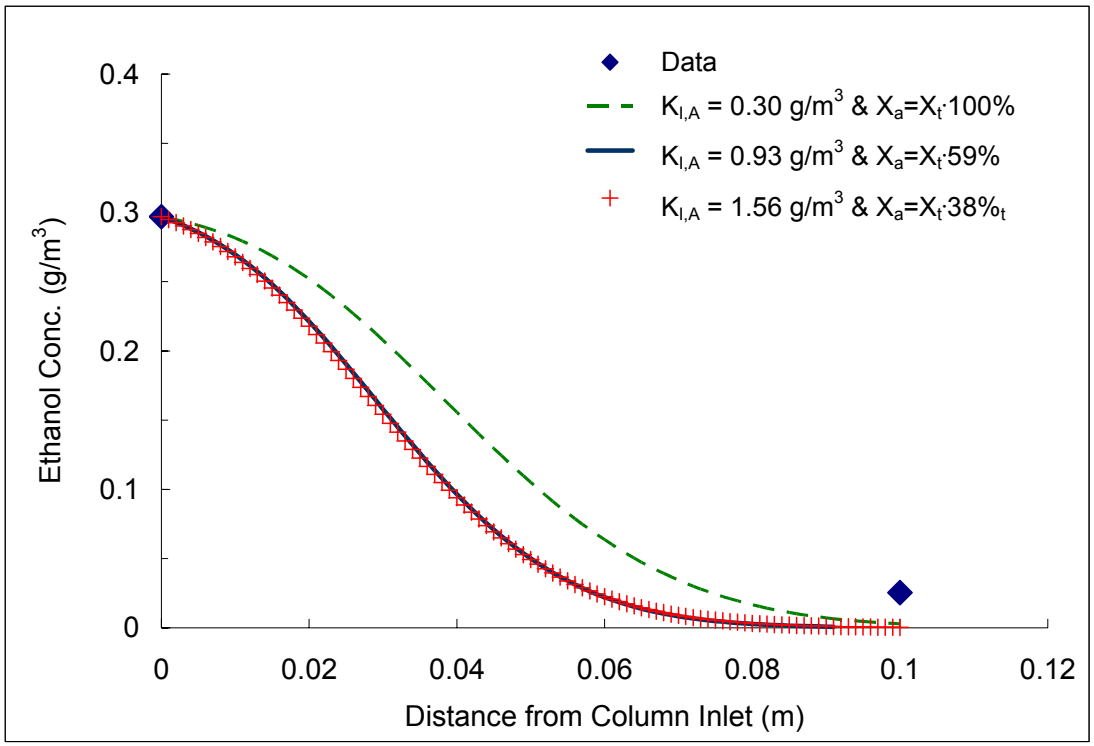

Figure 6.8. Predicted ethanol concentration profiles in the biofilter during Phase III-2 at an EBCT of 10 seconds for a range of inhibition constant ($K_{I,A}$) and active biomass fractions for the case that considers acetaldehyde inhibition of ethanol degradation.

To examine how the inhibition model describes the other two ethanol loadings in the presence of acetaldehyde during Phases III-1 and III-2, the $K_{I,A}$ value was set to 0.93 g/m^3 and the X_a value was set to 51,920 g/m^3 (59% of X_t) in the model. The model was then used to predict the ethanol concentration profiles along the biofilter height for both experimental phases. The experimental and predicted ethanol concentration profiles for three different ethanol influent concentrations during Phases III-1 and III-2 are shown in Figures 6.9 and 6.10, respectively. As seen in Figure 6.9, the predicted results for Phase III-1 agreed well with the experimental ethanol effluent concentrations. However, the inhibition model predicted complete ethanol removal at the 10 second EBCT in the

biofilter during Phase III-2 for all three ethanol loadings (Figure 6.10). This result is consistent with the complete removal observed for the two lowest ethanol influent concentrations of 0.10 and 0.20 g/m^3, but it does match the ethanol breakthrough observed at the highest ethanol influent concentration of 0.30 g/m^3. It is difficult to determine the reason for this discrepancy at the highest ethanol inlet concentration. Nevertheless, the experimental and model results indicate that ethanol breakthrough is not a significant concern.

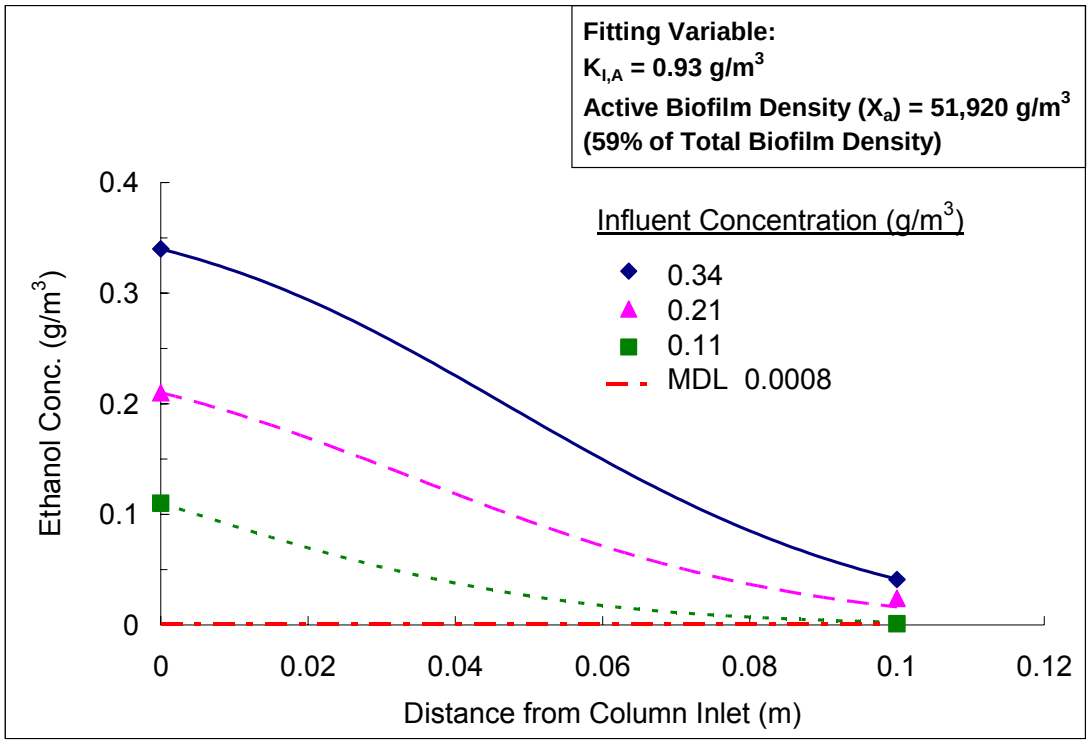

Figure 6.9. Comparison of the experimental data (symbols) and model predictions (lines) for the influent ethanol concentrations of 0.11, 0.21 and 0.34 g/m^3 in the biofilter at an EBCT of 5 seconds during Phase III-1. Model predictions were based on assuming acetaldehyde was converted to ethanol and acetaldehyde inhibited ethanol degradation in the biofilter.

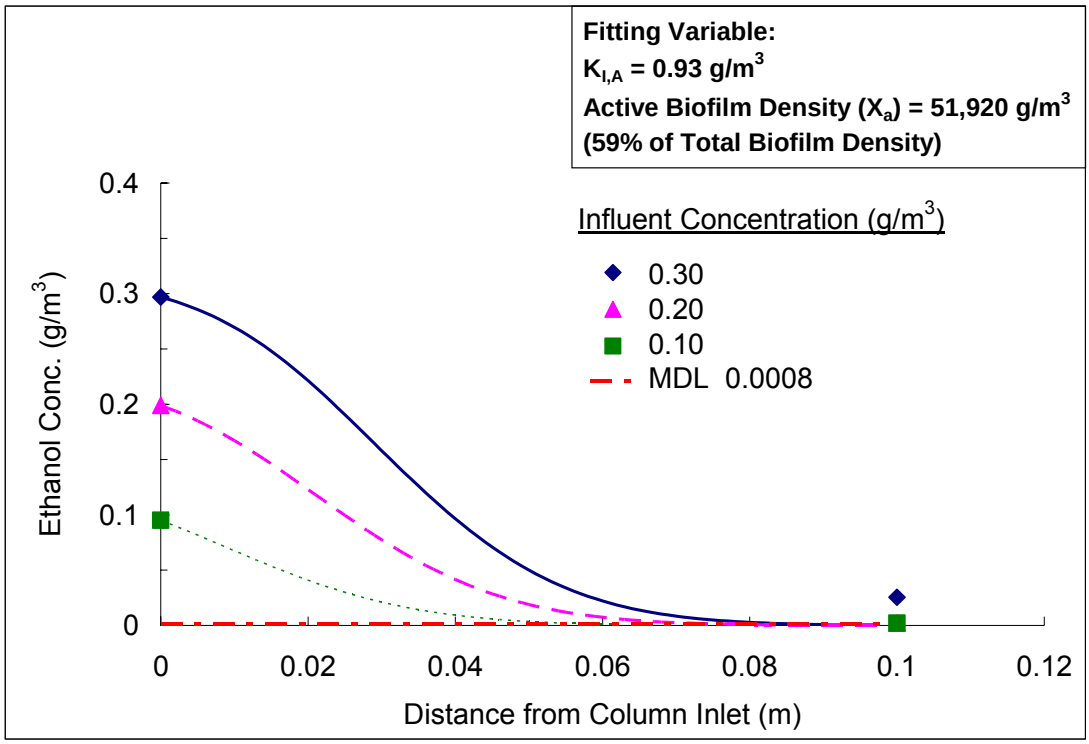

Figure 6.10. Comparison of the experimental data (symbols) and the model predictions (lines) for the influent ethanol concentrations of 0.10, 0.20 and 0.30 g/m^3 in the biofilter at an EBCT of 10 seconds during Phase III-2. Model predictions were based on assuming acetaldehyde was converted to ethanol and acetaldehyde inhibited ethanol degradation in the biofilter.

The active biomass fraction for the ethanol-degrading microbial community (38-59%) required in the model to fit the observed effluent ethanol concentrations (Figure 6.7) was much higher than the fraction (3.2%) required for acetaldehyde degradation. This significant difference in the active biomass fractions suggests that a more active ethanol-degrading microbial community was necessary for the observed ethanol removal efficiencies when inhibition of ethanol degradation by acetaldehyde occurred in the biofilter. Indeed, approximately 2 to 4 times higher loadings of ethanol than acetaldehyde were applied in the biofilter during Phase III, which might explain this

predicted increase in active ethanol-degrading biomass. Examining Figures 6.4 and 6.5 (the acetaldehyde concentration profiles) and Figures 6.9 and 6.10 (the ethanol concentration profiles in the presence of acetaldehyde inhibition) suggests that the acetaldehyde-degrading microbial community was probably more active and dominant in the upper section of the biofilter. Based on these figures, one can see that high acetaldehyde removals occurred at the upper biofilter section, where ethanol removal was significantly inhibited by the presence of acetaldehyde. Subsequently, acetaldehyde exerted less inhibition on ethanol degradation in the lower section of the biofilter, where most of the degradation of the influent ethanol actually took place.

Nevertheless, the model estimates the X_a range of the ethanol-degrading community to be from 33,440 to 51,920 g/m^3, which seems fairly reasonable when compared to values reported in the literature for similar pollutants. For instance, active biofilm densities up to 100,000 g/m^3 have been reported for biofilters removing readily degradable pollutants such as methanol and ethanol both in the absence and presence of other pollutants (Zarook *et al*., 1993; Baltzis *et al*., 1997; Sologar *et al*., 2003).

No Inhibition of Ethanol Degradation

The other scenario that was examined in the model was to assume that ethanol degradation in the biofilm was not affected by the presence of acetaldehyde. The Monod model (Equation 6.8) considering no inhibition of ethanol degradation by acetaldehyde and no ethanol formation from acetaldehyde degradation was used. As shown in Figures 6.11 and 6.12, the X_a value of 5,460 g/m^3 (approximately 6.2% of X_t) provided a good fit to the experimental data for both Phases III-1 and III-2 of the biofilter study. The fitted X_a value under the no inhibition scenario is slightly higher than that which was derived for acetaldehyde degradation (3.2% of X_t). Since the ethanol

loadings were higher than acetaldehyde loadings in the biofilter during this phase, it is reasonable that a higher fraction of active biomass degrading ethanol was observed.

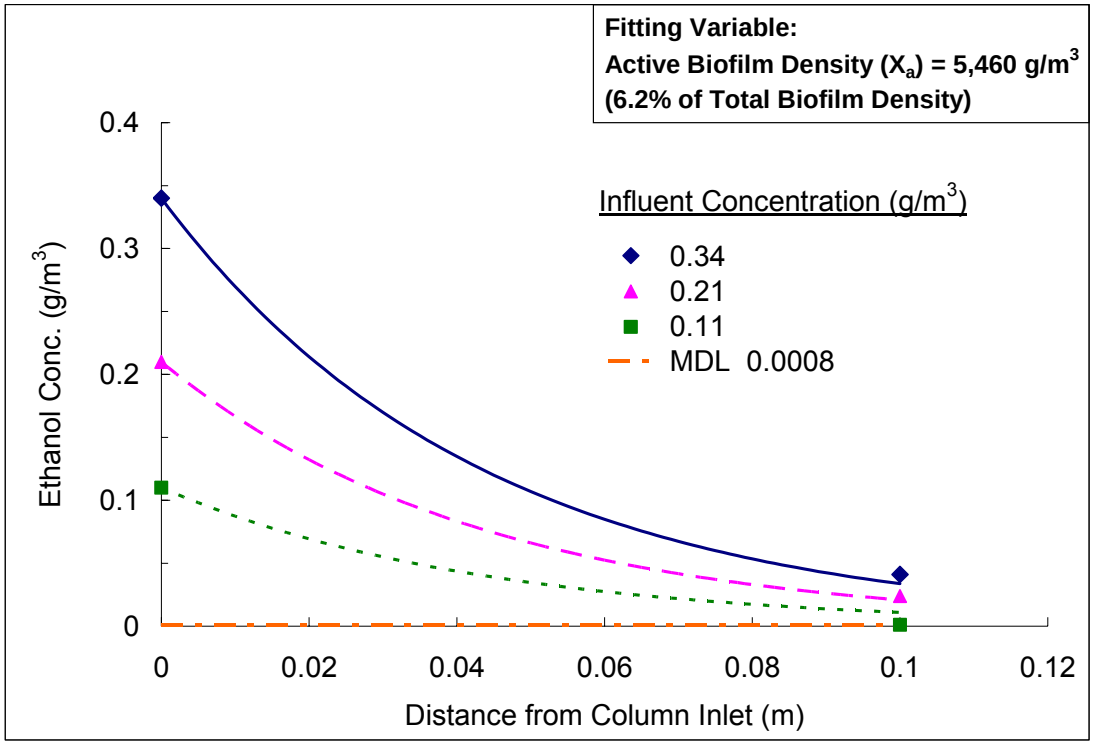

Figure 6.11. Comparison of the experimental data (symbols) and the model predictions (lines) for the influent ethanol concentrations of 0.11, 0.21 and 0.34 g/m^3 in the biofilter at an EBCT of 5 seconds during Phase III-1. Model predictions were based on assuming acetaldehyde was not converted to ethanol and acetaldehyde was not inhibited by ethanol degradation in the biofilter.

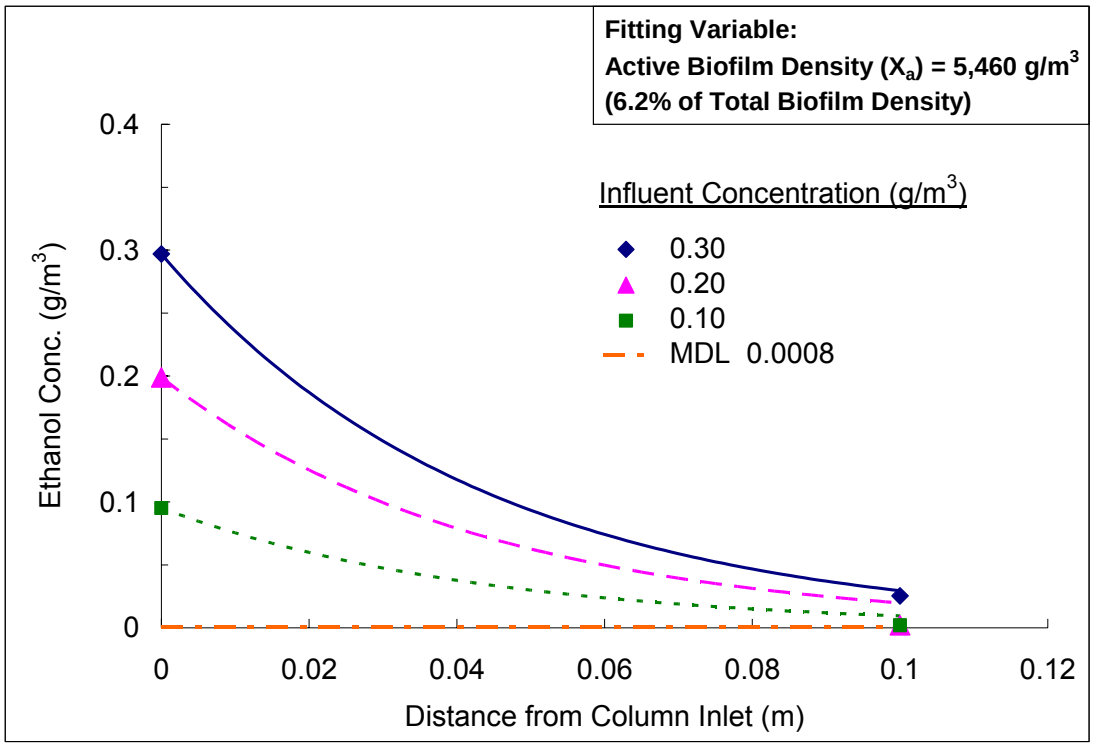

Figure 6.12. Comparison of the experimental data (symbols) and the model predictions (lines) for the influent ethanol concentrations of 0.10, 0.20 and 0.30 g/m^3 in the biofilter at an EBCT of 10 seconds during Phase III-2. Model predictions were based on assuming acetaldehyde was not converted to ethanol and acetaldehyde was not inhibited by ethanol degradation in the biofilter.

The kinetic data collected from the batch experiments with the aldehyde-enriched consortium indicate that ethanol degradation was inhibited by the presence of acetaldehyde. This enriched culture was used to inoculate the biofilter and thus it was expected that the inhibition observed in the batch experiments would also be observed in the biofilter. If the microbial community in the biofilter after 129 days of operation was similar to the aldehyde-enrichment culture used to inoculate the biofilter, then it would be appropriate to utilize these inhibition kinetics; however, the microbial population in the biofilter may have changed over time as observed by Park (2004). In this case, it would

be possible that Monod kinetics more accurately reflected the biodegradation kinetics actually occurring in the biofilter.

The shape of the predicted ethanol profiles for the modeling case where no inhibition was assumed (Figures 6.11 and 6.12) were distinctly different from those predicted for the case where acetaldehyde was assumed to inhibit ethanol degradation (Figures 6.9 and 6.10). Based on the limited data available in this study, it would appear that the Monod kinetics without inhibition fit the data better. However, additional experimental profile data at intermediate column depths would be required to definitively determine which modeling scenario most accurately reflected the kinetics in the biofilter. While such intermediate profile data is commonly collected for biofilters operated at long contact times of 30 seconds or greater, at the short contact times (5 to 10 seconds) evaluated in this research for these readily degradable compounds, it is more difficult to obtain this data.

6.3.3. Formaldehyde Removal

Even though no formaldehyde breakthroughs occurred during Phases III-1 and III-2 of the biofilter study, it is still meaningful to run the model to determine if any formaldehyde breakthrough was predicted. The X_a values that had been previously determined for acetaldehyde degradation (2,820 g/m^3) and ethanol degradation in the absence of inhibition (5,460 g/m^3) were used as two estimates of the active biomass fraction for the formaldehyde-degrading community. The model predictions suggest that both X_a values provide a similar fit to the experimental data; as an example, the model results assuming a 6.2% active formaldehyde-degrading biomass fraction in the biofilm are shown in Figure 6.13. The experimental data and model predictions are in

good agreement, suggesting complete removal of the formaldehyde loadings examined during Phase III.

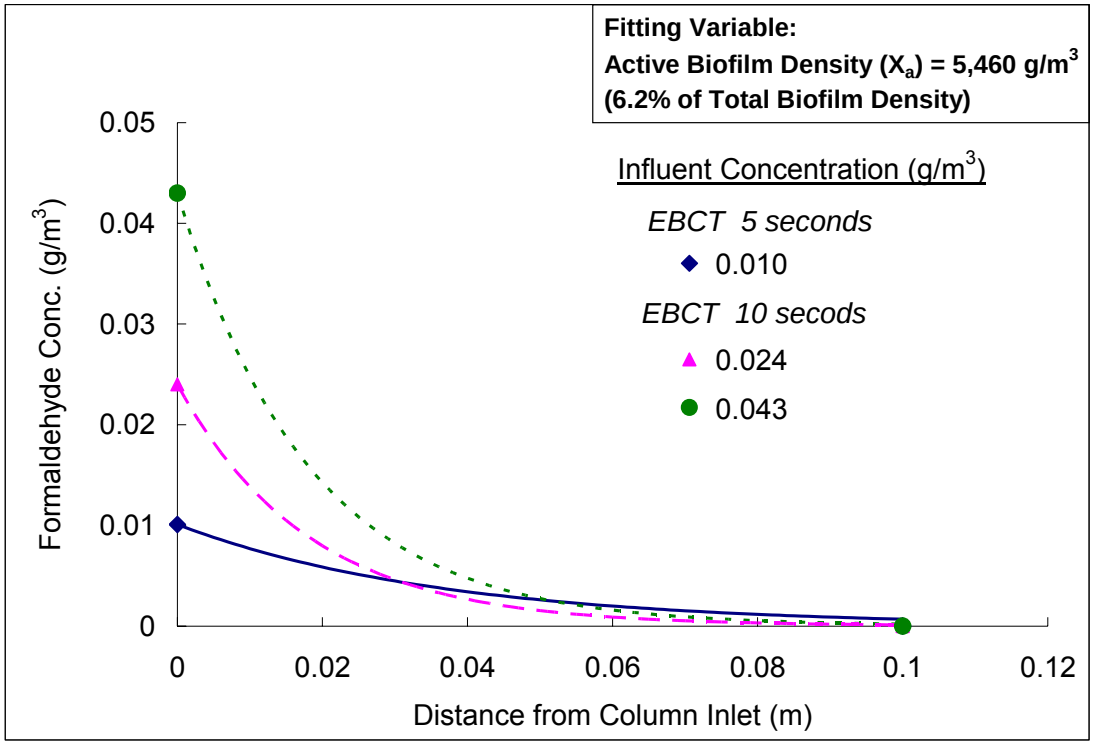

Figure 6.13. Comparison of the experimental data (symbols) and model predictions (lines) for the influent formaldehyde concentrations of 0.010 g/m^3 at an EBCT of 5 seconds during Phase III-1, and 0.024, 0.043 g/m^3 at an EBCT of 10 seconds during Phase III-2.

6.4. SUMMARY

A numerical model was developed to describe the performance of the Celite® biofilter system treating acetaldehyde during Phase I-5 and the substrate mixture of acetaldehyde, formaldehyde and ethanol during Phases III-1 and III-2 of the biofilter study. This model was established on the basis of considering pollutant transfer in the air and biofilm phases and including biodegradation in the biofilm phase, with substrate degradation kinetics and biofilter characteristic parameters incorporated. Nonlinear mass balance equations were solved numerically in Matlab® to provide pollutant concentration profiles along the height of the biofilter. This model was used to examine substrate degradation kinetics and mixture effects in the biofilter system.

The model was capable of describing acetaldehyde removals in the absence and presence of other substrates in the biofilter system. Assuming no inhibition, it was estimated by the model that approximately 3.2% of total biofilm density (X_t) was responsible for the acetaldehyde removal observed in the biofilter. Similarly, the model also confirmed that formaldehyde breakthroughs would not occur under the loadings that were supplied to the biofilter assuming that 3.2 to 6.2% of the biomass was actively degrading formaldehyde.

While the model results described acetaldehyde and formaldehyde removals adequately, it was difficult to determine the extent of inhibition of ethanol degradation by acetaldehyde in the biofilter. If a similar inhibition observed in the batch systems occurred in the biofilter system, an active fraction between 38 and 59% of the total biomass in the biofilter was required in the model to match the ethanol elimination observed in the biofilter. In this scenario, the acetaldehyde-degrading microbial community was most likely active in the upper section of the biofilter, while the ethanol-degrading microbial community was present in the lower biofilter section, where less

inhibition of ethanol degradation by acetaldehyde occurred. On the other hand, it would only require 6.2% of active biomass for ethanol removal in the biofilter system if no inhibition of ethanol degradation by acetaldehyde took place. This lack of inhibition could occur if there was a shift in the dominant microbial community between the enrichment culture used in the batch system to determine biodegradation kinetic parameters and the biofilm community that ultimately developed in the biofilter. Additional data would be required to determine whether substrate inhibition was occurring in the biofilter or not. However, the modeling results do elucidate the trade off between assuming no inhibition where a low active biomass fraction is required to fit experimental results and assuming inhibition and a much higher active biomass fraction to fit observations.

Chapter 7: Conclusions

Ethanol is widely used as an additive in reformulated gasoline, replacing MTBE, and is also considered an attractive biofuel option and renewable energy source. In the U.S., the majority of ethanol is produced from corn feedstock and production has soared to 7.7 billion gallons in 2008. Ethanol has the potential to reduce our dependence on fossil fuels; however, its production from corn stock is facing increasing scrutiny due to several environmental issues that have recently emerged. One significant environmental impact of corn-derived ethanol production is the emission of volatile organic compounds (VOCs) and hazardous air pollutants (HAPs). The most common VOC control technology implemented at ethanol production facilities is incineration, which can provide high pollutant destruction efficiencies but is costly and generates greenhouse emissions.

7.1. RESCEARCH CONCLUSIONS

The overall objective of this dissertation was to evaluate the feasibility of biofiltration as an alternative air pollution control technology to treat VOC emissions from corn-derived ethanol production facilities. Specifically, this research study focused on acetaldehyde, formaldehyde, ethanol and acetic acid, which represent both the hazardous and non-hazardous air pollutants emitted from these facilities. The key observations and specific conclusions that can be drawn from this dissertation research are summarized as follows:

1. In the single substrate batch reactors, an enriched aldehyde-degrading consortium was capable of completely degrading acetaldehyde, formaldehyde and ethanol.

Substrate degradation kinetics for acetaldehyde, formaldehyde and ethanol were estimated using nonlinear regression analysis of the Monod model.

- The maximum specific substrate utilization rates (k, mg/mg VSS/L) were determined to be in the following order: acetaldehyde (0.85) > formaldehyde (0.27) ≈ ethanol (0.23). These results suggest that the consortium has the highest degradation rate for acetaldehyde.
- The half-saturation constant (K_s, mg/L) for each substrate followed the order: acetaldehyde (3.5) ≈ formaldehyde (2.1) > ethanol (0.3), implying that ethanol is the most biodegradable pollutant for the consortium.

2. In dual substrate batch systems:
   - Acetaldehyde degradation was not inhibited by either formaldehyde or ethanol and its removal was described by the Monod model. In addition, aerobic acetaldehyde conversion to ethanol occurred both in the absence and presence of ethanol as a co-substrate.
   - Ethanol degradation was inhibited by acetaldehyde and its removal was described by a noncompetitive inhibition model with an estimated acetaldehyde inhibition constant ($K_{I,A}$) of 0.93±0.63 mg/L.
   - Formaldehyde degradation was inhibited in the dual substrate experiments, but not by acetaldehyde, ethanol (acetaldehyde degradation byproduct) or acetate (ethanol degradation byproduct). However, further research is required to determine the true cause of this inhibition.

The batch experimental results suggest that there is potential for two or more dominant microbial communities in the enriched consortium: an acetaldehyde-

degrading community (bacteria with similar functional capabilities to facultative bacteria *Zymomonas*) that reduces acetaldehyde to ethanol, and an ethanol-degrading community (bacteria with similar functional capabilities to acetic acid bacteria) that oxidizes ethanol to acetate.

3. The Celite® biofilter system successfully treated a series of simulated waste gas streams that progressed in complexity from a single VOC component to a four component mixture at relatively short EBCTs of 5 and 10 seconds.
   - Greater than 97% aldehyde removal was achieved in the biofilter when the waste gas stream contained a single aldehyde. It was also determined that a longer startup period was required for acetaldehyde than for formaldehyde.
   - No negative impacts on overall aldehyde removal were observed when formaldehyde and acetaldehyde were supplied simultaneously to the biofilter, suggesting that biofiltration is a feasible option to control HAP emissions from the ethanol plants.
   - High ethanol loadings (up to 213 $g/m^3/hr$) did not affect the removal of formaldehyde and acetaldehyde that were also present in the influent gas stream of the biofilter.
   - Extended feeding of acetic acid, however, gradually hindered biofilter performance, especially when the system pH declined. At a pH of 2.8 to 3.5, reduced removal efficiencies of acetaldehyde (30%), ethanol (33%), acetic acid (95%) and formaldehyde (97%) were observed.

While the presence of multiple substrates led to reductions in the rates of degradation for formaldehyde and ethanol in the batch experiments, the results

from the biofilter study indicated that the system pH is a more crucial operating parameter. This impact of pH on aldehyhde degradation in the biofilter was consistent with the batch experimental results. Thus, a biofilter system with proper pH control can be utilized to treat a gas stream with pollutant loadings representative of ethanol plant emissions.

4. A numerical model integrating pollutant degradation kinetics determined from batch kinetic data was successfully developed to examine the observed biofilter performance.
   - Although the extent to which ethanol degradation in the biofilter was inhibited by acetaldehyde cannot be definitively determined, the inhibition observed in the biofilter was not as pronounced as that seen within the batch experiments.
   - Pollutant removals are quite sensitive to the active biomass fraction in the biofilm.
   - When no substrate inhibition is assumed in the model, a low active biomass fraction is required to fit the experimental observations. However, when substrate inhibition is incorporated into the model, a much higher active biomass fraction must be used to fit experimental results.

These results reinforce the need for accurate estimates of active biomass fractions in the biofilm particularly in mixed substrate systems where substrate inhibition may be occurring.

7.2. PRACTICAL IMPLICATIONS

The work presented in this dissertation represents the first evaluation of biofiltration of VOC/HAP emissions from corn-derived ethanol production facilities. As previously noted, fundamental kinetic data for simultaneous biodegradation of ethanol plant air pollutants are not available in the published literature. Thus, batch kinetic data from this research provide fundamental insights to the degradation of substrate mixtures of dual aldehydes as well as dual aldehyde mixtures containing ethanol and acetic acid. The results of the biofilter study indicate that a biofiltration system is capable of treating simulated ethanol plant waste gases at short EBCTs, suggesting small biofilter systems would be sufficient and that this technology is an attractive option for ethanol plants. Based on the experimental conditions investigated during the biofilter study, pH appears to be the most crucial operating parameter that must be controlled for a successful biofiltration system.

Although the research indicates that biofiltration is a feasible treatment option, additional research will be required before biofiltration can be implemented as a full-scale treatment technology for VOC/HAP control at ethanol production facilities. First, biofilter performance at elevated temperatures must be investigated to evaluate the potential for treating various types of waste gas streams emitted from ethanol production plants. In addition, an alternative biofilter configuration such as a biotrickling filter, or a coupled system integrating a scrubber and a biofilter should be examined to determine if it is necessary and/or if it would provide better control of system pH. Finally, although the biofilter model developed in this research can cope with substrate inhibition, more research will be required to further delineate the types and levels of inhibition that will potentially occur within a biofilter system treating ethanol plant waste gases.

Appendix A

Computer Code Developed in Matlab®

I. Biofilter Modeling Program to Model Single Substrate (Acetaldehyde) Degradation in the Celite® Biofilter

```
function acethbvp_single_As425_delta300_Xa2820
global dsazero dcdza Sa Ca Conca z Cnewa Couta resultsa

Dea = 0.00000508; %Diffusivity for acetaldehyde
ma = 0.00273; %Henry's Law constant for acetaldehyde
ztop = 0.1; %Packed bed height
Cina = 0.093; %Influent concentration of acetaldehyde
n = 1; %Number of iterations
options = [];
Cnewa = Cina;
Conca = zeros(101,1);
z = zeros(100,1);
z(1,1) = .1 - ztop;
Conca(1,1) = Cnewa;
while n < 101
    Ca = Cnewa; %Acetaldehyde concentration in the gas phase
    Sa = Ca/ma; %Acetaldehyde concentration in the biofilm
    solinit = bvpinit(linspace(0,0.0003,100),[Sa 0]); %Initial solution guess for
              acetaldehyde degradation through the biofilm with biofilm thickness (delta)
              0.0003 m
    sol = bvp4c(@aceode,@acebc,solinit,options,Sa); %Solve for acetaldehyde
          degradation through the biofilm
    x=sol.x;
    y=sol.y;
    dsazero=y(2,1); %ds/dx at the biofilm/gas interface
    As = 425; %Biofilm specific surface area
    Ug = 70; % Superficial gas velocity
    dcdza = As*Dea*dsazero/Ug; %Change in acetaldehyde concentration with height
              at the point in the column
    Cnewa = Ca + Ca*dcdza*.01; %Calculate acetaldehyde concentration for the next
              point in the column
    n = n + 1;
    Conca(n,1) = Cnewa;
    z(n,1) = ztop*(n-1)*0.01; %Move down the column to the next point in column
              height
```

```
end
Couta = Conca(101,1);
resultsa = zeros(101,2);
resultsa(:,1) = z; %z
resultsa(:,2) = Conca; %Acetaldehyde concentration at each point along the column
plot(h,Conca,'--') %Plot the acetaldehyde concentration profile for review
axis([0 0.2 0 0.2])
title(['Change in Concentration vs. Height of Column Traveled'])
xlabel('z')
ylabel('Concentration g/m3')
fprintf('Concentration of acetaldehyde at the column outlet=%7.3f.\n',Couta) %Output
        acetaldehyde effluent concentration
csvwrite('Acetaldehyde_with
            Ethanol_EBCT5S_As425_delta300_Xa2820_Cin0.093.dat',resultsa); %Record
            acetaldehyde concentration through the column in a data file
%---------------------------------------
function dydx = aceode(x,y,Sa)
bea = 1; %beta
Dea = 0.00000508; %Diffusivity coefficient for acetaldehyde
Xe = 2820; %Active biofilm density for acetaldehyde degradation
Ksa = 3.5; %Half-saturation constant for acetaldehyde degradation
ka = 0.85; %Max specific utilization rate for acetaldehyde degradation


dydx = [ y(2)
            (bea*Xe*ka*y(1))/(Dea*(Ksa+y(1)))];

%---------------------------------------
function res = acebc(ya,yb,Sa)
res = [ ya(1) - Sa
            yb(2)];
```

II. Biofilter Modeling Program to Model Inhibition of Ethanol Degradation by Acetaldehyde in the Celite® Biofilter

```
function acethbvp_Eformation_AInhibition_Xe25960_Kia093_As425_delta300
global dsazero dcdza Sa Ca Conca z Cnewa Couta resultsa dsezero dcdze Se Ce Conce
        Cnewe Coute resultse

M = ['z','C'];
dlmwrite('EthanolFormation_AInhibtion_Xa2820_Acetaldehyde_Cina0.093_Kia0.93_
        As425_delta300.dat',M,','); %Create a data file with headers for data
dlmwrite('EthanolFormation_AInhibtion_Xe25960_Ethanol_Cine0.34_Cina0.093_
        Kia0.93_ As425_delta300.dat',M,','); %Create a data file with headers for data

Dea = 0.00000508; %Diffusivity coefficient for acetaldehyde
Dee = 0.00000468; %Diffusivity coefficient for ethanol
ma = 0.00237; %Henry's Law constant for acetaldehyde
me = 0.000205; %Henry's Law constant for ethanol
ztop = 0.1; %Packed bed height
Cina = 0.093; %Influent concentration of acetaldehyde
Cine = 0.34; %Influent concentration of ethanol
n = 1; %Number of iterations
options = [];
Cnewa = Cina;
Cnewe = Cine;
Conca = zeros(101,1);
Conce = zeros(101,1);
z = zeros(100,1);
z(1,1) = .1 - ztop;
Conca(1,1) = Cnewa;
Conce(1,1) = Cnewe;
while n < 101
    Ca = Cnewa; %Acetaldehyde concentration in the gas phase
    Sa = Ca/ma; %Acetaldehyde concentration in the biofilm
    Ce = Cnewe; %Ethanol concentration in the gas phase
    Se = Ce/me; %Ethanol concentration in the biofilm
    solinit = bvpinit(linspace(0,0.0003,100),[Sa 0]); %Initial solution guess for
            acetaldehyde degradation through the biofilm with biofilm thickness (delta)
            0.0003 m
    sol = bvp4c(@aceode,@acebc,solinit,options,Sa); %Solve for acetaldehyde
        degradation through the biofilm
    x=sol.x;
    y=sol.y;
    dsazero=y(2,1); %ds/dx at the biofilm/gas interface
    As = 425; %Biofilm specific surface area
    Ug = 70; %Superficial gas velocity
```

```
        dcdza = As*Dea*dsazero/Ug; %Change in acetaldehyde concentration with height
                at the point in the column
        Cnewa = Ca + Ca*dcdza*.01; %Calculate acetaldehyde concentration for the next
                 point in the column
        solinit = bvpinit(linspace(0,0.0003,100),[Se 0]); %Initial solution guess for ethanol
                degradation through the biofilm with biofilm thickness (delta) 0.0003 m
        sol = bvp4c(@ethode,@ethbc,solinit,options,Se,Sa); %Solve for ethanol degradation
              through the biofilm
        x=sol.x;
        y=sol.y;
        dsezero=y(2,1); %ds/dx at the biofilm/gas interface
        As = 425; %Biofilm specific surface area
        Ug = 70; %Superficial gas velocity
        dcdze = As*Dee*dsezero/Ug; %Change in ethanol concentration with height at the
                point in the column
        Cnewe = Ce + Ce*dcdze*.01; %Calculate ethanol concentration for the next point in
                 the column
        n = n + 1
        Conca(n,1) = Cnewa;
        Conce(n,1) = Cnewe;
        z(n,1) = ztop*(n-1)*0.01; %Move down the column to the next point in column
                height

end
Couta = Conca(101,1);
Coute = Conce(101,1);
resultsa = zeros(101,2);
resultse = zeros(101,2);
resultsa(:,1) = z; %z
resultsa(:,2) = Conca; %Acetaldehyde concentration at each point along the column
resultse(:,1) = z; %z
resultse(:,2) = Conce; %Ethanol concentration at each point along the column
%plot(z,Conca,'--') %Plot concentration profile of acetaldehyde if desired
%axis([0 0.2 0 0.2])
%title(['Change in Concentration vs. Height of column traveled'])
%xlabel('z')
%ylabel('Concentration g/m3')
fprintf('Concentration of acetaldehyde at the column outlet=%7.3f.\n',Couta) %Effluent
      acetaldehyde concentration
fprintf('Concentration of ethanol at the column outlet=%7.3f.\n',Coute) %Effluent ethanol
      concentration
dlmwrite('EthanolFormation_AInhibtion_Xa2820_Acetaldehyde_Cina0.093_Kia0.93_
        As425_delta300.dat',resultsa,'-append');
%Record acetaldehyde concentration through the column to the created data file
dlmwrite('EthanolFormation_AInhibtion_Xe25960_Ethanol_Cine0.34_Cina0.093_
```

```
            Kia0.93_ As425_delta300.dat',resultse,'-append');
%Record ethanol concentration through the column to the created data file
%---------------------------------------
function dydx = aceode(x,y,Sa)
bea = 1; %beta
Dea = 0.00000508; %Diffusivity coefficient for acetaldehyde
Xe = 2820; %Active biofilm density for acetaldehyde degradation
Ksa = 3.5; %Half-saturation constant for acetaldehyde degradation
ka = 0.85; %Max specific utilization rate for acetaldehyde degradation


dydx = [ y(2)
            (bea*Xa*ka*y(1))/(Dea*(Ksa+y(1)))];

%---------------------------------------
function res = acebc(ya,yb,Sa)
res = [ ya(1) - Sa
            yb(2)];

%---------------------------------------
function dydx = ethode(x,y,Se,Sa)
bee = 1; %beta
Dee = 0.00000468; %Diffusivity coefficient for ethanol
Xe = 25960; %Active biofilm density for ethanol degradation
Kse = 0.32; % Half-saturation constant for ethanol degradation
ke = 0.23; % Max specific utilization rate for ethanol degradation
Cia = 0.93; %Inhibition constant
Xa = 2820; %Active biofilm density for acetaldehyde degradation
Ksa = 3.5; %Half-saturation constant for acetaldehyde degradation
ka = 0.85; %Max specific utilization rate for acetaldehyde degradation

dydx = [ y(2)
            (bee*Xe*ke*y(1))/(Dee*(Kse+y(1))*(1+Sa/Cia))-.4*(ka*Xa*Sa)/(Ksa+Sa)];

%---------------------------------------
function res = ethbc(ya,yb,Se,Sa)
res = [ ya(1) - Se
            yb(2)];
```

Bibliography

Archer Daniels Midland (ADM). (2002). "VOC Emissions Test Results for Feed Dryers 1-5: Super Stack/RTO CO_2 Scrubber/RTO." Prepared by Archer Daniels Midland Co., Decatur, Illinois.

Adroer, N., Casas, C., de Mas, C., and Solà, C. (1990). "Mechanism of Formaldehyde Biodegradation by *Pseudomonas putida*." *Applied Microbiology and Biotechnology*, 33(2), 217-220.

American Engineering Testing (AET), (2005). "Report of Compliance Emission Testing for Pine Lakes Corn Processors located in Steamboat Rock, Iowa." Prepared by American Engineering Testing, Inc., St. Paul, Minnesota.

Alvarez-Cohen, L. and Speitel, G.E. Jr. (2001). "Kinetics of Aerobic Cometabolism of Chlorinated Solvents." *Biodegradation*, 12(2), 105-126.

Alonso, C., Suidan, M.T., Sorial, G.A., Smith, F.L., Biswas, P., Smith, P.J., and Brenner, R.C. (1997). "Gas treatment in trickle-bed biofilters: Biomass, how much is enough?" *Biotechnology and Bioengineering*, 54(6), 583-594.

Amoore, J.E., and Hautala, E. (1983). "Odor as an aid to chemical safety: Odor thresholds compared with threshold limit values and volatilities for 214 industrial chemicals in air and water dilution." *Journal of Applied Toxicology*, 3(6), 272-290.

Andrawes, F.F. (1984). "Detection of Traces of Formaldehyde in Pure Air by Gas Chromatography and Helium Ionization Detection." *Journal of Chromatographic Science*, 22(11), 506-508.

APHA, AWWA, and WEF. (1998). "Standard Methods for the Examination of Water and Wastewater." American Public Health Association: American Water Works Association: Water Environmental Federation, Washington, D.C.

Arulneyam, D., and Swaminathan, T. (2000). "Biodegradation of Ethanol Vapour in a Biofilter." *Bioprocess Engineering*, 22(1), 63-67.

Arcangeli, J.P., and Arvin. E. (1992). "Toluene Biodegradation and Biofilm Growth in an Aerobic Fixed-Film Reactor." *Applied Microbiology and Biotechnology*, 37(4), 510-517.

Arcangeli, J.P., and Arvin. E. (1997). "Modeling of the Cometabolic Biodegradation of Trichloroethylene by Toluene-Oxidizing Bacteria in a Biofilm System." *Environmental Science and Technology*, 31(11), 3044–3052.

Azachi, M., Henis, Y., Oren, A., Gurevich, P., and Sarig, S. (1995). "Transformation of Formaldehyde by a *Halomonas sp.*" *Canadian Journal of Microbiology*, 41(6), 548-553.

Aziz, C.E. (1997). "Cometabolic degradation of chlorinated solvent mixtures by OB3b PP358." Dissertation, The University of Texas at Austin, Austin, Texas.

Baltzis, C., Wojdyla, S.M., and Zarook, S.M. (1997). "Modeling Biofiltration of VOC Mixtures under Steady-State Conditions." *Journal of Environmental Engineering-ASCE*, 123(6), 599-605.

Bangs, K.M. (2005). "Treatment of Air Pollutants Emitted from Corn-Derived Ethanol Production Facilities." Thesis, The University of Texas at Austin, Austin, Texas.

Barber, R.D., and Donohue, T.J. (1998). "Function of a Glutathione-Dependent Formaldehyde Dehydrogenase in *Rhodobacter sphaeroides* Formaldehyde Oxidation and Assimilation." *Biochemistry*, 37(2), 530-537.

Betterton, E.A., and Hoffmann, M.R. (1988). "Henry's law constants of some environmentally important aldehydes." *Environmental Science and Technology*, 22(12), 1415-1418.

Bhattacharya, S., and Baltzis, B.C. (2001). "Long Term Operation and Performance of a Biotrickling Filter Treating ortho-Dichlorobenzene and Ethanol Mixtures." Proceedings of the Air & Waste Management Association's Annual Conference & Exhibition, 94th, Orlando, FL, United States, June 24-28, 2001.

Bielefeldt, A.R. and Stensel, H.D. (1999). "Modeling Competitive Inhibition Effects During Biodegradation of BTEX Mixtures." *Water Research*, 33(3), 707-714.

Boenigk, R., Dürre, P., and Gottschalk, G. (1989). "Carrier-Mediated Acetate Transport in *Acetobacterium woodii*." *Archives of Microbiology*, 152(6), 589-593.

Bonastre, N., de Mas, C., and Solà, C. (1986). "Vavilin Equation in Kinetic Modeling of Formaldehyde Biodegradation." *Biotechnology and Bioengineering*, 28(4), 616-619.

Brady, D., and Pratt, G.C. (2006). "Volatile Organic Compound Emissions from Dry Mill Ethanol Production." Environmental Bulletin No.8. Minnesota Pollution Control Agency, St. Paul, Minnesota.

Chang, M.K., Voice, T.C., and Criddle, C.S. (1993). "Kinetics of Competitive Inhibition and Cometabolism in the Biodegradation of Benzene, Toluene, and *p*-Xylene by Two *Pseudomonas* Isolates." *Biotechnology and Bioengineering*, 41(11), 1057-1065.

Chemfinder. http://www.chemfinder.com. Accessed on April 2007.

Chinnawirotpisan, P., Theeragool, G., Limtong, S., Toyama, H., Adachi, O., Matsushita, K. (2003). "Quinoprotein Alcohol Dehydrogenase Is Involved in Catabolic Acetate Production, while NAD-dependent Alcohol Dehydrogenase in Ethanol Assimilation in *Acetobacter pasteurianus* SKU1108." *Journal of Bioscience and Bioengineering*, 96(6), 564-571.

Christen, P., Domenech, F., Michelena, G., Auria, R., and Revah, S. (2002). "Biofiltration of Volatile Ethanol Using Sugar Cane Bagasse Inoculated with *Candida utilis*." *Journal of Hazardous Materials*, 89(2-3), 253-265.

Corsi, R.L., and Seed, L. (1995). "Biofiltration of BTEX: Media, Substrate, and Loadings Effects." *Environmental Progress*, 14(3), 151-158.

Cox, H.H.J., Moerman, R.E., van Baalen, S., van Heiningen, W.N.M., Doddema, H.J., and Harder, W. (1997). "Performance of a Styrene-Degrading Biofilter Containing the Yeast *Exophiala jeanselmei*." *Biotechnology and Bioengineering*, 53(3), 259-266.

Cox, H.H.J., Sexton, T., Shareefdeen, Z.M., and Deshusses, M.A. (2001). "Thermophilic Biotrickling Filtration of Ethanol Vapors." *Environmental Science and Technology*, 35(12), 2612-2619.

Datta, I., Fulthorpe, R.R., Sharma, S., and Allen, D.G. (2007). "High-Temperature Biotrickling Filtration of Hydrogen Sulphide." *Applied Microbiology and Biotechnology*, 74(3), 708-716.

Deshusses, M.A., Hamer, G., and Dunn, I.J. (1995a). "Behavior of Biofilters for Waste Air Biotreatment. 1. Dynamic Model Development." *Environmental Science and Technology*, 29(4), 1048-1058.

Deshusses, M.A., Hamer, G., and Dunn, I.J. (1995b). "Behavior of Biofilters for Waste Air Biotreatment. 2. Experimental Evaluation of a Dynamic Model." *Environmental Science and Technology*, 29(4), 1059-1068.

Deshusses, M.A., Hamer, G., and Dunn, I.J. (1996). "Transient-State Behavior of a Biofilter Removing Mixtures of Vapors of MEK and MIBK from Air." *Biotechnology and Bioengineering*, 49(5), 587-598.

Devinny, J.S., and Hodge, D.S. (1995). "Formation of Acidic and Toxic Intermediates in Overloaded Ethanol Biofilters." *Journal of the Air & Waste Management Association*, 45(2), 125-131.

Devinny, J.S., and Ramesh, J. (2005). "A Phenomenological Review of Biofilter Models." *Chemical Engineering Journal*, 113(2-3), 187-196.

Dirk-Faitakis, C., and Allen, D.G. (2005). "Development and simulation studies of an unsteady state biofilter model for the treatment of cyclic air emissions of an α-pinene gas stream." *Journal of Chemical Technology and Biotechnology*, 80(7), 737-745.

Domenech, F., Christen, P., Paca, J., and Revah, S. (1999). "Ethanol Utilization for Metabolite Production by *Candida utilis* Strains in Liquid Medium." *Acta Biotechnologia*, 19(1), 27-36.

Dupasquier, D., Revah, S. and Auria, R. (2002). "Biofiltration of Methyl tert-Butyl Ether Vapors by Cometabolism with Pentane: Modeling and Experimental Approach." *Environmental Science and Technology*, 36 (2), 247–253.

Eiroa, M., Kennes, C., and Veiga, M.C. (2004). "Formaldehyde Biodegradation and Its Inhibitory Effect on Nitrification." *Journal of Chemical Technology and Biotechnology*, 79(5), 499-504.

Eiroa, M., Kennes, C., and Veiga, M.C. (2005). "Simultaneous Nitrification and Formaldehyde Biodegradation in an Activated Sludge Unit." *Bioresource Technology*, 96(17), 1914-1918.

Fargione, J.; Hill, J.; Tilman, D.; Polasky, S.; and Hawthorne, P. (2008). "Land Clearing and the Biofuel Carbon Debt." *Science*, 319(5867), 1235-1238.

Farrell, A.E., Plevin, R.J., Turner, B.T., Jones, A.D., O'Hare, M., and Kammen, D.M. (2006). "Ethanol Can Contribute to Energy and Environmental Goals." *Science*, 311(5760), 506-508.

Ferranti, M.M., and Conca, A. (2000). "Formaldehyde Biological Removal from Exhaust Air in the Composite Panel Board Industry from Pilot Tests to Industrial Plant." Proceedings of the Air & Waste Management Association's 93th Annual Conference & Exhibition, Salt Lake City, UT, United States, June 18-22, 2000.

Fortin, N.Y., and Deshusses, M.A. (1999). "Treatment of Methyl tert-Butyl Ether Vapors in Biotrickling Filters. 1. Reactor Startup, Steady-State Performance, and Culture Characteristics." *Environmental Science and Technology*, 33 (17), 2980-2986.

Gaffney, J.S., Streit, G.E., Spall, W.E., and Hall, J.H. (1987). "Beyond Acid Rain." *Environmental Science and Technology*, 21(12), 519-524.

Garner, L.G. (2002). "Biofiltration- A Disruptive Technology for Sustainable Air Pollution Control." Proceedings of the Air & Waste Management Association's 95th Annual Conference & Exhibition, Baltimore, MD, United States, June 23-27, 2002.

Glancer-Šoljan, M., Šoljan, V., Dragičević, T.L., and Cačić, L. (2001). "Aerobic Degradation of Formaldehyde in Wastewater from the Production of Melamine Resins." *Food Technology and Biotechnology*, 39(3), 197-202.

Gómez-Manzo, S., Contreras-Zentella, M., González-Valdez, A., Sosa-Torres, M., Arreguín-Espinoza, R., and Escamilla-Marván, E. (2008). "The PQQ-alcohol dehydrogenase of *Gluconacetobacter diazotrophicus*." *International Journal of Food Microbiology*, 125(1), 71-78.

Gonzalez-Gil, G., Kleerebezem, R., and Lettinga, G. (2002). "Conversion and Toxicity Characteristics of Formaldehyde in Acetoclastic Methanogenic Sludge." *Biotechnology and Bioengineering*, 79(3), 314-322.

Grady, C.P.L., and Lim, H.C. (1980). *Biological Wastewater Treatment*, Marcel Dekker Inc., New York.

Grady, C.P.L., Smets, B.F., and Barbeau, D.S. (1996). " Variability in Kinetic Parameter Estimates: A Review of Possible Causes and A Proposed Terminology." *Water Research*, 30(3), 742-748.

Gribbins, M.J., and Loehr, R.C. (1998). "Effect of Media Nitrogen Concentration on Biofilter Performance." *Journal of the Air & Waste Management Association*, 48(3), 216-226.

Gunsch, C.K. (2004). "Linking Gene Expression to Performance in a Fungal Vapor-Phase Bioreactor Treating Ethylbenzene." Dissertation, The University of Texas at Austin, Austin, Texas.

Hanson, R.S. and Hanson, T.E. (1996). "Methanotrophic Bacteria." *Microbiological Reviews*, 60(2), 439-471.

Hidalgo, A., Lopategi, A., Prieto, M., Serra, J.L., and Llama, M.J. (2002). "Formaldehyde Removal in Synthetic and Industrial Wastewater by *Rhodococcus erythropolis* UPV-1." *Applied Microbiology and Biotechnology*, 58(2), 260-263.

Hodge, D.S., and Devinny, J.S. (1995) "Modeling Removal of Air Contaminants by Biofiltration." *Journal of Environmental Engineering-ASCE*, 121(1), 21-32.

Höllrigl, V., Hollmann, F., Kleeb, A.C., Buehler K., and Schmid, A. (2008). "TADH, the Thermostable Alcohol Dehydrogenase from Thermus sp. ATN1: a Versatile New

Biocatalyst for Organic Synthesis." *Applied Microbiology and Biotechnology*, 81(2), 263-273.

Ibrahim, M.A., Yamamoto, M., Yasuda, Y., Fukunaga, K., and Nakao, K. (2001a). "Removal of Acetaldehyde and Propionaldehyde from Waste Gas in Packed Column with Immobilized Activated Sludge Gel Beads." *Journal of Chemical Engineering of Japan*, 34(10), 1195-1203.

Ibrahim, M.A., Mizuno, H., Yasuda, Y., Fukunaga, K., and Nakao, K. (2001b). "Removal of Mixtures of Acetaldehyde and Propionaldehyde from Waste Gas in Packed Column with Immobilized Activated Sludge Gel Beads." *Biochemical Engineering Journal*, 8(1), 9-18.

Interpoll Laboratories (Interpoll). (2001). "Results of the August 2 &3, 2001 VOC Emission Compliance Testing at the Ethanol 2000 Facility Located in Bingham Lake, Minnesota." Submitted to Environmental Resource Group, Minneapolis, Minnesota.

Interpoll Laboratories (Interpoll). (2003). "Results of the August 26-29, 2003 Air Emission Compliance Testing at the Exol Ethanol Facility Located in Albert Lea, Minnesota." Submitted to Exol, Albert Lea, Minnesota.

Interpoll Laboratories. (Interpoll). (2005). "Results of the June 14-15, 2005 Air Emission Compliance Testing at the Heartland Corn Products Facility Located in Winthrop, Minnesota." Submitted to Natural Resource Group, Minneapolis, Minnesota.

Kalnenieks, U., Galinina., N., Toma, M., and Skārds, I. (1996). "Electron Transport Chain in Aerobically Cultivated *Zymomonas mobilis*." *FEMS Microbiology Letters*, 143(2-3), 185-189.

Kalnenieks, .U, Galinina, N., Toma, M.M., and Marjutina, U. (2002). "Ethanol Cycle in An Ethanologenic Bacterium." *FEBS Letters*, 522(1-3), 6-8.

Kalnenieks, U., Galinina, N., Toma, M. M., Pickford, J. L., Rutkis, R., and Poole, R. K. (2006). "Respiratory Behaviour of a *Zymomonas mobilis adhB adhB::kan*^{r} Mutant Supports the Hypothesis of Two Alcohol Dehydrogenase Isoenzymes Catalysing Opposite Reactions." *FEBS Letters*, 580(21), 5084-5088.

Kastner, J.R., and Das, K.C. (2005). "Comparison of Chemical Wet Scrubbers and Biofiltration for Control of Volatile Organic Compounds using GC/MS Techniques and Kinetic Analysis." *Journal of Chemical Technology and Biotechnology*, 80(10), 1170-1179.

Kaszycki, P., Tyszka, M., Malec, P., and Koloczek, H. (2001). "Formaldehyde and Methanol Biodegradation with the Methylotrophic Yeast *Hansenula polymorpha*. An Application to Real Wastewater Treatment ." *Biodegradation*, 12(3), 169-177.

Kato, N., Yamagami, T., Kitayama, Y., Shimao, M., and Sakazawa, C. (1984). "Dismutation and Cross-Dismutation of Aldehydes, and Alcohol: Aldehyde Oxidoreduction by Resting-Cells of *Pseudomonas putida* F61-a." *Journal of Biotechnology*, 1(5-6), 295-306.

Kennes, C., and Viega, M. C. (2002). *Bioreactors for Waste Gas Treatment*, Kluwer Acadimic Publishers, The Netherlands.

Kim, H., Kim, S., and Dale, B.E. (2009). "Biofuels, Land Use Change, and Greenhouse Gas Emissions: Some Unexplored Variables." *Environmental Science and Technology*, 43(3), 961–967.

Kinoshita, S., Kakizono, T., Kadota, K., Das, K., and Taguchi H. (1985). "Purification of two alcohol dehydrogenases from *Zymomonas mobilis* and their properties." *Applied Microbiology and Biotechnology*, 22(4), 249-254.

Kolb, B. (2005). Personal communication, Bob Kolb, Ronning Engineering Co., Inc., Overland Park, Kansas.

Kondo, T. and Kondo, M. (1996). "Efficient Production of Acetic Acid from Glucose in a Mixed Culture of *Zymomonas mobilis* and *Acetobacter sp*." *Journal of Fermentation and Bioengineering*, 81(1), 42-46.

Kong, Z., Farhana, L., Fulthorpe, R.R., and Allen, D.G. (2001). "Treatment of Volatile Organic Compounds in a Biotrickling Filter under Thermophilic Conditions." *Environmental Science and Technology*, 35(21), 4347-4352.

Kovárová-Kovar, K., and Egli, T. (1998). "Growth Kinetics of Suspended Microbial Cells: From Single-Substrate-Controlled Growth to Mixed-Substrate Kinetics." *Microbiology and Molecular Biology Reviews*, 62(3): 646-666.

Krailas, S., Pham, Q.T., Amal, R., Jiang, J.K., and Heitz, M. (2000). "Effect of Inlet Mass Loading, Water and Total Bacteria Count on Methanol Elimination Using Upward Flow and Downward Flow Biofilters." *Journal of Chemical Technology and Biotechnology,* 75(4), 299-305.

Kwon, S. (2007). "Biological Pretreatment of Produced Water for Reuse Applications." Dissertation, The University of Texas at Austin, Austin, Texas.

Leson, G., and Winer, A.M. (1991). "Biofiltration: An Innovative Air Pollution Control Technology for VOC Emissions." *Journal of the Air & Waste Management Association*, 41(8), 1045-1054.

Lovanh, N., Hunt, C.S., and Alvarez, P.J.J. (2002). "Effect of Ethanol on BTEX Biodegradation Kinetics: Aerobic Continuous Culture Experiments." *Water Research*, 36(15), 3739-3746.

Lu, Z. and Hegemann, W. (1998). "Anaerobic Toxicity and Biodegradation of Formaldehyde in Batch Cultures." *Water Research*, 32(1), 209-215.

Luong, J.H.T. (1987). "Generalization of Monod Kinetics for Analysis of Growth Data with Substrate Inhibition." *Biotechnology and Bioengineering*, 29(2), 242-248.

Madigan, M.T., Martinko, J.M., and Parker, J. (2003). *Brock Biology of Microorganisms*. Prentice Hall.

Matsushita, K., Yakushi, T., Takaki, Y., Toyama, H., and Adachi, O. (1995). "Generation Mechanism and Purification of an Inactive Form Convertible In Vivo to the Active Form of Quinoprotein Alcohol Dehydrogenase in *Gluconobacter suboxydans*." *Journal of Bacteriology*, 177(22), 6552-6559.

Matsushita, K., Inoue, T., Adachi, O., and Toyama, H. (2005). "*Acetobacter aceti* Possesses a Proton Motive Force-Dependent Efflux System for Acetic Acid." *Journal of Bacteriology*, 187(13), 4346-4352.

Matteau, Y., and Ramsay, B. (1999). "Thermophilic Toluene Biofiltration." *Journal of the Air & Waste Management Association*, 49(3), 350-354.

McAloon, A., Taylor, F., Yee, W., Ibsen, K., and Wooley, R. (2000). "Determining the Cost of Producing Ethanol from Corn Starch and Lignocellulosic Feedstocks." A joint study sponsored by the U.S. Department of Agriculture and U.S. Department of Energy, National Renewable Energy Laboratory, Golden, Colorado. NREL/TP-580-28893.

Mehta, R.J. (1975). "A Novel Inducible Formaldehyde Dehydrogenase of *Pseudomonas sp*. (RJ_1)." *Antonie van Leeuwenhoek*, 41(1), 89-95.

Minnesota Department of Health. (2003). "Public Health Assessment: Gopher State Ethanol/Minnesota Brewing Corporation, City of St. Paul." Prepared by the Minnesota Department of Health, Ramsey County, Minnesota.

Moe, W.M., and Irvine, R.L. (2000). "Polyurethane Foam Medium for Biofiltration. II: Operation and Performance." *Journal of Environmental Engineering-ASCE*, 126(9), 826-832.

Mohseni, M., and Allen, D.G. (2000). "Biofiltration of Mixtures of Hydrophilic and Hydrophobic Volatile Organic Compounds." *Chemical Engineering Science*, 55(9), 1545-1558.

Muraoka, H., Watabe, Y., and Ogasawara, N. (1982). Effect of Oxygen Deficiency on Acid Production and Morphology of Bacterial Cells in Submerged Acetic Fermentation by *Acetoacter aceti*. *Journal of Fermentation Technology*, 60(3), 171-180.

Muraoka, H., Watabe, Y., Ogasawara, N., and Takahashi, H. (1983). "Trigger of Damage by Oxygen Deficiency to the Acid Production System during Submerged Acetic Fermentation with *Acetoacter aceti*." *Journal of Fermentation Technology*, 61(1), 89-93.

Nakano, S., and Fukaya, M. (2008). "Analysis of Proteins Responsive to Acetic Acid in *Acetobacter*: Molecular Mechanisms Conferring Acetic Acid Resistance in Acetic Acid Bacteria." *International Journal of Food Microbiology*, 125(1), 54-59.

Oliveira, S.V.W.B., Moraes, E.M., Adorno, M.A.T., Varesche, M.B.A., Foresti, E., and Zaiat, M. (2004). "Formaldehyde Degradation in an Anaerobic Packed-Bed Bioreactor." *Water Research*, 38(7), 1685-1694.

Omil, F., Méndez, D., Vidal, G., Méndez, R., and Lema, J.M. (1999). "Biodegradation of Formaldehyde under Anaerobic Conditions." *Enzyme and Microbial Technology*, 24(5-6), 255-262.

Ottengraf, S.P.P., and van der Oever, A.H.C. (1983). "Kinetics of Organic Compound Removal from Waste Gases with a Biological Filter." *Biotechnology and Bioengineering*, 25(12), 3089-3102.

Ottengraf, S.P.P., Meesters, J.J.P., van der Oever, A.H.C., and Rozema, H.R. (1986). "Biological Elimination of Volatile Xenobiotic Compounds in Biofilters." *Bioprocess Engineering*, 1(2), 61-69.

Park, Y.S., Ohtake, H., Fukaya, M., Okumura, H., Kawamura, Y., and Toda, K. (1989). "Effects of Dissolved Oxygen and Acetic Acid Concentrations on Acetic Acid Production in Continuous Culture of *Acetobacter aceti*." *Journal of Fermentation and Bioengineering*, 68(2), 96-101.

Park, J. (2004). "Biodegradation of Paint VOC Mixtures in Biofilters." Dissertation, The University of Texas at Austin, Austin, Texas.

Pimentel, D., and Patzek, T.W. (2005). "Ethanol Production Using Corn, Switchgrass, and Wood; Biodiesel Production Using Soybean and Sunflower." *Natural Resources Research*, 14(1), 65-76.

Pineda, J., Auria, R., Perez-Guevara, F., and Revah, S. (2000) "Biofiltration of Toluene Vapors Using a Model Support." *Bioprocess Engineering*, 23(5), 479-486.

Pirnie-Fisker, E.F., and Woertz, J.R. (2007). "Degradation of Ethanol Plant By-Products by *Exophiala lecanii-corni* and *Saccharomyces cerevisiae* in Batch Studies." *Applied Microbiology and Biotechnology*, 74(4), 902-910.

Prado, Ó.J., Veiga, M.C., and Kennes, C. (2004). "Biofiltration of Waste Gases Containing a Mixture of Formaldehyde and Methanol." *Applied Microbiology and Biotechnology*, 65(2), 235-242.

Prado, Ó.J., Veiga, M.C., and Kennes, C. (2006). "Effect of Key Parameters on the Removal of Formaldehyde and Methanol in Gas-Phase Biotrickling Filters." *Journal of Hazardous Materials*, 138(3), 543-548.

Qu, M., and Bhattacharya, S.K. (1997). "Toxicity and Biodegradation of Formaldehyde in Anaerobic Methanogenic Culture." *Biotechnology and Bioengineering*, 55(5), 727-736.

Rajagopalan, S., vanCompernolle, R., Meyer, C.L., Cano, M.L., and Sun, P.T. (1998). "Comparison of Methods for Determining Biodegradation Kinetics of Volatile Organic Compounds." *Water Environment Research*, 70(3), 291-298.

Renewable Fuels Association (RFA). http://www.ethanolrfa.org. Accessed on Feburary 2009.

Rittmann, B.E., and McCarty, P.L. (2001). *Environmental Biotechnology: Principles and* Applications, McGraw-Hill, New York.

Roe, A.J., McLaggan, D., Davidson, I., O'Byrne, C., and Booth, I.R. (1998). "Perturbation of Anion Balance during Inhibition of Growth of Escherichia coli by Weak Acids." *Journal of Bacteriology*, 180(4), 767–772.

Russell, J.B. (1992). "Another Explanation for the Toxicity of Fermentation Acids at Low pH: Anion Accumulation verse Uncoupling." *Journal of Applied Bacteriology*, 73(5), 363-370.

Searchinger, T., Heimlich, R., Houghton, R. A., Dong, F., Elobeid, A., Fabiosa, J., Tokgoz, S., Hayes, D., and Yu, T. (2008). "Use of U.S. Croplands for Biofuels Increases Greenhouse Gases Through Emissions from Land-Use Change." *Science*, 319(5867), 1238-1240.

Shapouri, H., Duffield, J.A., and Wang, M. (2002). "The Energy Balance of Corn Ethanol: An Update." U.S. Department of Agriculture, Office of the Chief Economist. Office of Energy Policy and New Uses. Agricultural Economic Report No. 814.

Shapouri, H., and Salassi, M. (2006). "The Economic Feasibility of Ethanol Production from Sugar in the United States". U.S. Department of Agriculture, Office of the Chief Economist, Office of Energy Policy and New Uses, and Louisiana State University (LSU).

Shinagawa, E., Toyama, H., Matsushita, K., Tuitemwong, P., Theeragool, G., and Adachi, O. (2006). "A Novel Type of Formaldehyde-Oxidizing Enzyme from the Membrane of *Acetobacter sp.* SKU 14." *Bioscience, Biotechnology, and Biochemistry*, 70(4), 850-857.

Shinagawa, E., Toyama, H., Matsushita, K., Tuitemwong, P., Theeragool, G., and Adachi, O. (2008). Formaldehyde Elimination with Formaldehyde and Formate Oxidase in Membrane of Acetic Acid Bacteria. *Journal of Bioscience and Bioengineering*, 105(3), 292-295.

Simkins, S., and Alexander, M. (1984). "Models for Mineralization Kinetics with the Variables of Substrate Concentration and Population Density." *Applied and Environmental Microbiology*, 47(6), 1299-1306.

Smith, L.H., McCarty, P.L., and Kitanidis, P.K. (1998). "Spreadsheet Method for Evaluation of Biochemical Reaction Rate Coefficients and Their Uncertainties by Weighted Nonlinear Least-Squares Analysis of the Integrated Monod Equation." *Applied and Environmental Microbiology*, 64(6), 2044-2050.

Sologar, V.S., Lu, Z.J., and Allen, D.G. (2003). "Biofiltration of Concentrated Mixtures of Hydrogen Sulfide and Methanol." *Environmental Progress*, 22(2), 129-136.

Song, J., and Kinney, K.A. (2000). "Effect of Vapor-Phase Bioreactor Operation on Biomass Accumulation, Distribution, and Activity: Linking Biofilm Properties to Bioreactor Performance." *Biotechnology and Bioengineering*, 68(5), 508-516.

Song, J. (2001). "Control and Characterization of Biomass Activity and Distribution in Vapor-Phase Bioreactors for VOC Removal." Dissertation, The University of Texas at Austin, Austin, Texas.

Song, J., Kinney, K.A., and John, P. (2003). "Influence of Nitrogen Supply and Substrate Interactions on the Removal of Paint VOC Mixtures in a Hybrid Bioreactor." *Environmental Progress*, 22(2), 137-144.

Stanley, G.A., Douglas, N.G., Every, E.J., Tzanatos, T., and Pamment, N.B. (1993). "Inhibition and Stimulation of Yeast Growth by Acetaldehyde." *Biotechnology Letters*, 15, 1199-1204.

Strauss, J.M., Riedel, K.J., and du Plessis, C.A. (2004). "Mesophilic and Thermophilic BTEX Substrate Interactions for a Toluene-Acclimatized Biofilter." *Applied Microbiology and Biotechnology*, 64(6), 855-861.

Sugiyama, M., Suzuki, S., Tonouchi, N., Yokozeki. K. (2003). "Cloning of the Xylitol Dehydrogenase Gene from Gluconobacter oxydans and Improved Production of Xylitol from D-Arabitol." *Bioscience, Biotechnology, and Biochemistry*, 67(3), 584-591.

Swanson, W.J., and Loehr, R.C. (1997). "Biofiltration: Fundamentals, Design and Operations Principles, and Applications." *Journal of Environmental Engineering-ASCE*, 123(6), 538-546.

Tang, H.M., Hwang, S.J., and Hwang, S.C. (1996). "Waste Gas Treatment in Biofilters." *Journal of the Air & Waste Management Association*, 46(4), 349-354.

Tayama, K., Fukaya, M., Okumura, H., Kawamura, Y., and Beppu, T. (1989). "Purification and Characterization of Membrane-bound Alcohol Dehydrogenase from *Acetobacter polyoxoyenes* sp. nov." *Applied Microbiology and Biotechnology*, 32(2) 181-185.

Terán Pérez, W., Domenech, F., Roger, P., and Christen, P. (2002). "Effect of Mineral Salts Addition on the Behavior of an Ethanol Biofilter." *Environmental Technology*, 23(9), 981-988.

Trivić, S., Leskova, V., and Winston, G.W. (1999). "Aldehyde Dismutase Activity of Yeast Alcohol Dehydrogenase." *Biotechnology Letters*, 21(3), 231-234.

U.S. Congress. (2007). Energy Indenpedance and Security Act of 2007 (H.R.6), 110th Congress, 1st session.

U.S. Department of Energy. http://www.afdc.energy.gov/afdc/ethanol/e85.html. Accessed on April 2007.

U.S. Environmental Protection Agency. (1990). The Clean Air Act (CAA) Amendments of 1990, Title Ⅰ, Part A, Section 112 (b).

U.S. Environmental Protection Agency. (1994a). "Emission Factor Documentation for AP-42, Section 9.9.7, Corn Wet Milling, Final Report." Prepared by Midwest Research Institute, Kansas City, Missouri.

U.S. Environmental Protection Agency. (1994b). "Air Emissions Models for Waste and Wastewater." Prepared for USEPA, Office of Air Quality Planning and Standards, Research Triangle Park, NC (Contract No. 68D10118).

U.S. Environmental Protection Agency. (1996). "Sampling for Selected Aldehyde and Ketone Emissions from Stationary Sources." USEPA Test Method 0011.

U.S. Environmental Protection Agency. (1997). "Emission Factor Documentation for AP-42, Section 9.12.3, Distilled Spirits, Final Report." Prepared by Midwest Research Institute, Kansas City, Missouri.

U.S. Environmental Protection Agency. (2002). Headquarters Press Release, Washington D.C., "United States Settles with 12 Minnesota Ethanol Companies," October 2, 2002.

U.S. Environmental Protection Agency. (2003). Headquarters Press Release, Washington D.C., "Federal; Multi-state Deal Secures Significant Air Pollution Reductions from Industrial Giant Archer Daniels Midland," April 9, 2003.

U.S. Environmental Protection Agency. (2005a). Headquarters Press Release, Washington D.C., "Federal, Multi-State Clean Air Act Settlement with Cargill, Inc., Secures Major Pollution Reductions," September 1, 2005.

U.S. Environmental Protection Agency. (2005b). "The Potential Role of Combined Heat and Power Systems in Destroying Volatile Organic Compounds from Dried Distiller's Grain Solids Dryers in the Ethanol Industry." Developed under contract for the EPA CHP Partnership by ERG, Energy and Environmental Analysis, Inc., and Power Equipment Associates, Inc.

U.S. Environmental Protection Agency. (2006). Method316 - Sampling and Analysis for Formaldehyde Emissions from Stationary Sources in the Mineral Wool and Wool Fiberglass Industries. http://www.epa.gov/ttn/emc/methods/method316.html. Accessed on July 2006.

U.S. Environmental Protection Agency. Health Effects Notebook for Hazardous Air Pollutants. http://www.epa.gov/ttn/atw/hlthef/hapindex.html. Accessed on April 2007.

U.S. Environmental Protection Agency. Integrated Risk Information System (IRIS). http://www.epa.gov/NCEA/iris/subst/0290.htm#carc. Accessed on Feburary 2009.

van Groenestijin, J.W., and Hessslink, P.G.M. (1994). "Biotechniques for Air Pollution Control." *Biodegradation*, 4(4), 282-301.

Velonia, K., and Smonou, I. (2000). "Dismutation of Aldehydes Catalyzed by Alcohol Dehydrogenases." *Journal of the Chemical Society, Perkin Transactions 1*, 14, 2283-2287.

Vorholt, J.A. (2002). "Cofactor-Dependent Pathways of Formaldehyde Oxidation in Methylotrophic Bacteria." *Archives of Microbiology*, 178(4), 239-249.

Wahman, D.G. (2006). "Cometabolism of Trihalomethanes by Nitrifying Biofilters under Drinking Water Treatment Plant Conditions." Dissertation, The University of Texas at Austin, Austin, Texas.

Woertz, J.R., Kinney, K.A., McIntosh, N.D.P., and Szaniszlo, P.J.(2001). "Removal of Toluene in a Vapor-Phase Bioreactor Containing a Strain of the Dimorphic Black Yeast *Exophiala lecanii-corni*." *Biotechnology and Bioengineering*, 75(5), 550-558.

Yamazaki, T., Tsugawa, W., and Sode, K. (2001). "Biodegradation of Formaldehyde by a Formaldehyde-Resistant Bacterium Isolated from Seawater." *Applied Biochemistry and Biotechnology*, 91-93(1-9), 213-217.

Yang, H., Minuth, B., and Allen, D.G. (2002). "Effects of Nitrogen and Oxygen on Biofilter Performance." *Journal of the Air & Waste Management Association*, 52(3), 279-286.

Yaws, C.L. (1999). *Chemical Properties Handbook*, McGraw-Hill, New York.

Zarook, S.M., Baltzis, B.C., Oh, Y.S., and Bartha, R. (1993). "Biofiltration of Methanol Vapor." *Biotechnology and Bioengineering*, 41(5), 512-524.

Zarook, S.M., Shaikh, A.A., Ansar, Z., and Baltzis, B.C. (1997). "Biofiltration of Volatile Organic Compound (VOC) Mixtures under Transient Conditions." *Chemical Engineering Science*, 52(21-22), 4135-4142.

Zhang, Y., Liss, S.N., and Allen, D.G. (2008). "Modeling the Biofiltration of Dimethyl Sulfide in the Presence of Methanol in Inorganic Biofilters at Steady State." *Biotechnology Progress*, 24(4), 845-851.

Zhou, Q., Huang, Y.L., Tseng, D.-H., Shim, H., and Yang, S.-T. (1998). "A Trickling Fibrous-Bed Bioreactor for Biofiltration of Benzene in Air." *Journal of Chemical Technology and Biotechnology*, 73(4), 359-368.

Vita

Li-Jung Chen was born in Taipei, Taiwan on August 19, 1977, the daughter of Yu-Mei Chang and Chia-Mu Chen. She graduated from Song Shan Senior High School in Taipei in 1995 and then entered National Chung Hsing University (NCHU) in Taichung. After receiving her degree of Bachelor of Science in Engineering in June 1999, she continued her graduate study at the Environmental Microbiology Laboratory in NCHU and received her degree of Master of Science in Engineering in June 2001. Upon graduation, she joined Apollo Technology Co. Ltd in Taipei as an environmental engineer for two years. In August 2003, she entered the Graduate School of The University of Texas at Austin.

Permanent address: 2F, No.122, Ln. 67, Lin-Shen N. Rd., 104 Taipei, Taiwan, R.O.C.

This dissertation was typed by the author.